

# The QCD Sphaleron Rate

A First-Principles Determination from Inverse-Problem Techniques

*Multi-canonical methods and Lattice Field Theory*

---

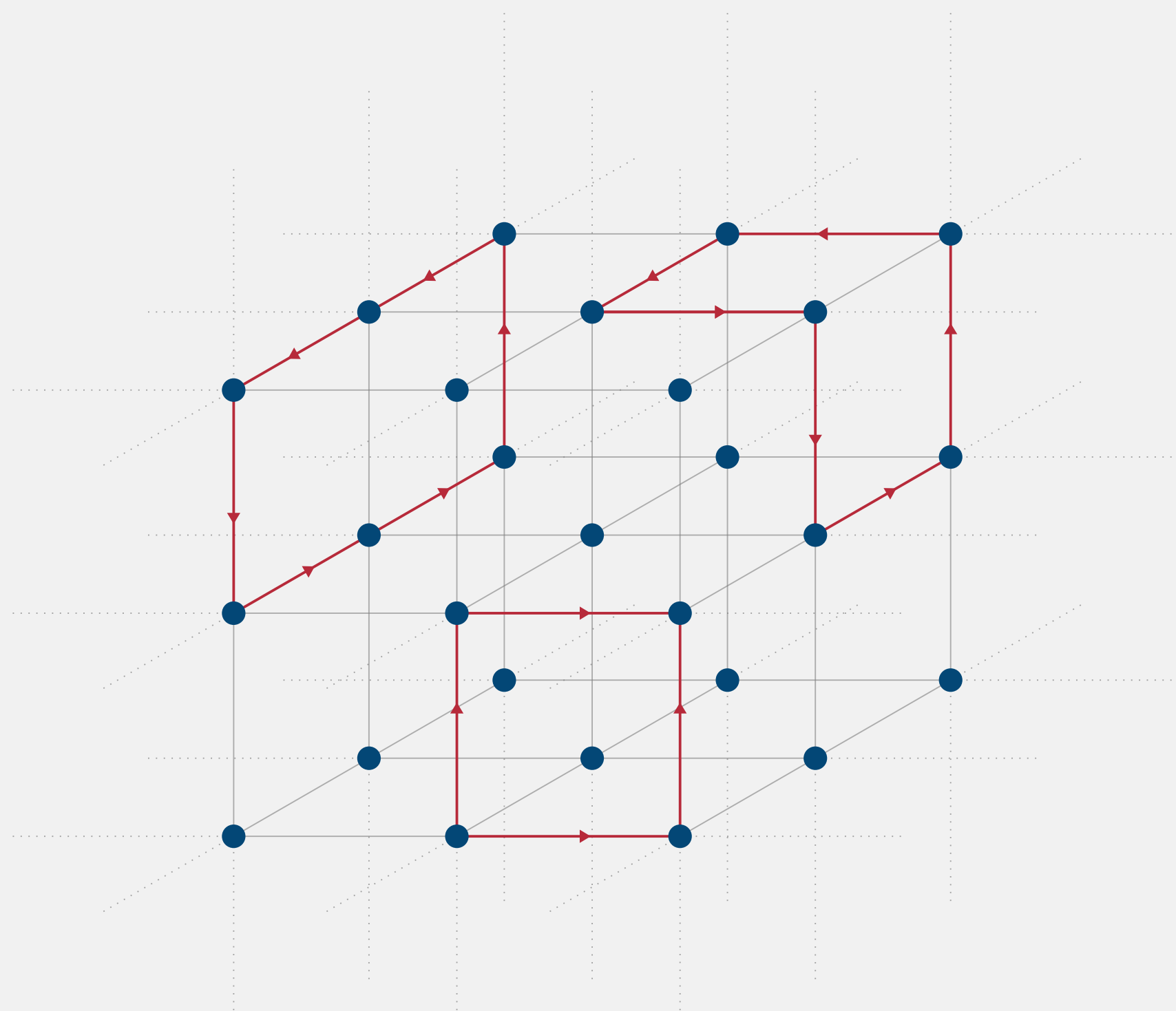
Roberto Dionisio

*roberto.dionisio@phd.unipi.it*

Università di Pisa

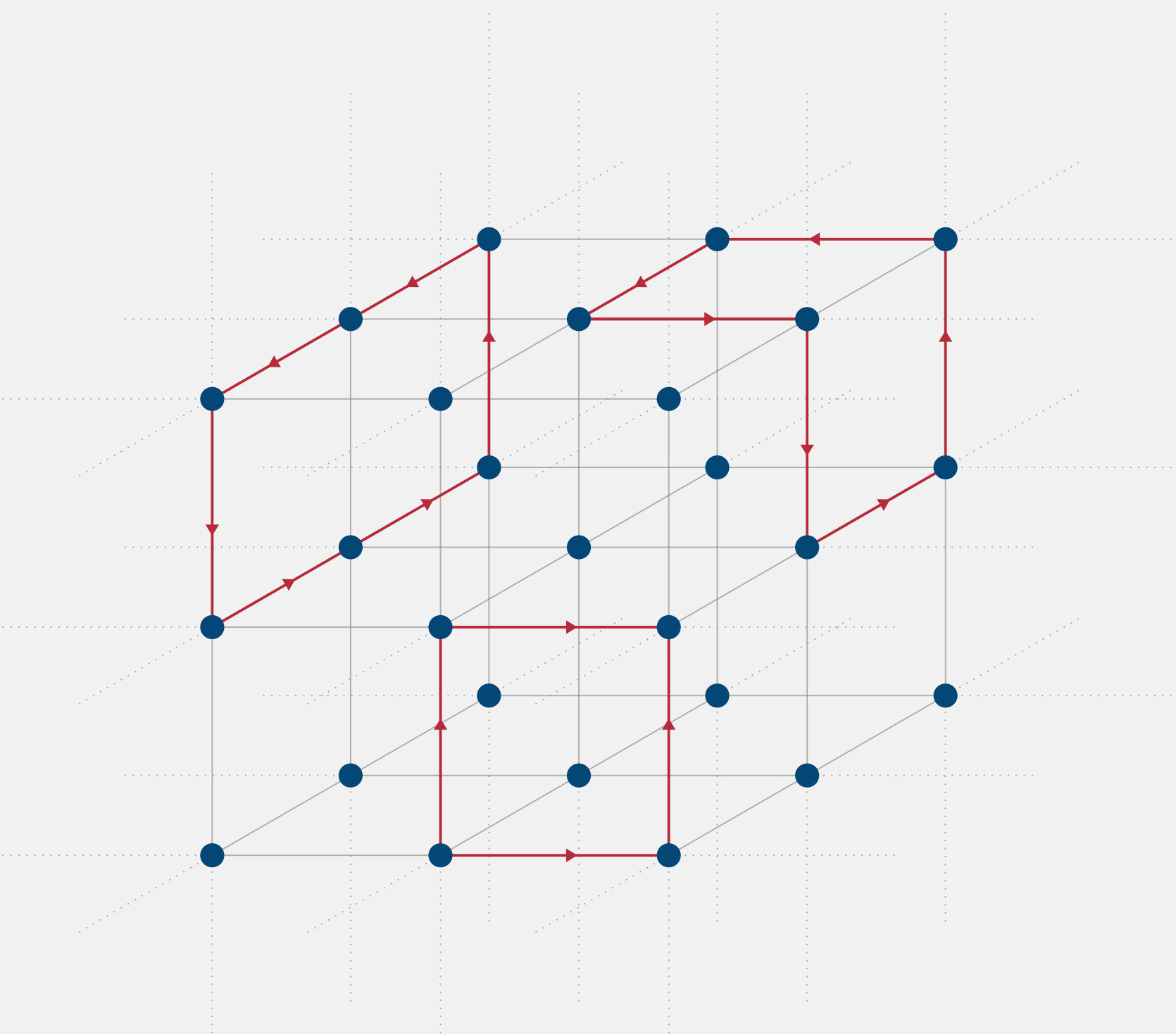
November 26, 2025

# Outline



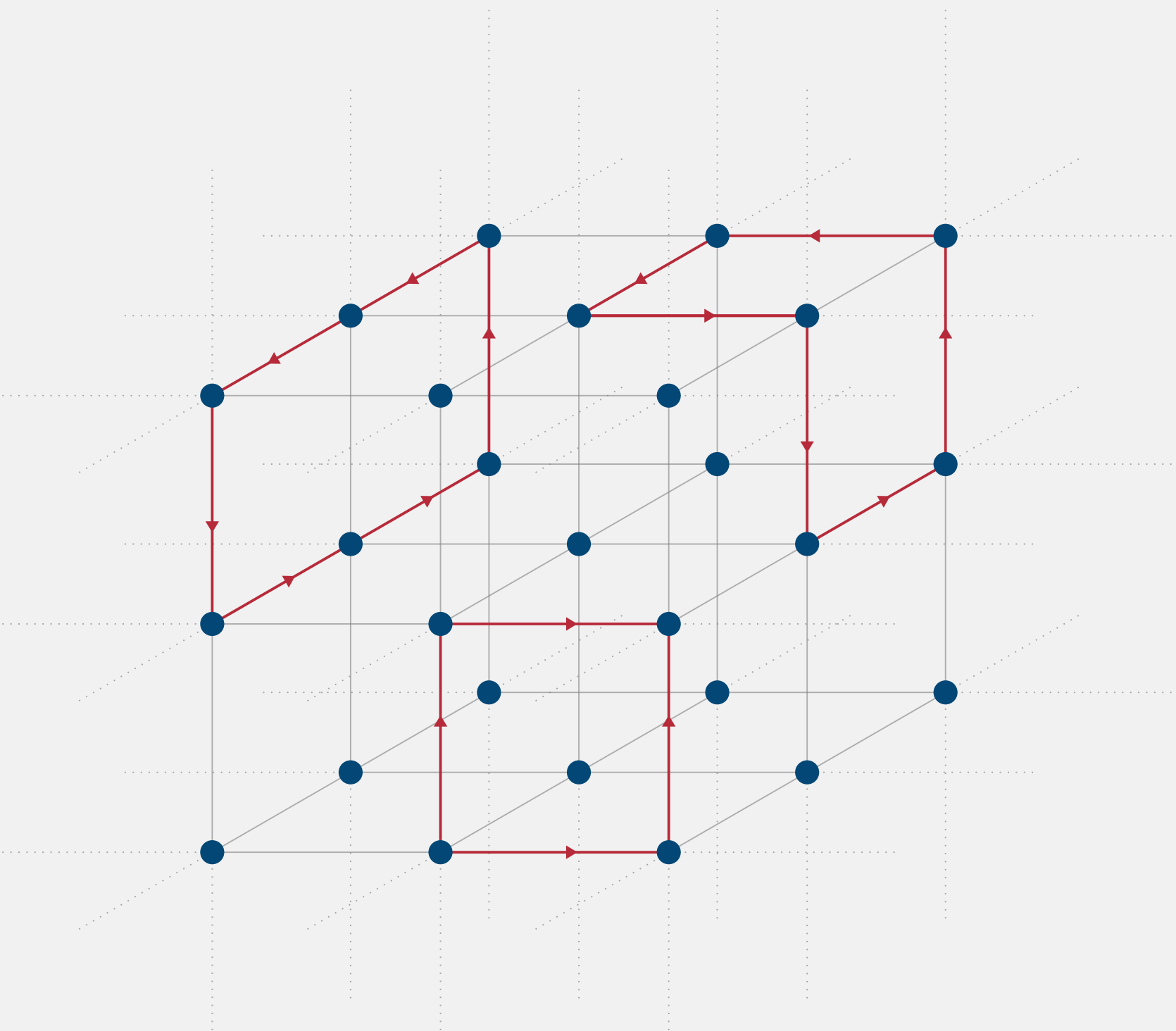
# Outline

## 1. Physics motivation



## 1. Physics motivation

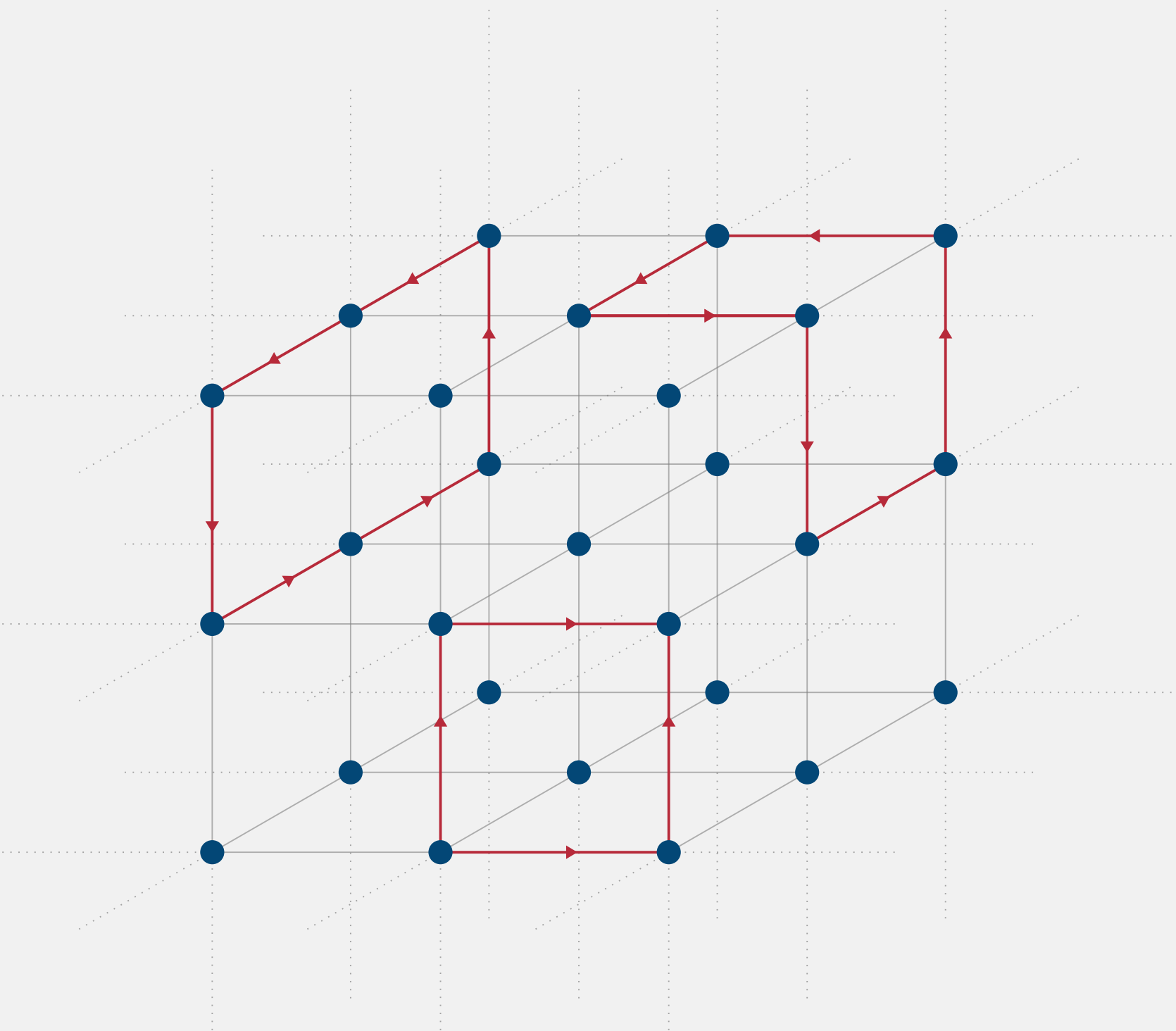
- What are sphaleron transitions? Why do we care?



## 1. Physics motivation

- What are sphaleron transitions? Why do we care?

## 2. The inverse problem

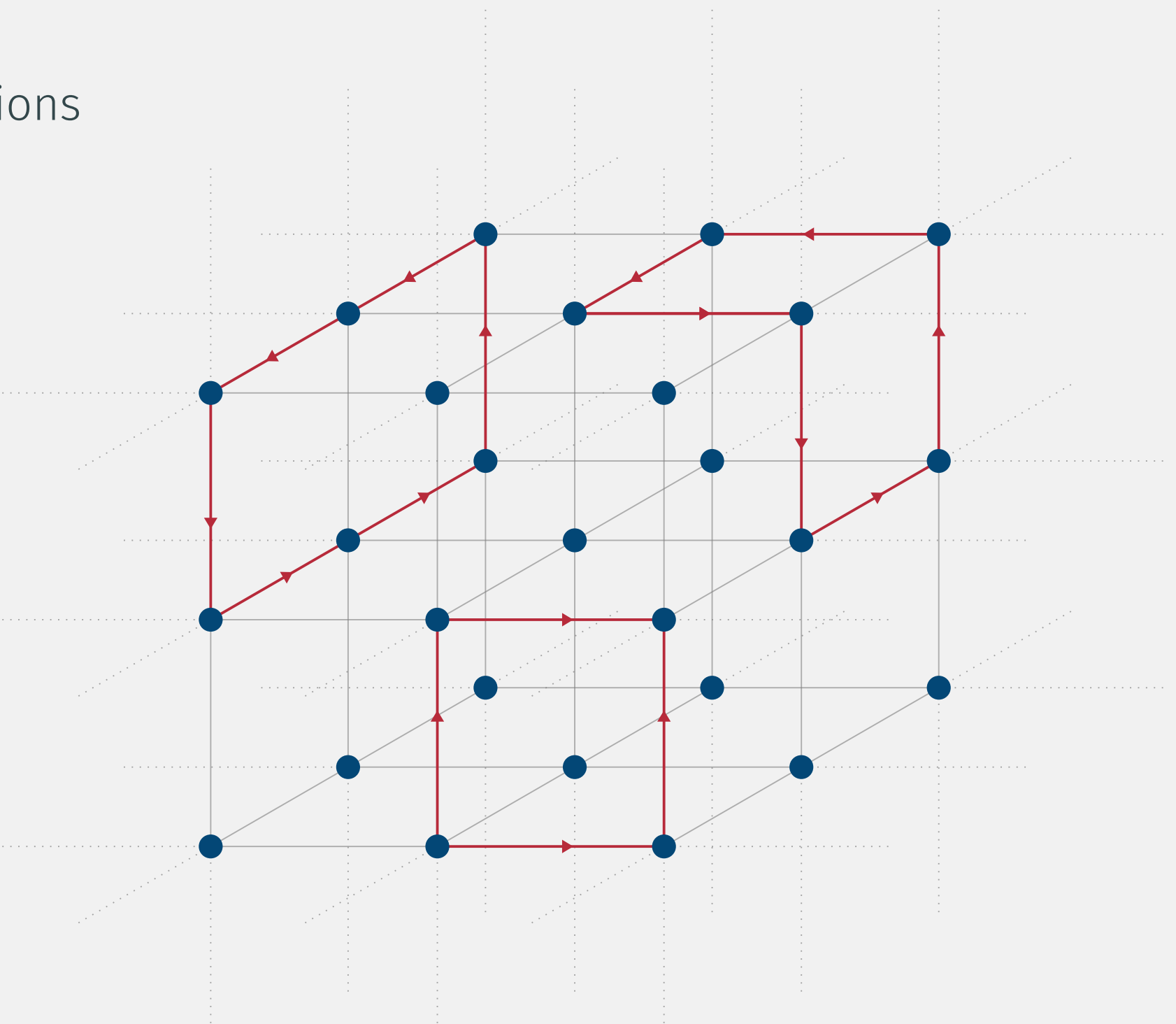


## 1. Physics motivation

- What are sphaleron transitions? Why do we care?

## 2. The inverse problem

- From Euclidean Correlators to Spectral functions
- Ill-posedness



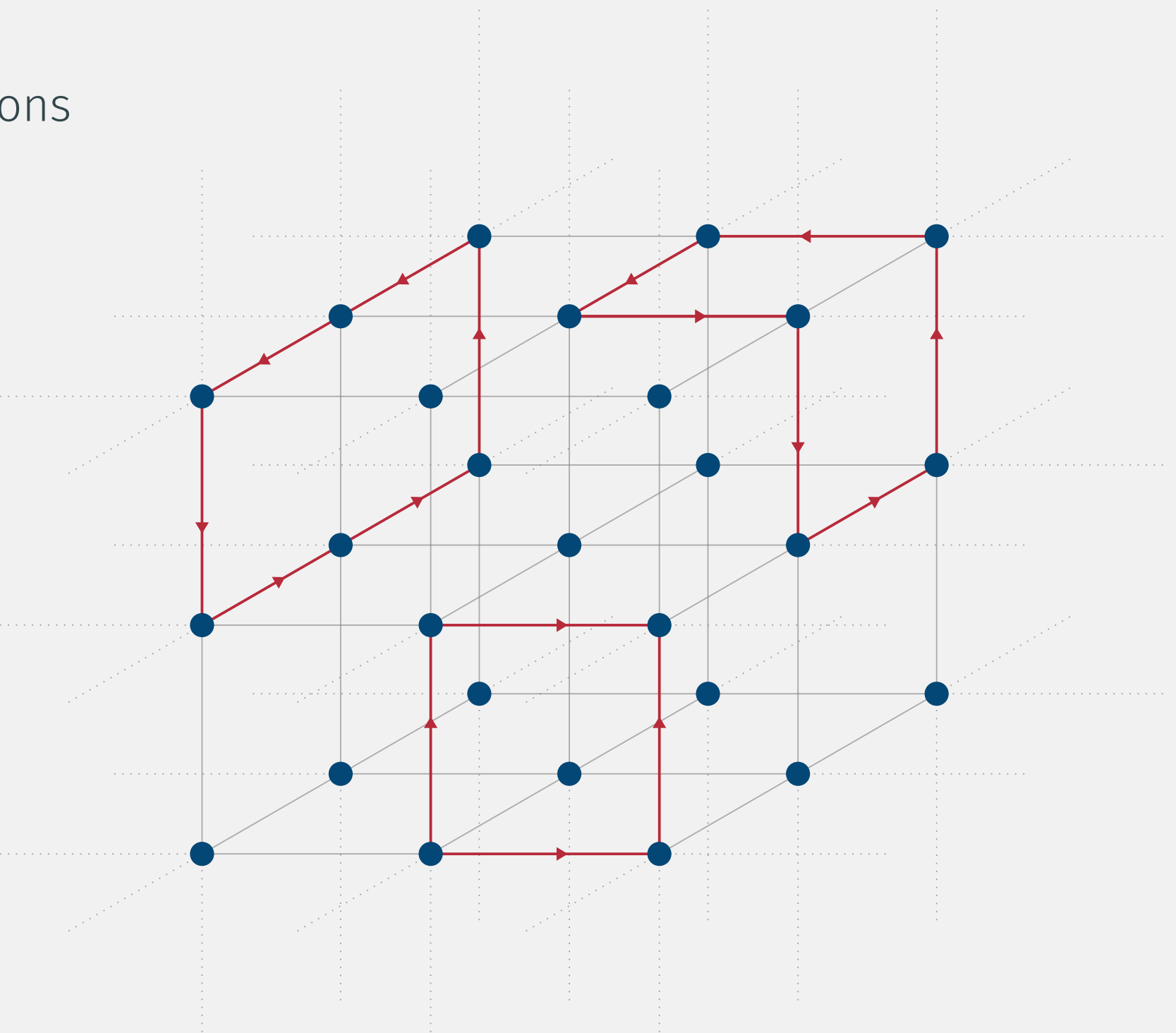
## 1. Physics motivation

- What are sphaleron transitions? Why do we care?

## 2. The inverse problem

- From Euclidean Correlators to Spectral functions
- Ill-posedness

## 3. Mock data tests



## 1. Physics motivation

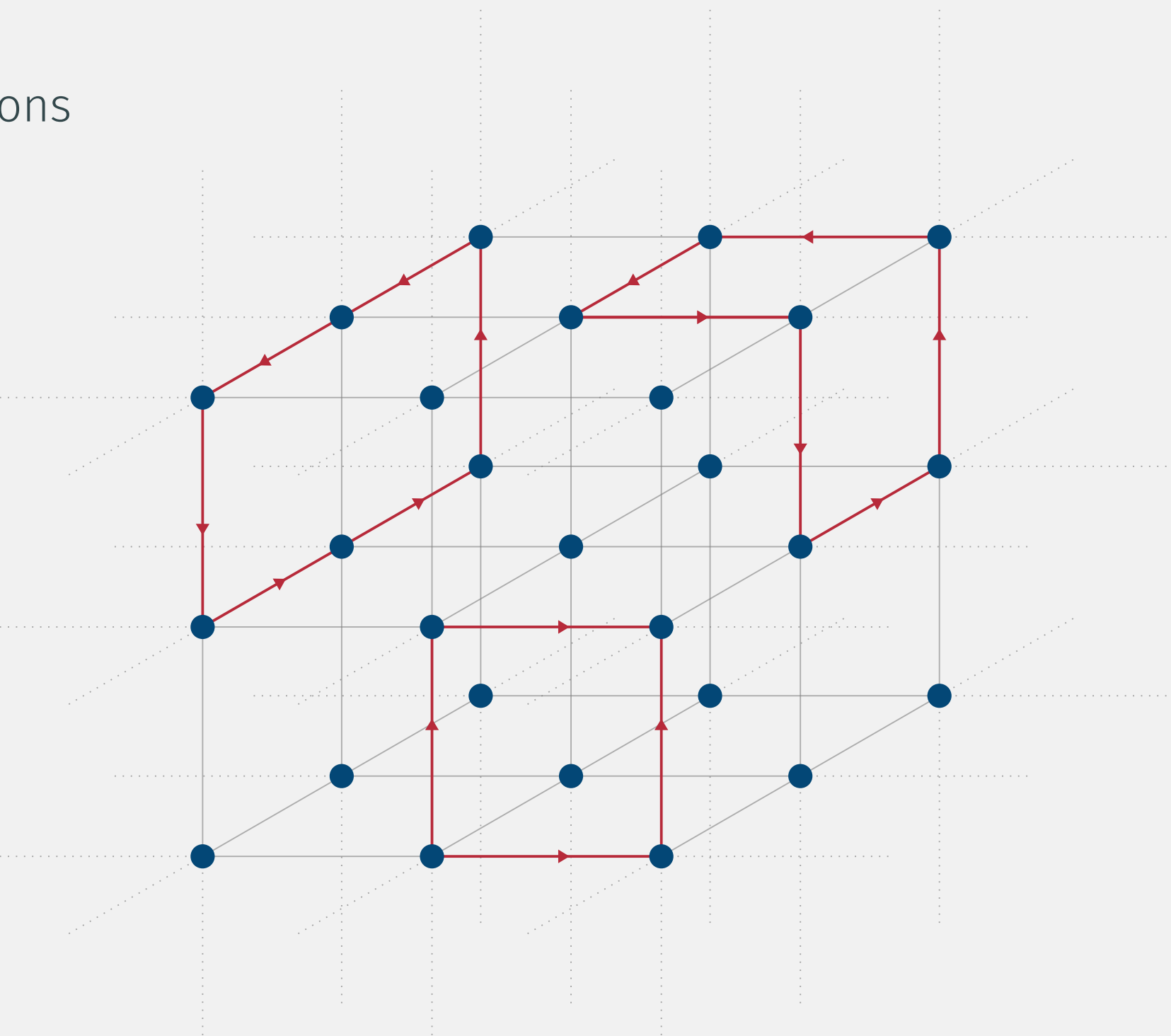
- What are sphaleron transitions? Why do we care?

## 2. The inverse problem

- From Euclidean Correlators to Spectral functions
- Ill-posedness

## 3. Mock data tests

- Instabilities & Regularization



## 1. Physics motivation

- What are sphaleron transitions? Why do we care?

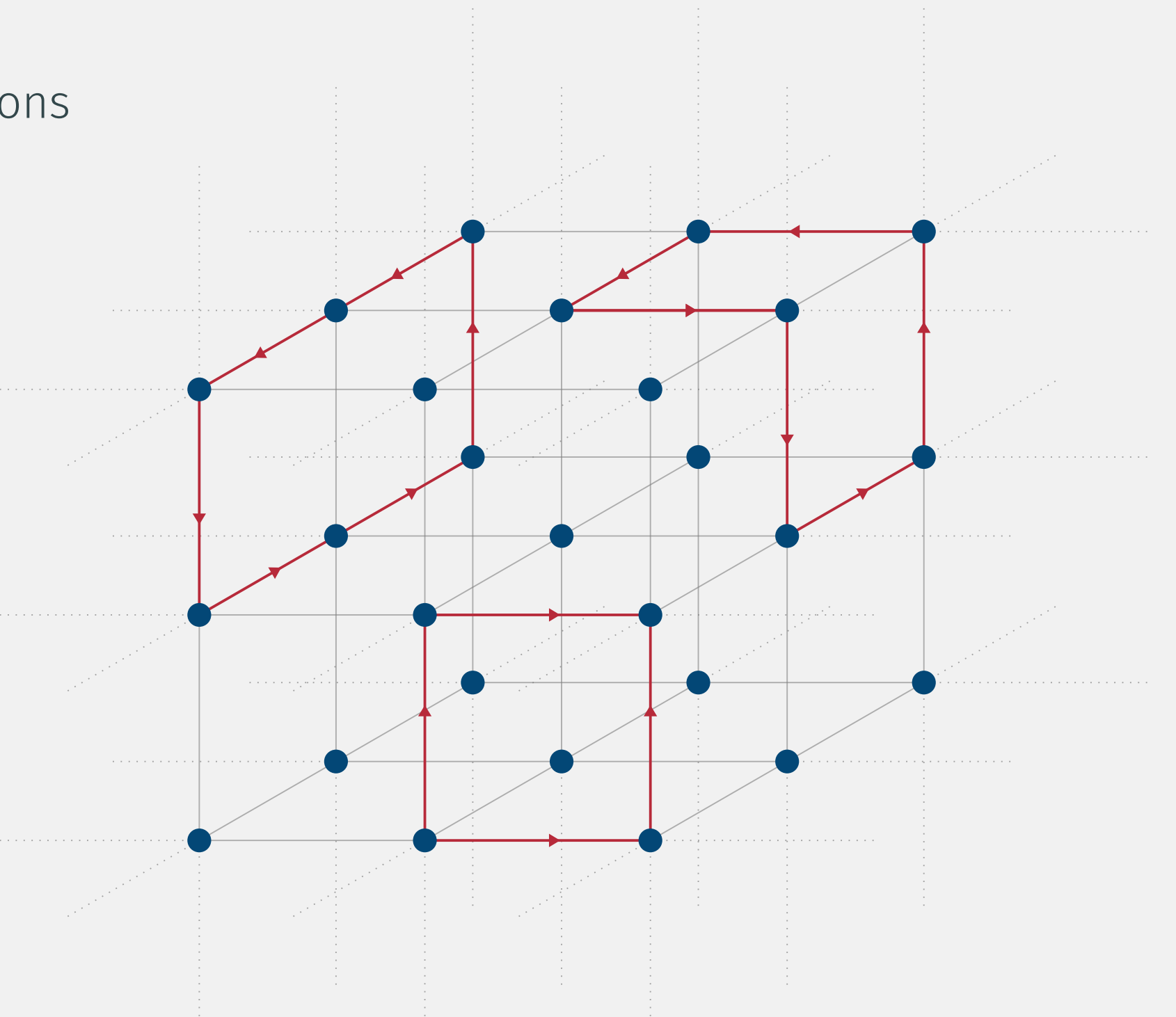
## 2. The inverse problem

- From Euclidean Correlators to Spectral functions
- Ill-posedness

## 3. Mock data tests

- Instabilities & Regularization

## 4. Algorithmic strategy



## 1. Physics motivation

- What are sphaleron transitions? Why do we care?

## 2. The inverse problem

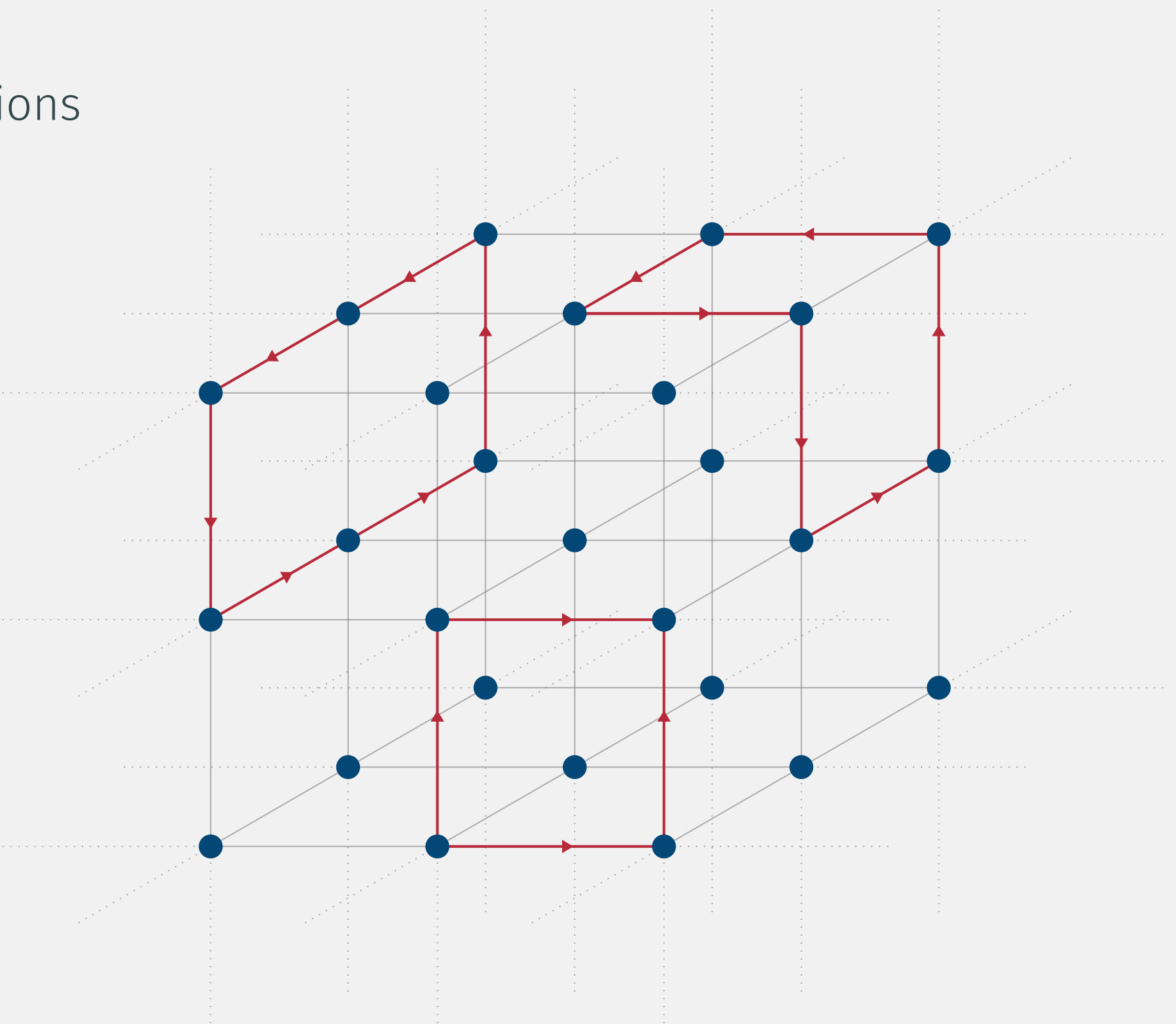
- From Euclidean Correlators to Spectral functions
- Ill-posedness

## 3. Mock data tests

- Instabilities & Regularization

## 4. Algorithmic strategy

- Modified Backus–Gilbert (HLT)



# Outline

## 1. Physics motivation

- What are sphaleron transitions? Why do we care?

## 2. The inverse problem

- From Euclidean Correlators to Spectral functions
- Ill-posedness

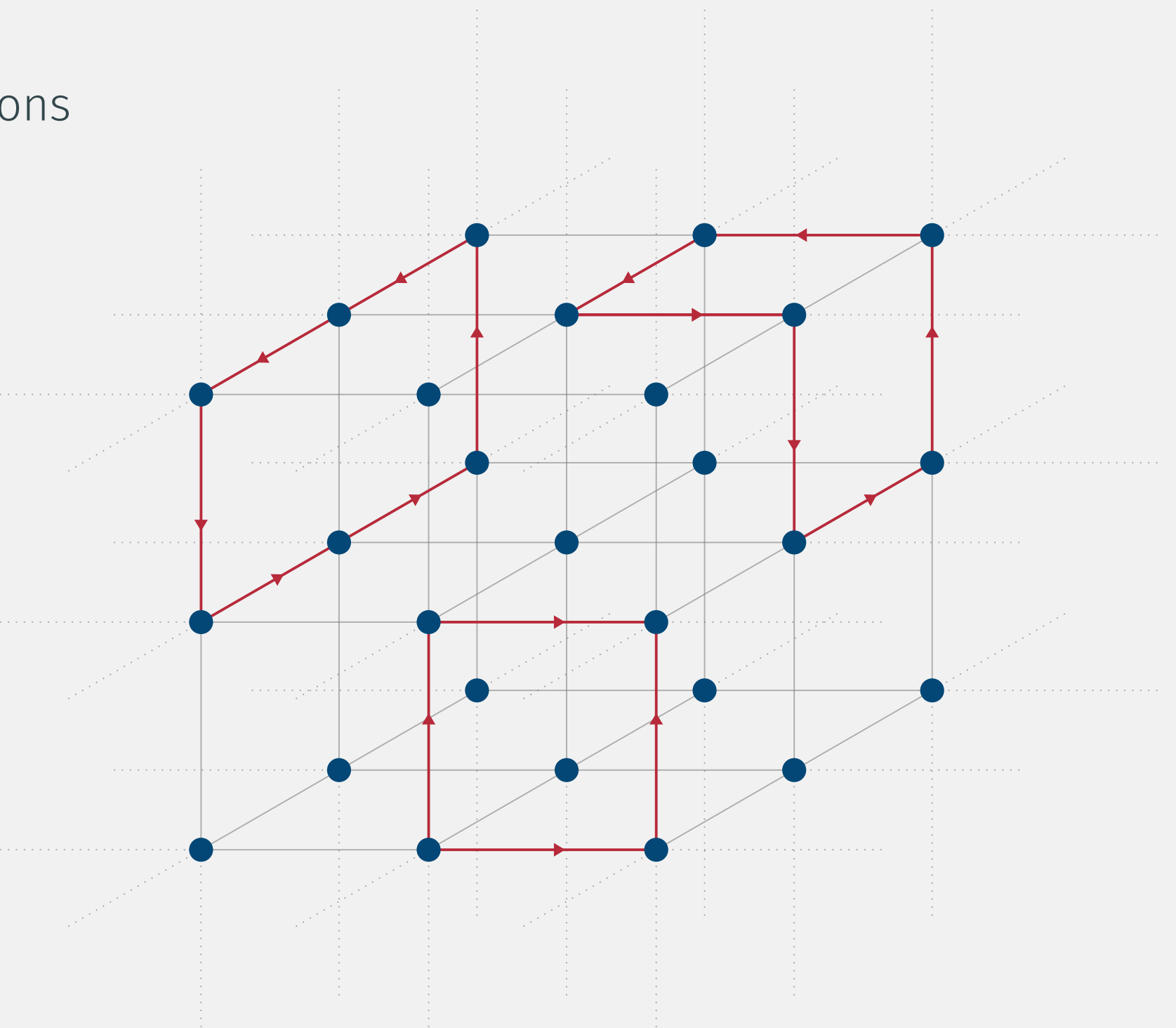
## 3. Mock data tests

- Instabilities & Regularization

## 4. Algorithmic strategy

- Modified Backus–Gilbert (HLT)

## 5. Lattice QCD calculation



# Outline

## 1. Physics motivation

- What are sphaleron transitions? Why do we care?

## 2. The inverse problem

- From Euclidean Correlators to Spectral functions
- Ill-posedness

## 3. Mock data tests

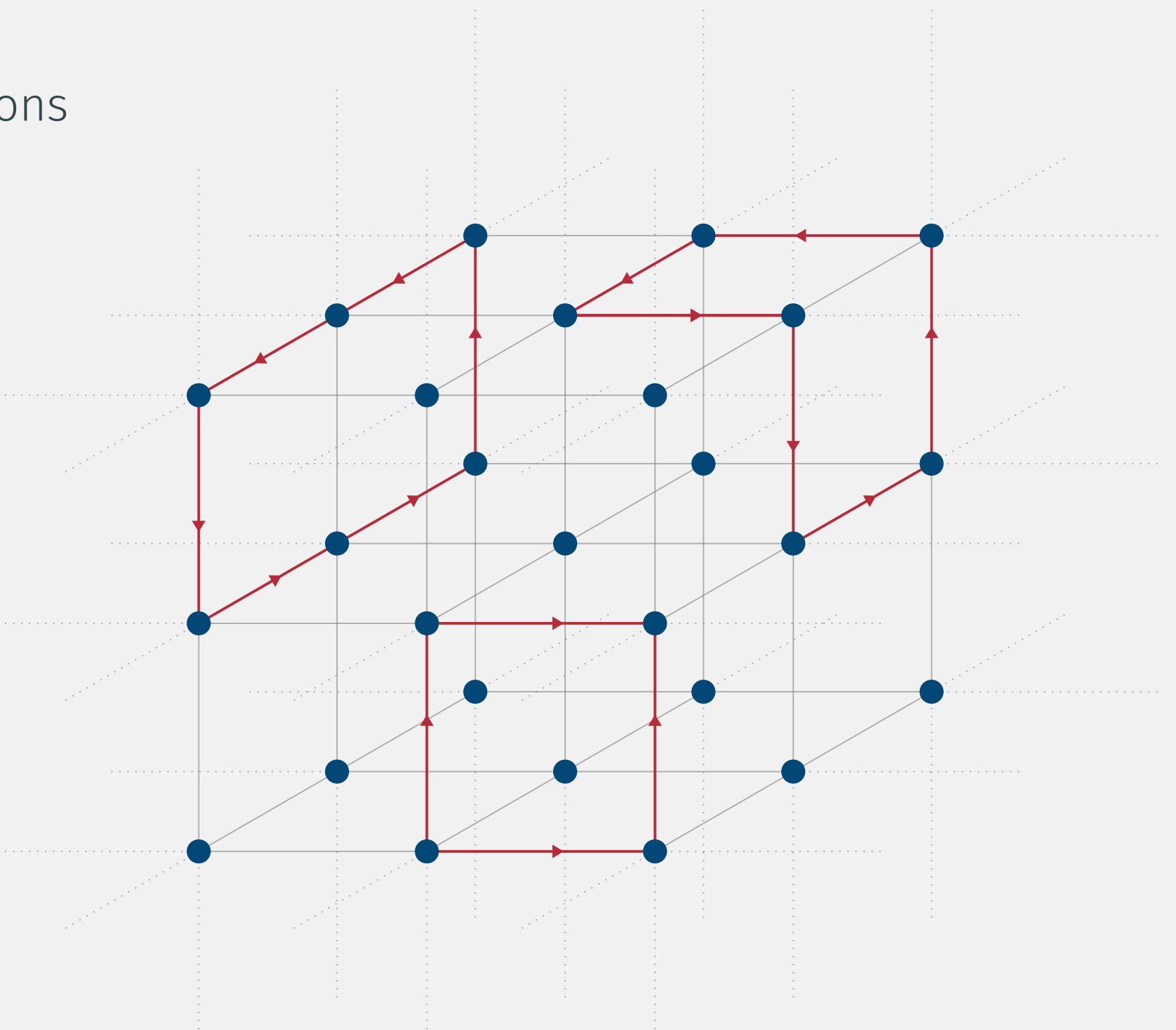
- Instabilities & Regularization

## 4. Algorithmic strategy

- Modified Backus–Gilbert (HLT)

## 5. Lattice QCD calculation

- Finite  $\vec{p}$  Correlators & Double Extrapolation



# Outline

## 1. Physics motivation

- What are sphaleron transitions? Why do we care?

## 2. The inverse problem

- From Euclidean Correlators to Spectral functions
- Ill-posedness

## 3. Mock data tests

- Instabilities & Regularization

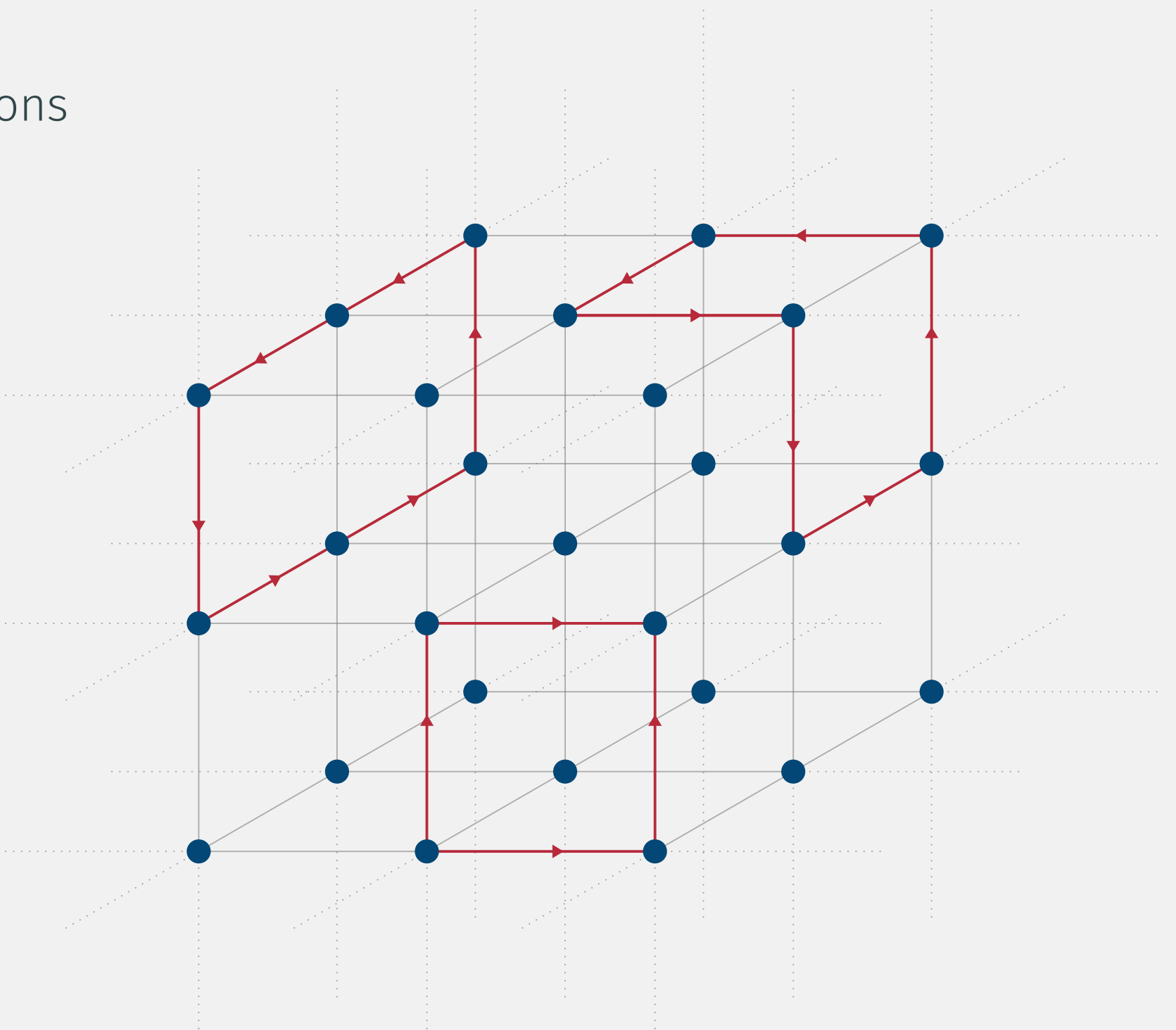
## 4. Algorithmic strategy

- Modified Backus–Gilbert (HLT)

## 5. Lattice QCD calculation

- Finite  $\vec{p}$  Correlators & Double Extrapolation

## 6. Final results & outlook



# QCD Topology



Full QCD Euclidean action:

Full QCD Euclidean action:

$$S_{\text{QCD}} = \int d^4x \frac{1}{2g^2} \text{Tr} [G_{\mu\nu}(x)G_{\mu\nu}(x)] + \int d^4x \sum_f \bar{\psi}_f(x)(\gamma_\mu D_\mu + m_f)\psi_f(x) + \theta Q$$

Full QCD Euclidean action:

$$S_{\text{QCD}} = \int d^4x \frac{1}{2g^2} \text{Tr} [G_{\mu\nu}(x)G_{\mu\nu}(x)] + \int d^4x \sum_f \bar{\psi}_f(x)(\gamma_\mu D_\mu + m_f)\psi_f(x) + \theta Q$$

# QCD Topology

Full QCD Euclidean action:

$$S_{\text{QCD}} = \int d^4x \frac{1}{2g^2} \text{Tr} [G_{\mu\nu}(x)G_{\mu\nu}(x)] + \int d^4x \sum_f \bar{\psi}_f(x)(\gamma_\mu D_\mu + m_f)\psi_f(x) + \theta Q$$

The  $\theta$ -term couples to the **topological charge**:

$$Q = \frac{1}{32\pi^2} \int d^4x \varepsilon_{\mu\nu\rho\sigma} \text{Tr}[G_{\mu\nu}G_{\rho\sigma}]$$

# QCD Topology

Full QCD Euclidean action:

$$S_{\text{QCD}} = \int d^4x \frac{1}{2g^2} \text{Tr}[G_{\mu\nu}(x)G_{\mu\nu}(x)] + \int d^4x \sum_f \bar{\psi}_f(x)(\gamma_\mu D_\mu + m_f)\psi_f(x) + \theta Q$$

The  $\theta$ -term couples to the **topological charge**:

$$Q = \frac{1}{32\pi^2} \int d^4x \varepsilon_{\mu\nu\rho\sigma} \text{Tr}[G_{\mu\nu}G_{\rho\sigma}]$$

- In the continuum:  $Q$  in  $\mathbb{Z}$
- Each integer labels a distinct **topological sector**

# QCD Topology

Full QCD Euclidean action:

$$S_{\text{QCD}} = \int d^4x \frac{1}{2g^2} \text{Tr}[G_{\mu\nu}(x)G_{\mu\nu}(x)] + \int d^4x \sum_f \bar{\psi}_f(x)(\gamma_\mu D_\mu + m_f)\psi_f(x) + \theta Q$$

The  $\theta$ -term couples to the **topological charge**:

$$Q = \frac{1}{32\pi^2} \int d^4x \varepsilon_{\mu\nu\rho\sigma} \text{Tr}[G_{\mu\nu}G_{\rho\sigma}]$$

- In the continuum:  $Q$  in  $\mathbb{Z}$
- Each integer labels a distinct **topological sector**

*Topological sectors are separated by **energy barriers**  
transitions between vacua are rare but physically important*

# Why QCD topology matters



# Why QCD topology matters

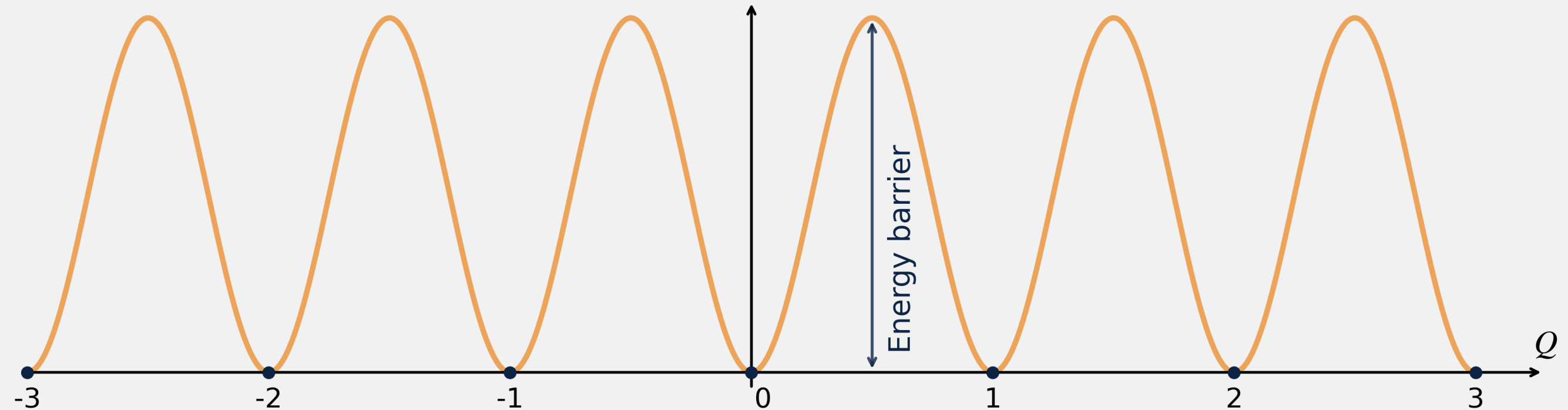


- Different  $Q$ -sectors correspond to **distinct vacua** with non-trivial topological structure

# Why QCD topology matters

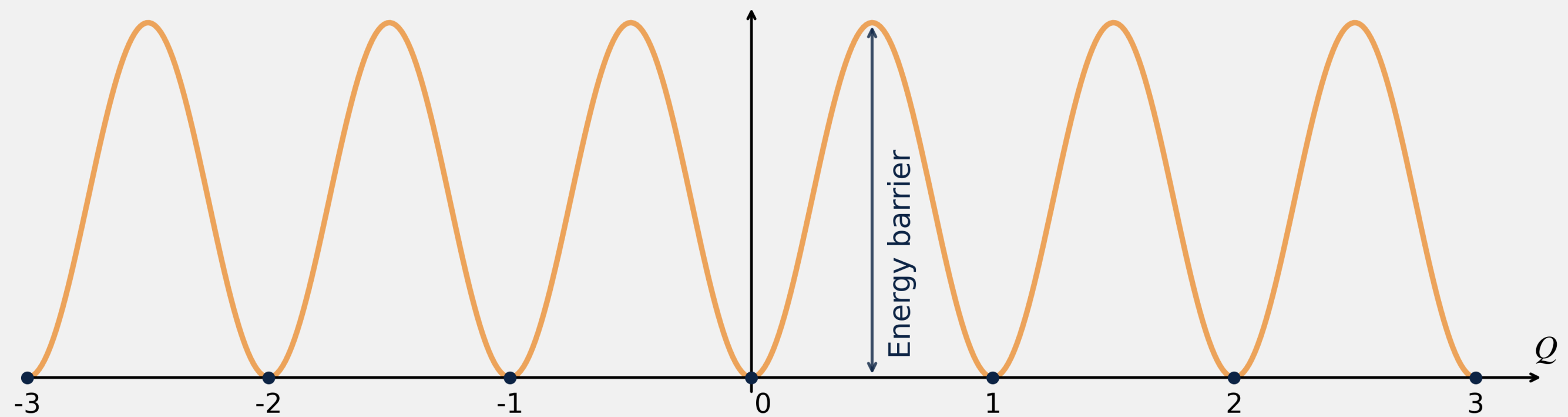


- Different  $Q$ -sectors correspond to **distinct vacua** with non-trivial topological structure



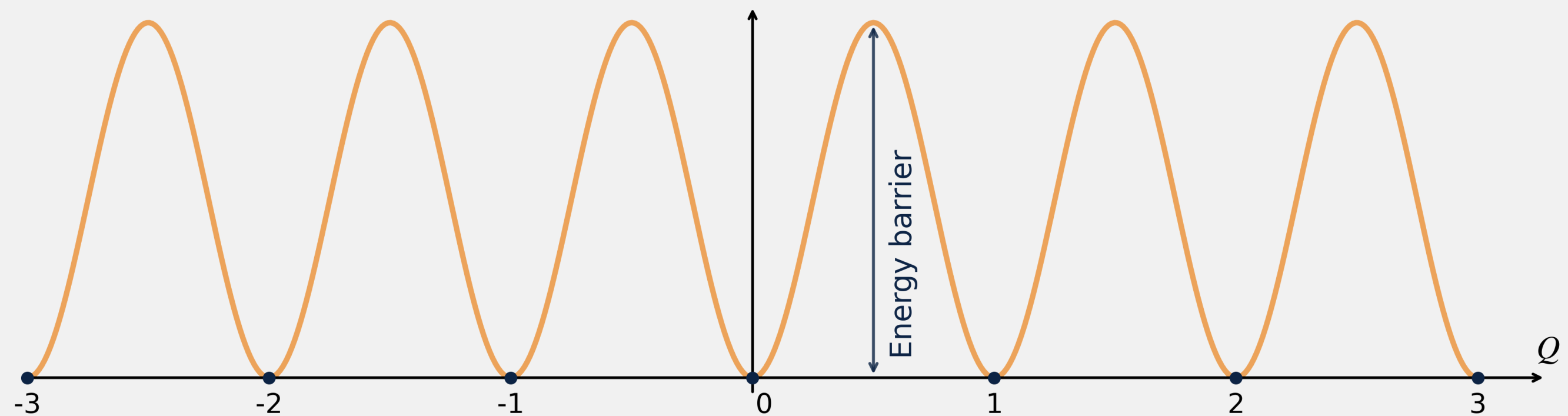
# Why QCD topology matters

- Different  $Q$ -sectors correspond to **distinct vacua** with non-trivial topological structure



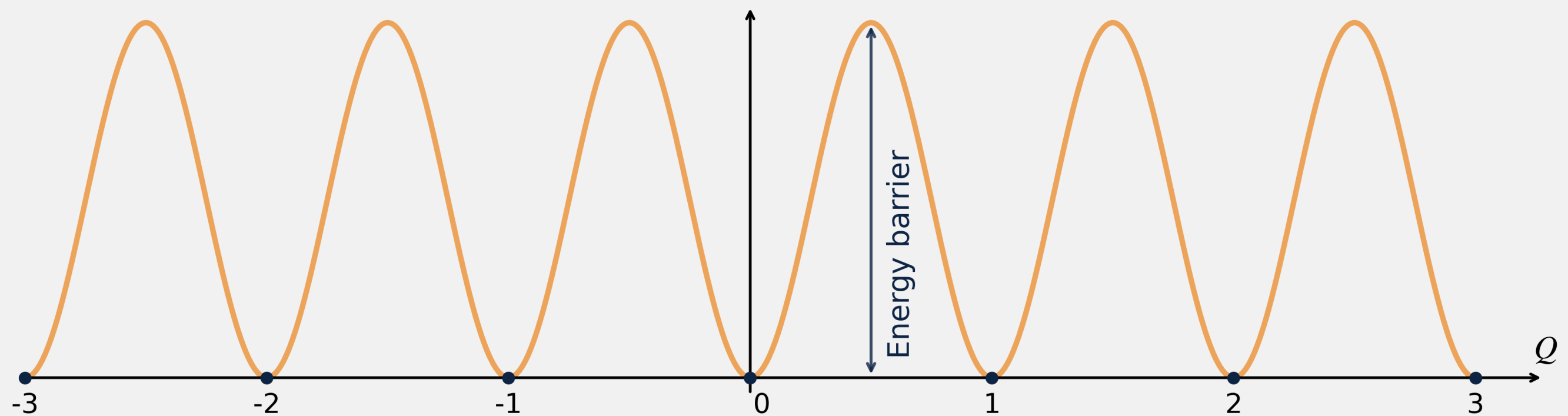
# Why QCD topology matters

- Different  $Q$ -sectors correspond to **distinct vacua** with non-trivial topological structure
- Topology underlies key QCD phenomena:
  - Witten–Veneziano mechanism  $\rightarrow m_{\eta'}$
  - Strong-CP problem ( $\theta$ -term)
  - Topological susceptibility in QCD thermodynamics



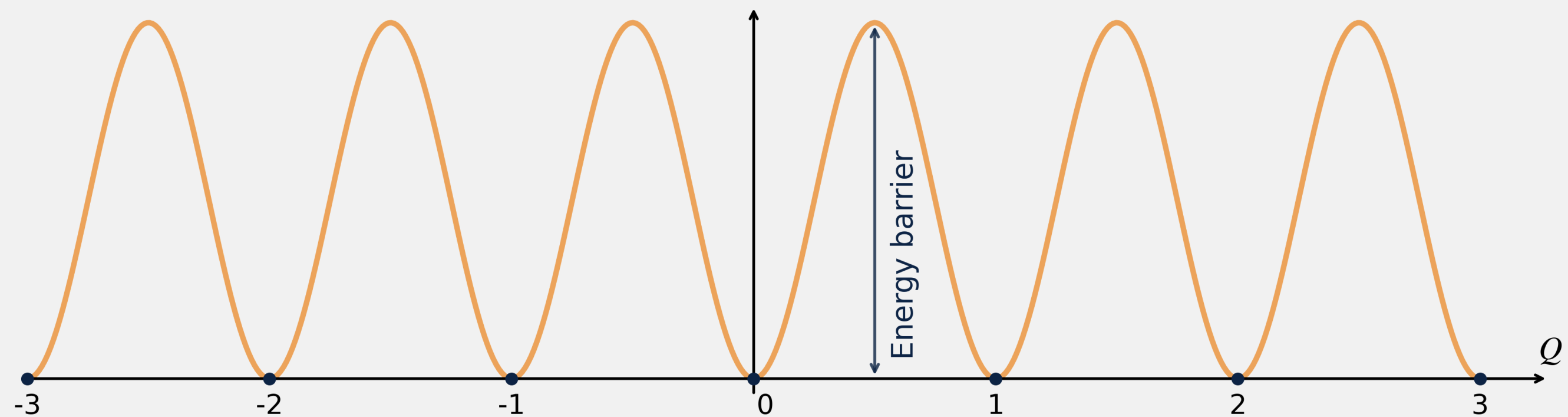
# Why QCD topology matters

- Different  $Q$ -sectors correspond to **distinct vacua** with non-trivial topological structure
- Topology underlies key QCD phenomena:
  - Witten–Veneziano mechanism  $\rightarrow m_{\eta'}$
  - Strong-CP problem ( $\theta$ -term)
  - Topological susceptibility in QCD thermodynamics



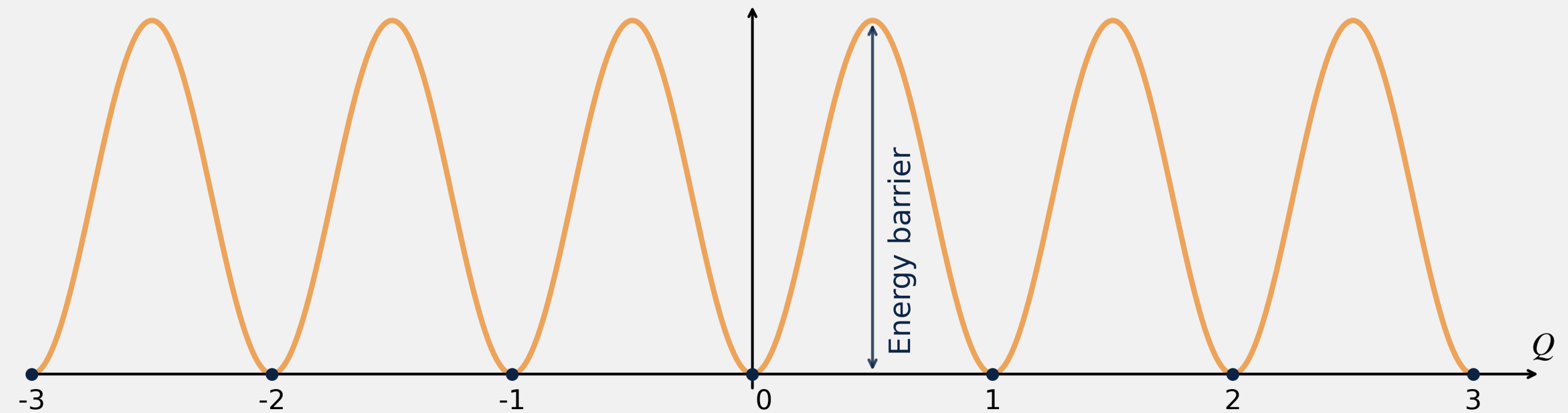
# Why QCD topology matters

- Different  $Q$ -sectors correspond to **distinct vacua** with non-trivial topological structure
- Topology underlies key QCD phenomena:
  - Witten–Veneziano mechanism  $\rightarrow m_{\eta'}$
  - Strong-CP problem ( $\theta$ -term)
  - Topological susceptibility in QCD thermodynamics



Understanding QCD topology is essential  
for **hadron physics** and **finite-temperature QCD**.

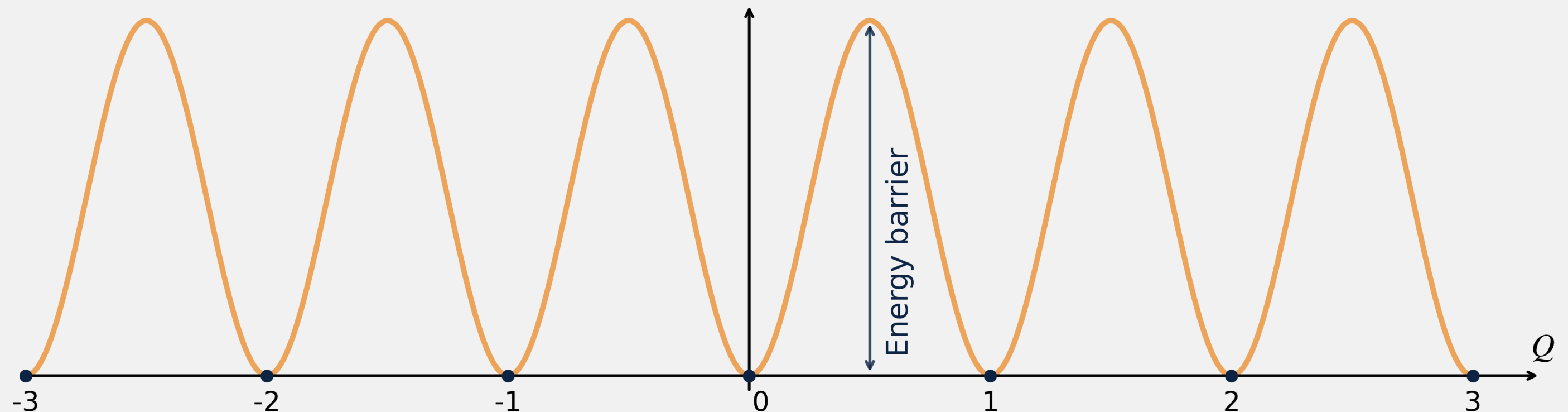
# The QCD Sphaleron Rate



# The QCD Sphaleron Rate

σφαλερός (*sphalerós*)

1. *slippery*, likely to make one stumble
2. ready to fall



# The QCD Sphaleron Rate

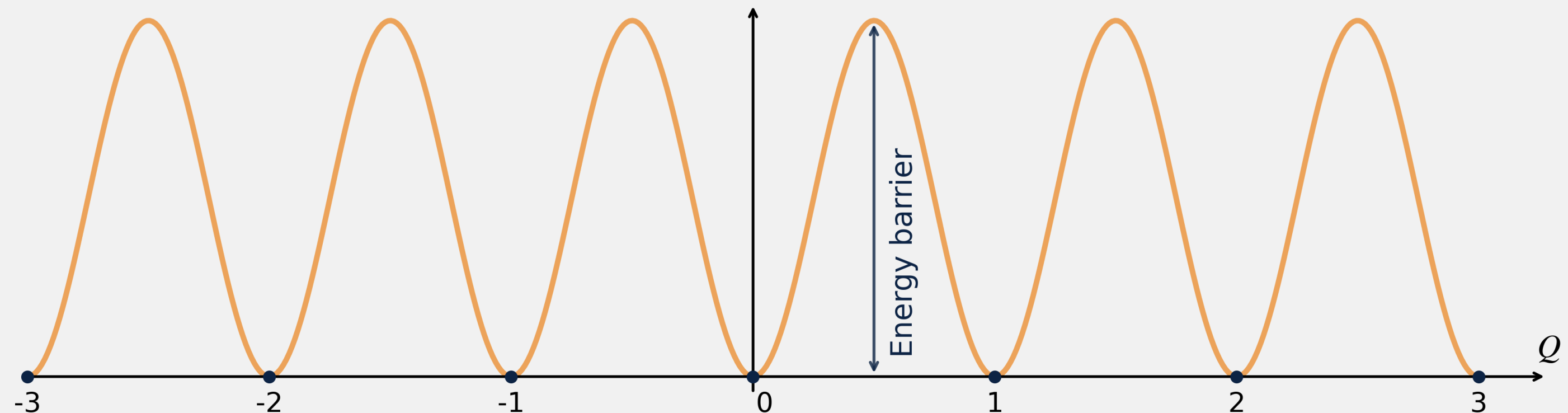


σφαλερός (*sphalerós*)

1. *slippery*, likely to make one stumble
2. ready to fall

Sphaleron Rate:

Rate of **real time** thermal transitions above sphaleron barriers separating topologically-inequivalent QCD vacua



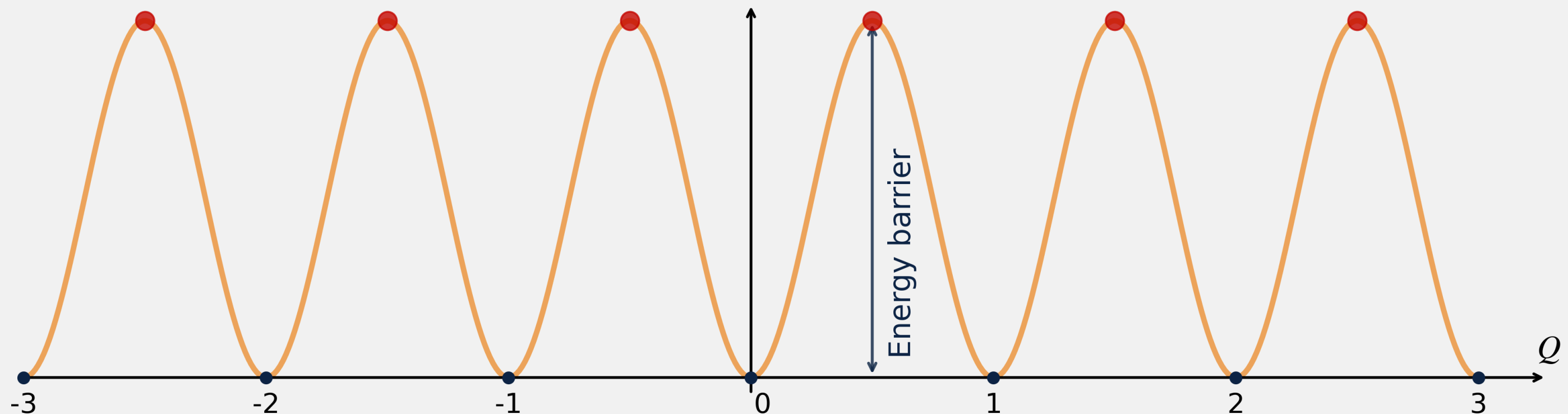
# The QCD Sphaleron Rate

σφαλερός (*sphalerós*)

1. *slippery*, likely to make one stumble
2. ready to fall

**Sphaleron Rate:**

Rate of **real time** thermal transitions above sphaleron barriers separating topologically-inequivalent QCD vacua



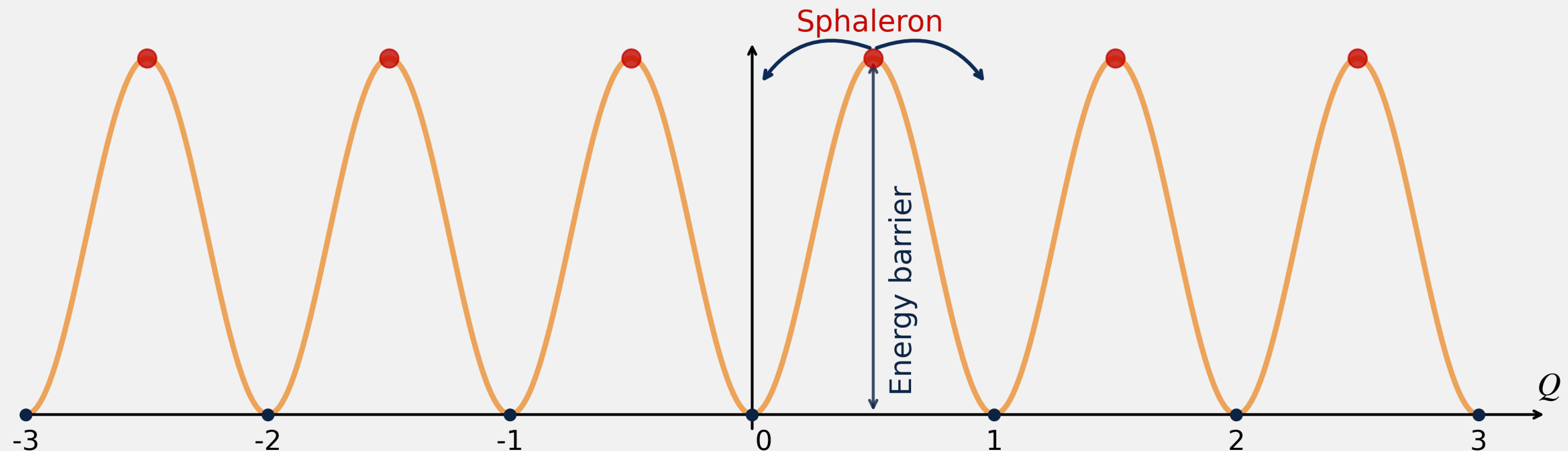
# The QCD Sphaleron Rate

σφαλερός (*sphalerós*)

1. *slippery*, likely to make one stumble
2. ready to fall

**Sphaleron Rate:**

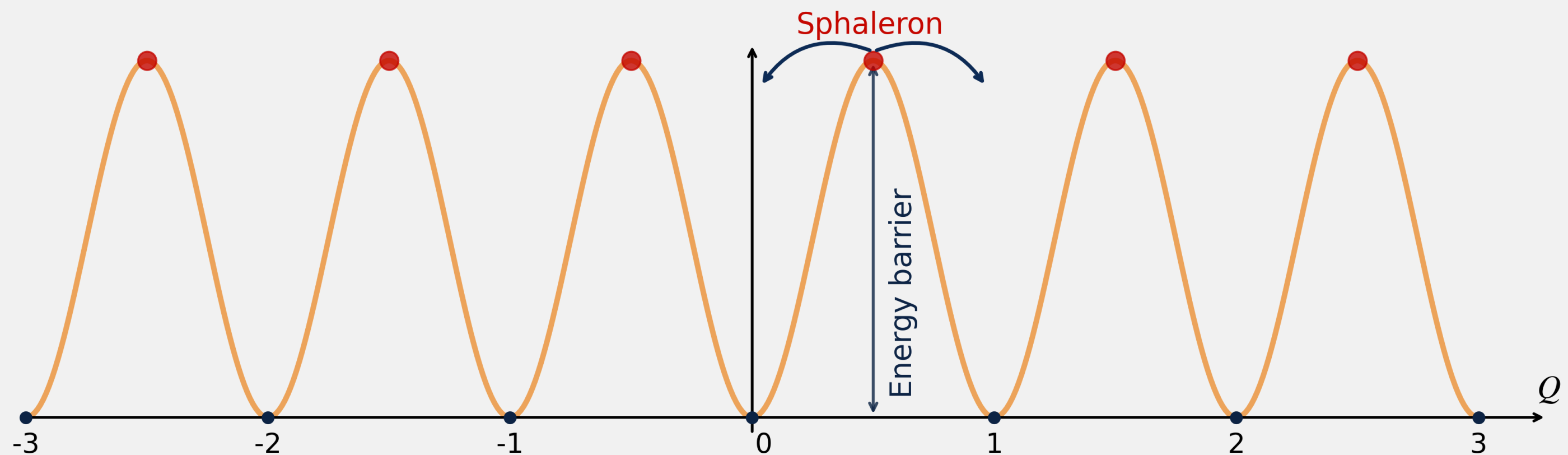
Rate of **real time** thermal transitions above sphaleron barriers separating topologically-inequivalent QCD vacua



# The QCD Sphaleron Rate

## Sphalerop Rate:

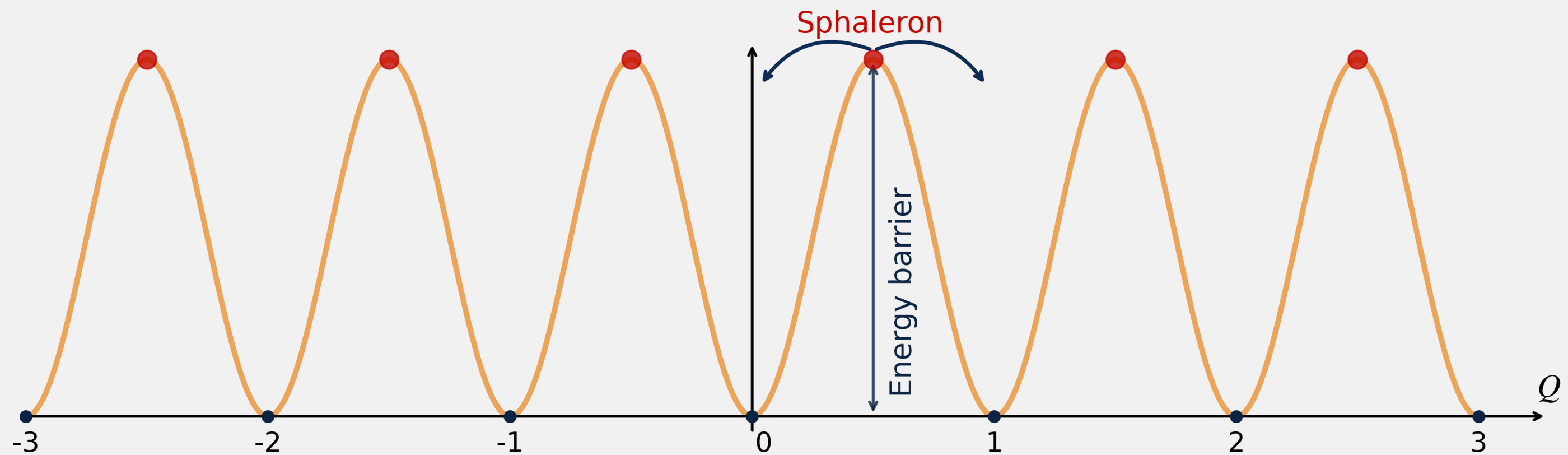
*Rate of **real time** thermal transitions above sphaleron barriers separating topologically-inequivalent QCD vacua*



# The QCD Sphaleron Rate

**Sphaleron Rate:**  
*Rate of **real time** thermal transitions above sphaleron barriers separating topologically-inequivalent QCD vacua*

$$\Gamma_{\text{sphal}} \equiv \int dt d^3x \langle q(\vec{x}, t) q(\vec{0}, 0) \rangle_T$$



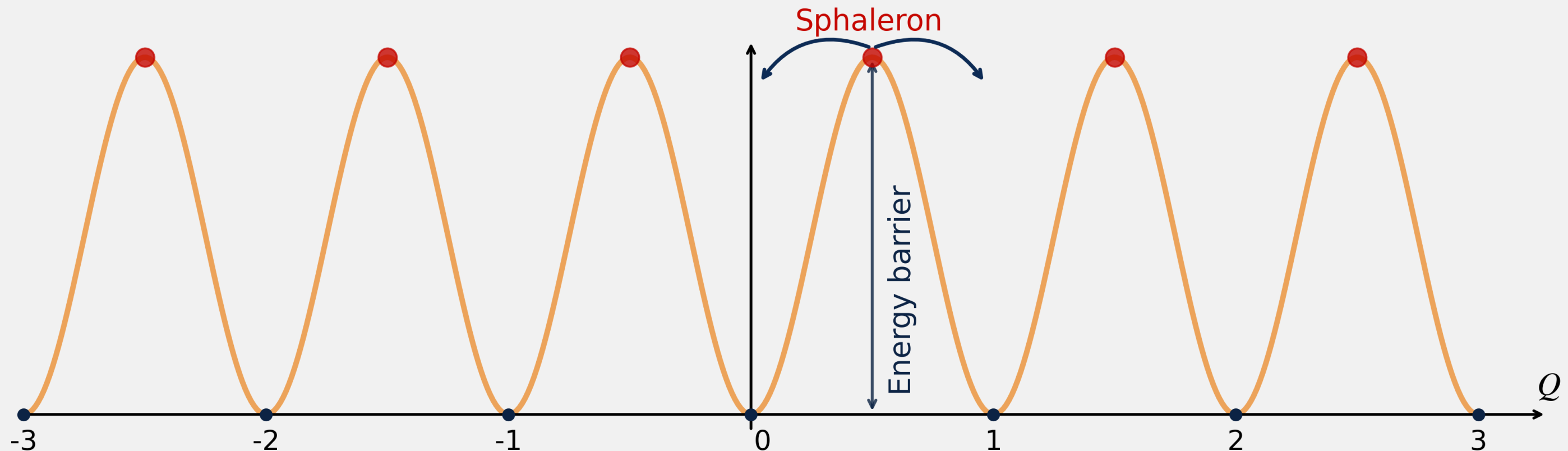
# The QCD Sphaleron Rate

## Sphaleron Rate:

Rate of **real time** thermal transitions above sphaleron barriers separating topologically-inequivalent QCD vacua

$$\Gamma_{\text{sphal}} \equiv \int dt d^3x \langle q(\vec{x}, t) q(\vec{0}, 0) \rangle_T$$

$$\langle \mathcal{O} \rangle_T = \frac{1}{\text{Tr}\{e^{-\mathcal{H}/T}\}} \text{Tr}\{e^{-\mathcal{H}/T} \mathcal{O}\}$$



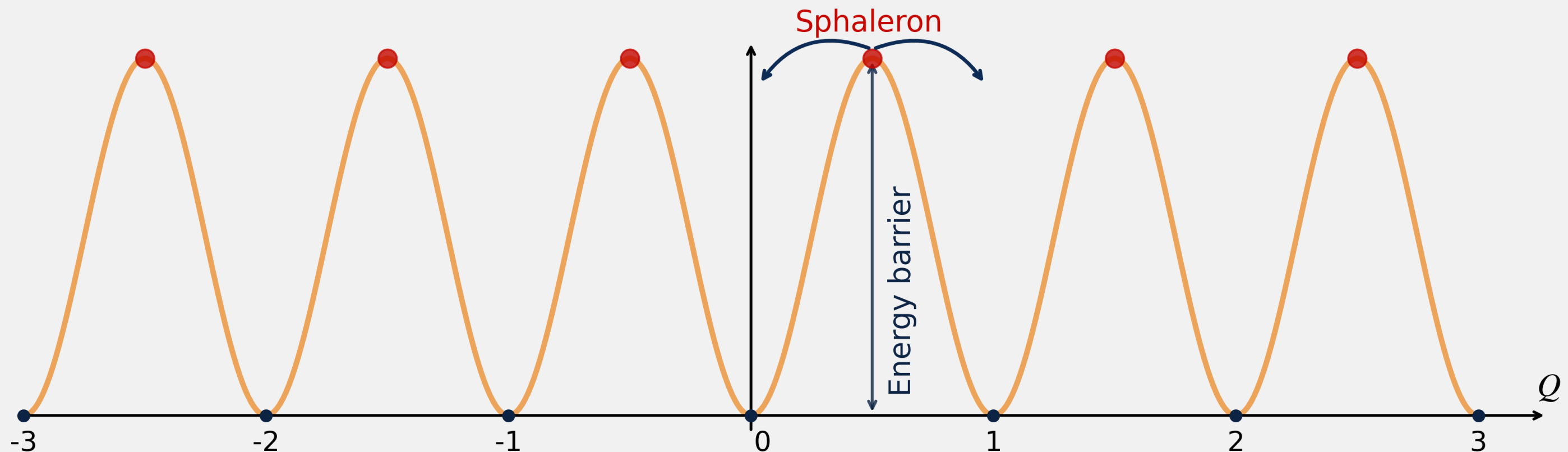
# The QCD Sphaleron Rate

## Sphaleron Rate:

Rate of **real time** thermal transitions above sphaleron barriers separating topologically-inequivalent QCD vacua

$$\Gamma_{\text{sphal}} \equiv \int dt d^3x \langle q(\vec{x}, t) q(\vec{0}, 0) \rangle_T$$

$$\langle \mathcal{O} \rangle_T = \frac{1}{\text{Tr}\{e^{-\mathcal{H}/T}\}} \text{Tr}\{e^{-\mathcal{H}/T} \mathcal{O}\}$$



**Why do we care?**

# 1) Chiral Magnetic Effect

Early stage of the Universe ( $10^{-6}$ s) → Quark-Gluon plasma

# 1) Chiral Magnetic Effect

Early stage of the Universe ( $10^{-6}$ s) → Quark-Gluon plasma

- **Helicity/Chirality** in the  $m_q \rightarrow 0$

$$\hat{h} = \frac{\vec{s} \cdot \vec{p}}{|\vec{p}|}$$

# 1) Chiral Magnetic Effect

Early stage of the Universe ( $10^{-6}$ s) → Quark-Gluon plasma



- **Helicity/Chirality** in the  $m_q \rightarrow 0$

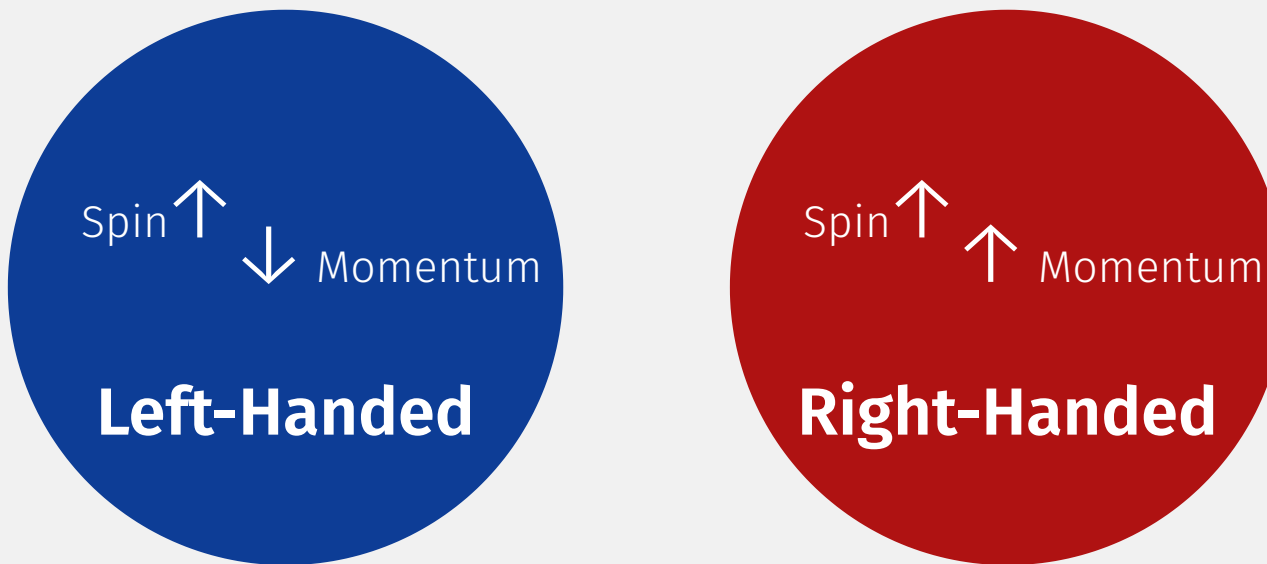
$$\hat{h} = \frac{\vec{s} \cdot \vec{p}}{|\vec{p}|}$$

- **Left-Handed (L):**  
Spin is *anti-parallel* to momentum.

$$\hat{h}\psi_L = -1\psi_L$$

# 1) Chiral Magnetic Effect

Early stage of the Universe ( $10^{-6}$ s) → Quark-Gluon plasma



- **Helicity/Chirality** in the  $m_q \rightarrow 0$

$$\hat{h} = \frac{\vec{s} \cdot \vec{p}}{|\vec{p}|}$$

- **Left-Handed (L):**  
Spin is *anti-parallel* to momentum.

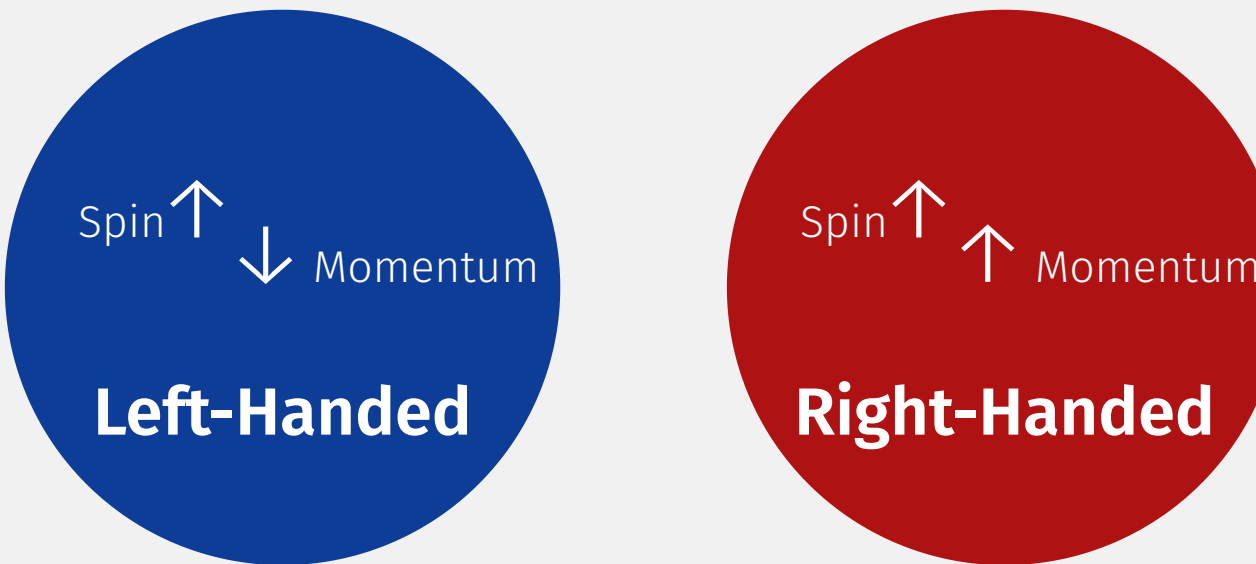
$$\hat{h}\psi_L = -1\psi_L$$

- **Right-Handed (R):**  
Spin is *parallel* to momentum.

$$\hat{h}\psi_R = +1\psi_R$$

# 1) Chiral Magnetic Effect

Early stage of the Universe ( $10^{-6}$ s) → Quark-Gluon plasma



- **Helicity/Chirality** in the  $m_q \rightarrow 0$

$$\hat{h} = \frac{\vec{s} \cdot \vec{p}}{|\vec{p}|}$$

- **Left-Handed (L):**  
Spin is *anti-parallel* to momentum.

$$\hat{h}\psi_L = -1\psi_L$$

- **Right-Handed (R):**  
Spin is *parallel* to momentum.

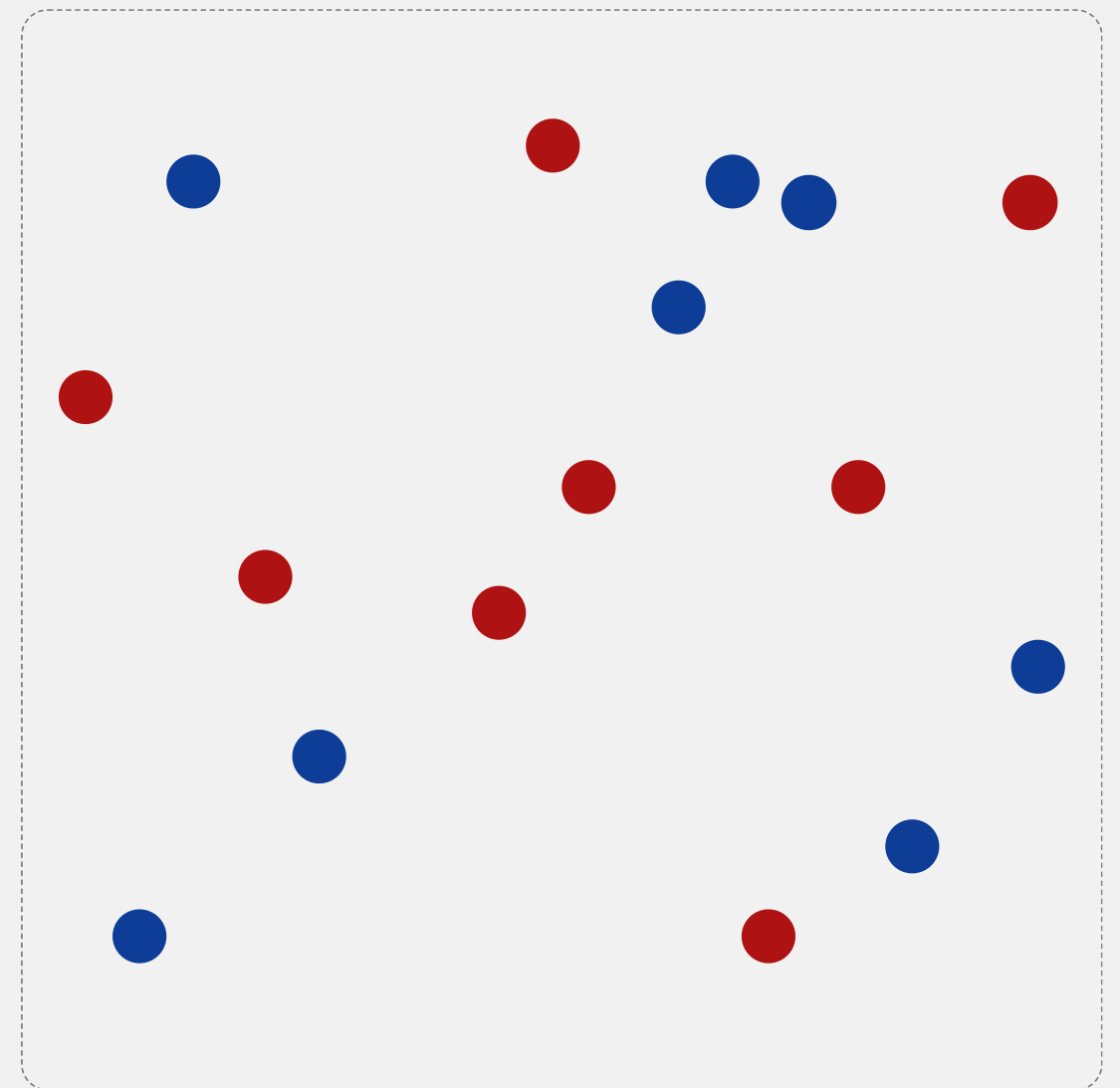
$$\hat{h}\psi_R = +1\psi_R$$

- **Why it matters:**  
Sphaleron transitions change topology ( $Q$ ), generating an axial charge density  $N_5$ :

$$\Delta N_5 = (N_L - N_R) \propto \Delta Q$$

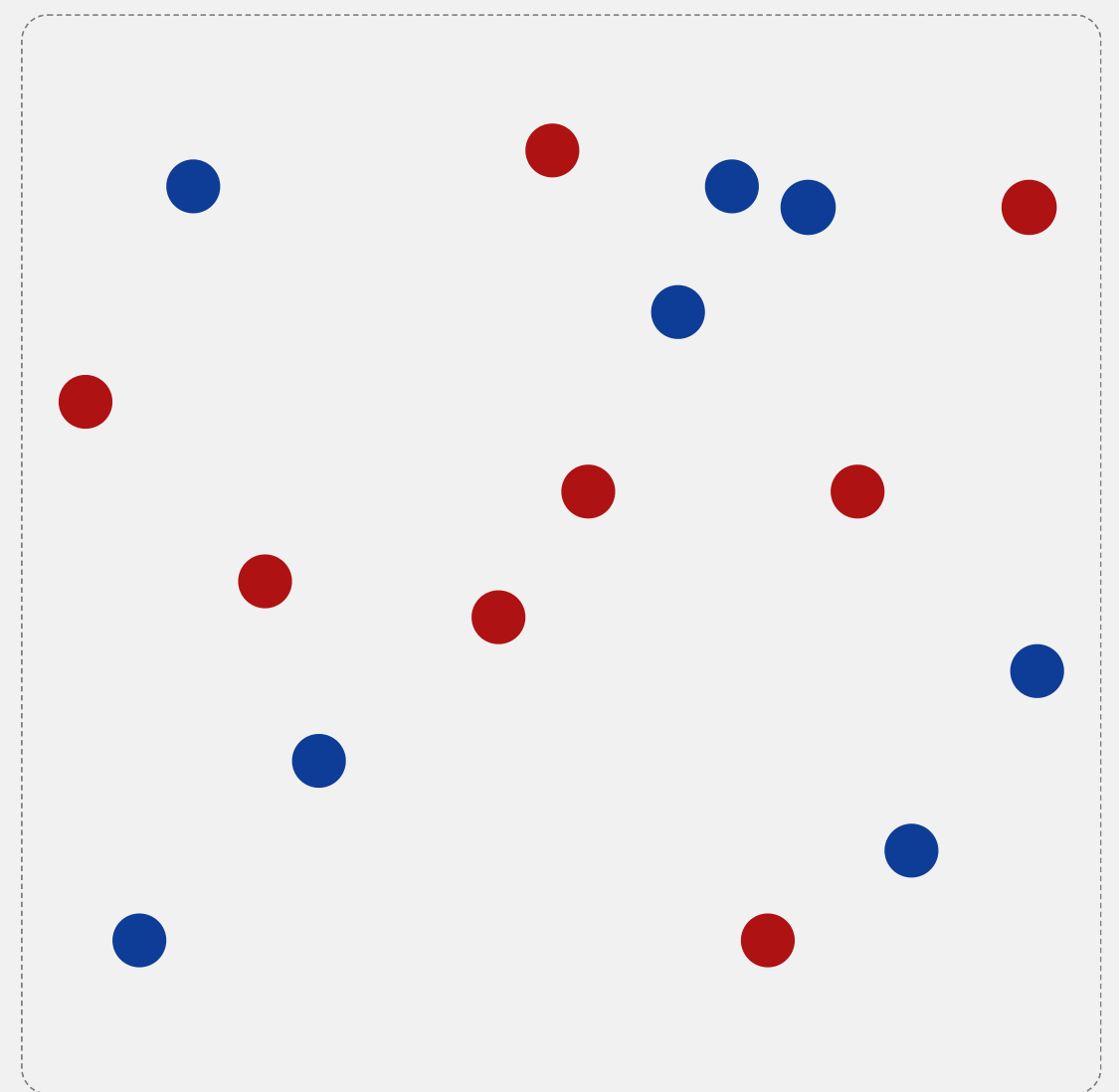
# 1) Chiral Magnetic Effect

Early stage of the Universe ( $10^{-6}$ s) → Quark-Gluon plasma



# 1) Chiral Magnetic Effect

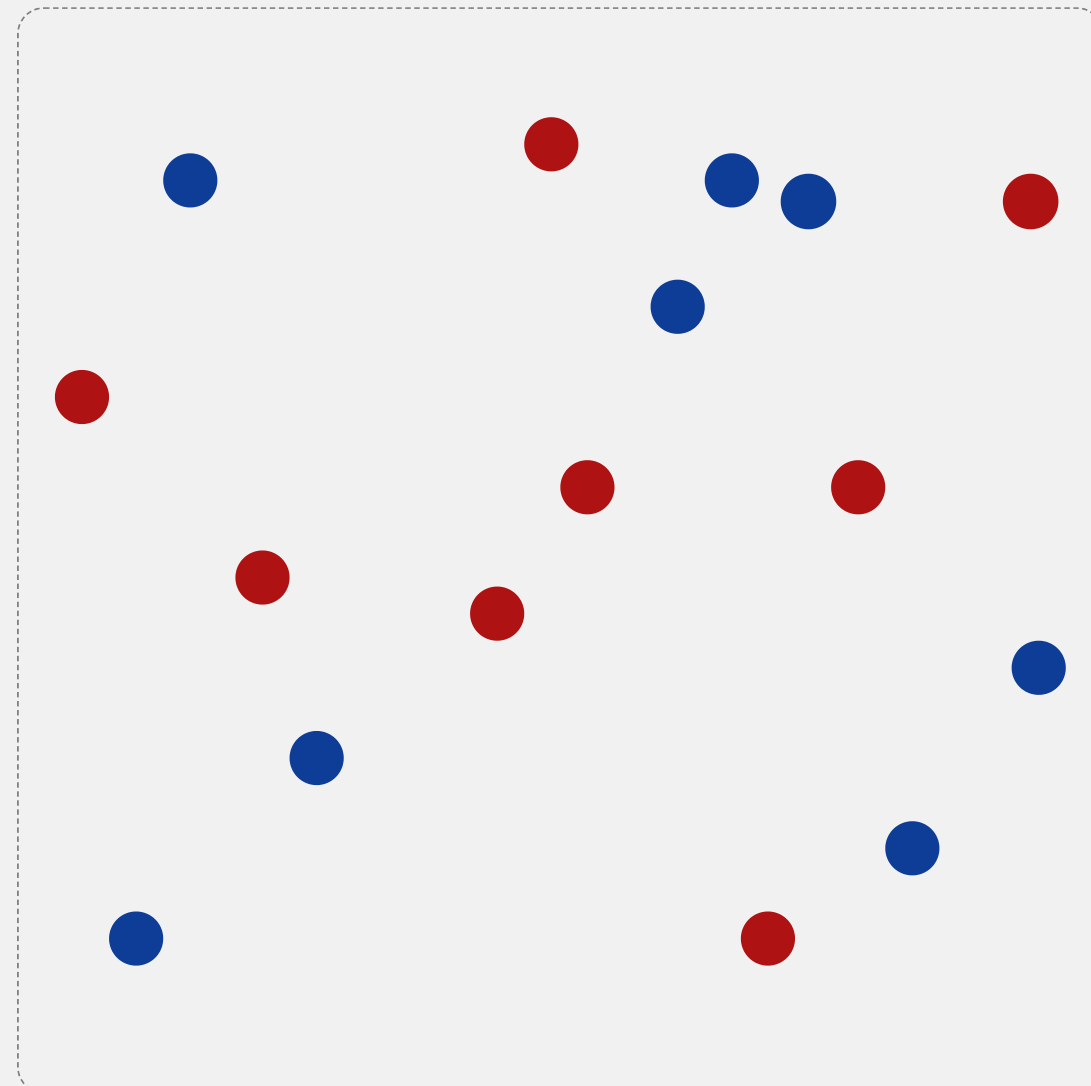
Early stage of the Universe ( $10^{-6}$ s) → Quark-Gluon plasma



1. At  $T \gg T_c$  ( $\sim 155$  MeV) → Deconfinement

# 1) Chiral Magnetic Effect

Early stage of the Universe ( $10^{-6}$ s) → Quark-Gluon plasma

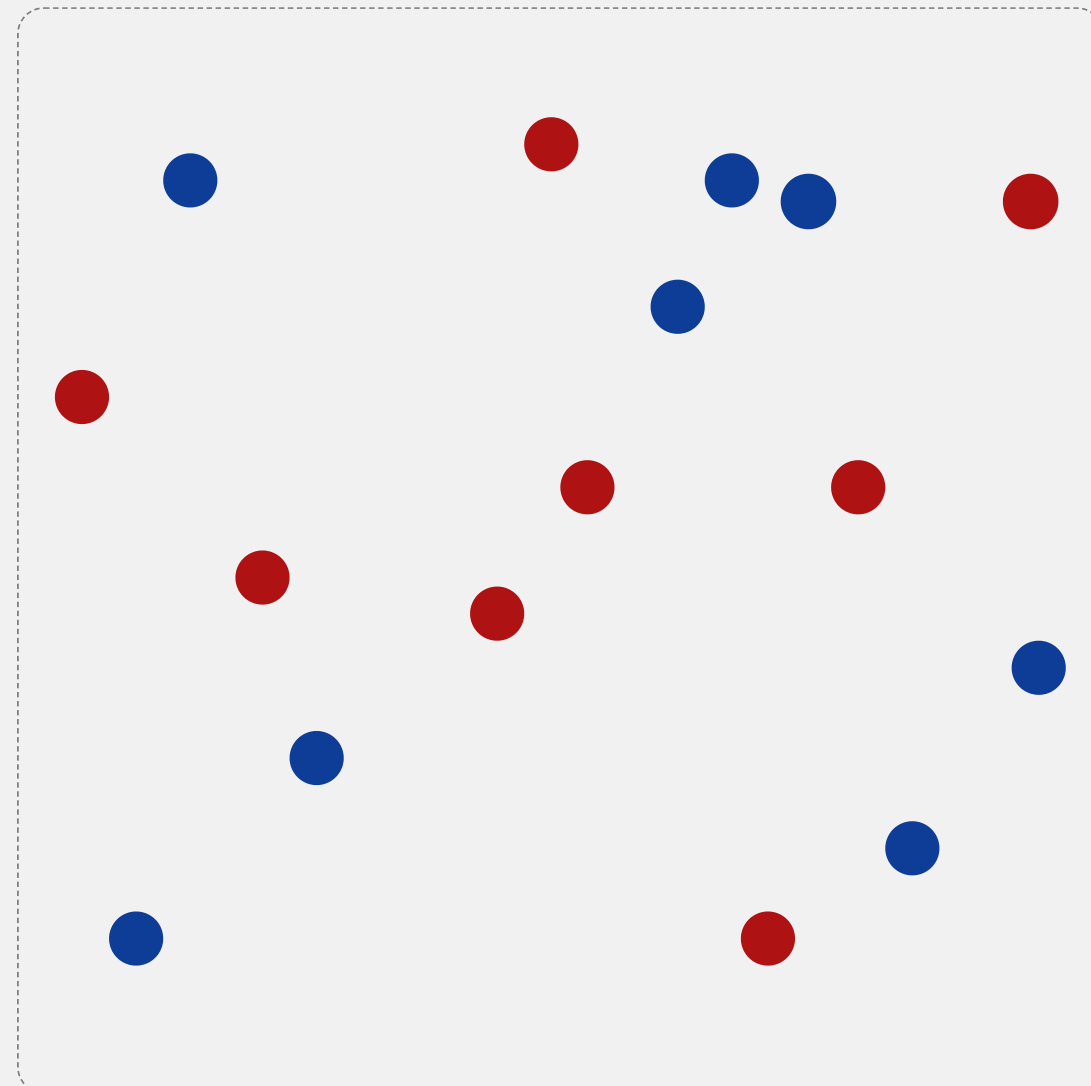


1. At  $T \gg T_c$  ( $\sim 155$  MeV) → **Deconfinement**
2. QCD interactions are vector-like  
preserve CP globally at  $\theta = 0$

$$\underbrace{\langle N_L - N_R \rangle}_{N_5} = 0$$

# 1) Chiral Magnetic Effect

Early stage of the Universe ( $10^{-6}$ s) → Quark-Gluon plasma



1. At  $T \gg T_c$  ( $\sim 155$  MeV) → **Deconfinement**

2. QCD interactions are vector-like  
preserve CP globally at  $\theta = 0$

$$\underbrace{\langle N_L - N_R \rangle}_{N_5} = 0$$

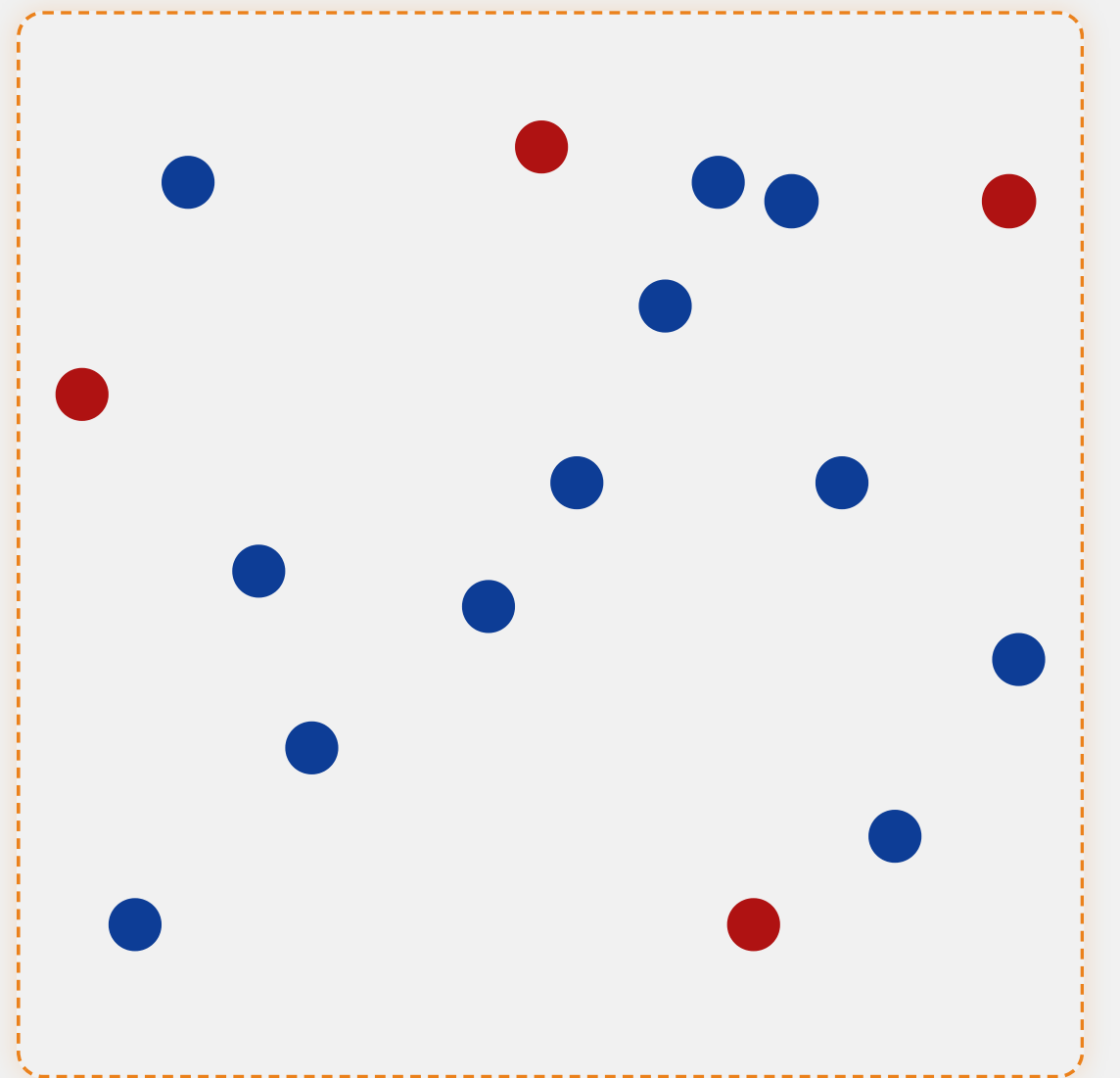
3. **But** topology can induce local imbalance:  
via Atiyah-Singer Index Theorem

$$Q = \int d^4x q(x) = N_L - N_R \equiv N_5$$

⇒ Fluctuations of  $Q$  drive  $N_5 \neq 0$

# 1) Chiral Magnetic Effect

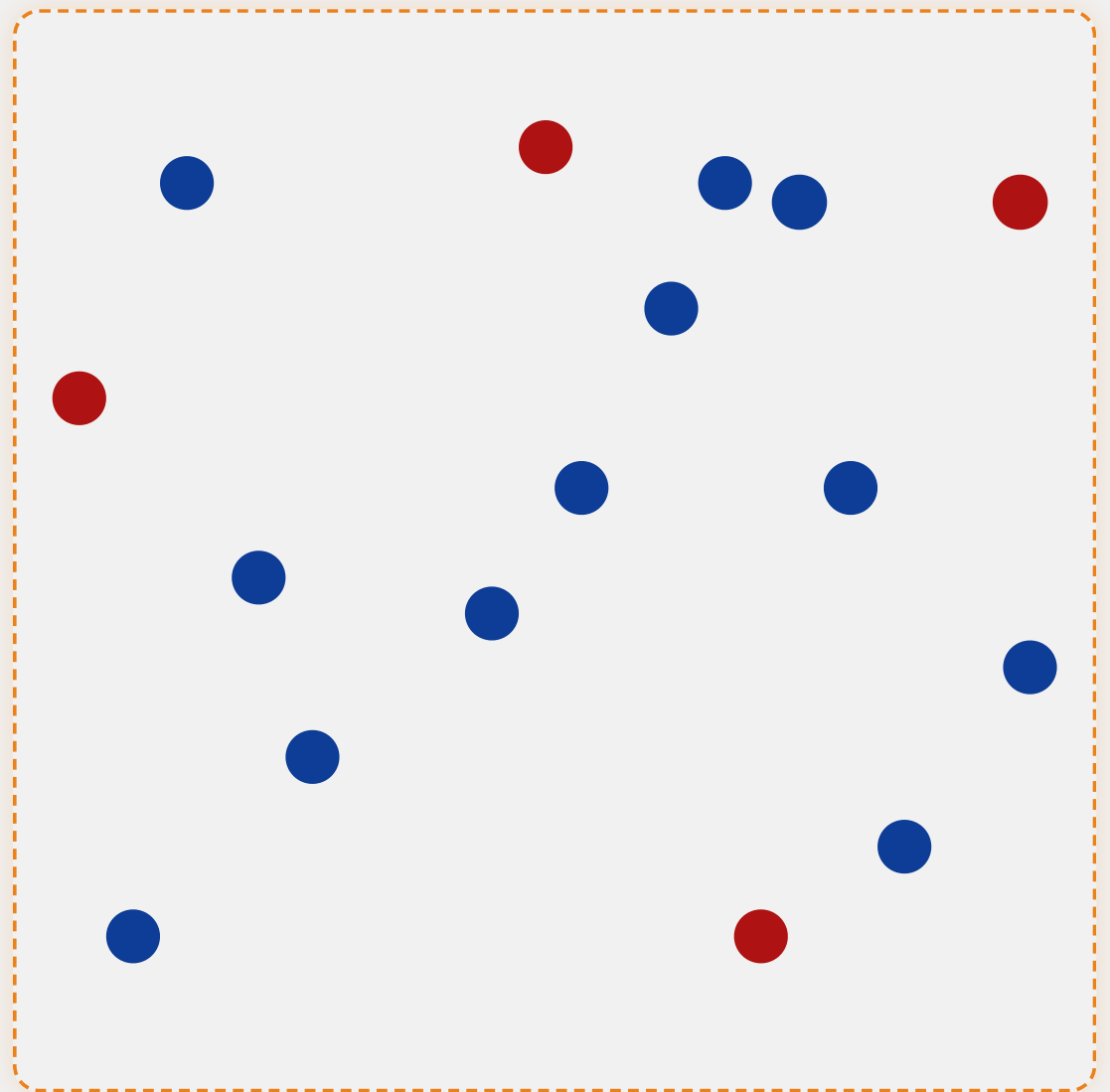
Sphaleron Transition occurs! ( $N_R \rightarrow N_L$ )



# 1) Chiral Magnetic Effect

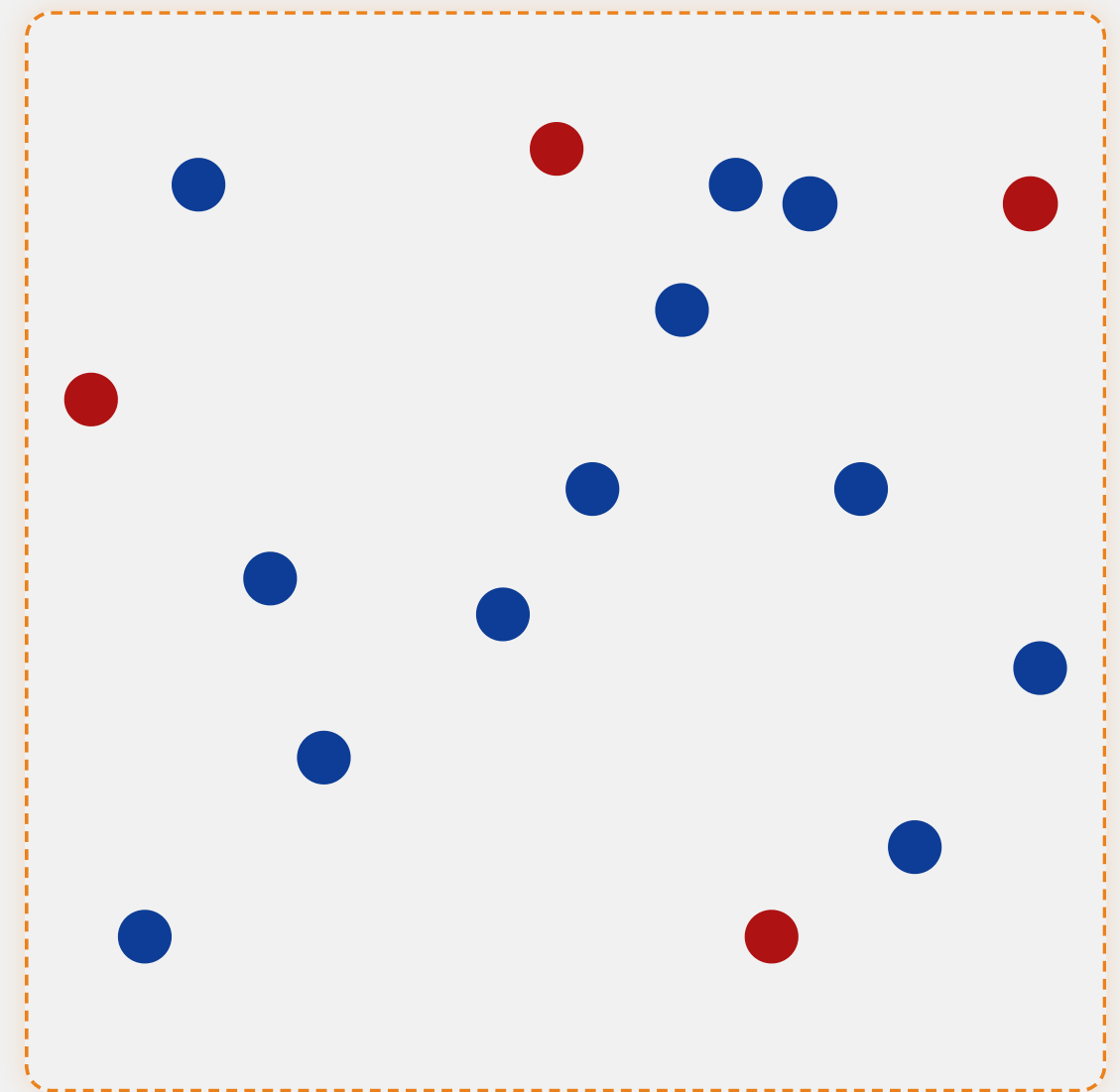
Sphaleron Transition occurs! ( $N_R \rightarrow N_L$ )

Finite Sphaleron Rate ( $\Gamma_{\text{sphal}} \neq 0$ )



# 1) Chiral Magnetic Effect

Sphaleron Transition occurs! ( $N_R \rightarrow N_L$ )

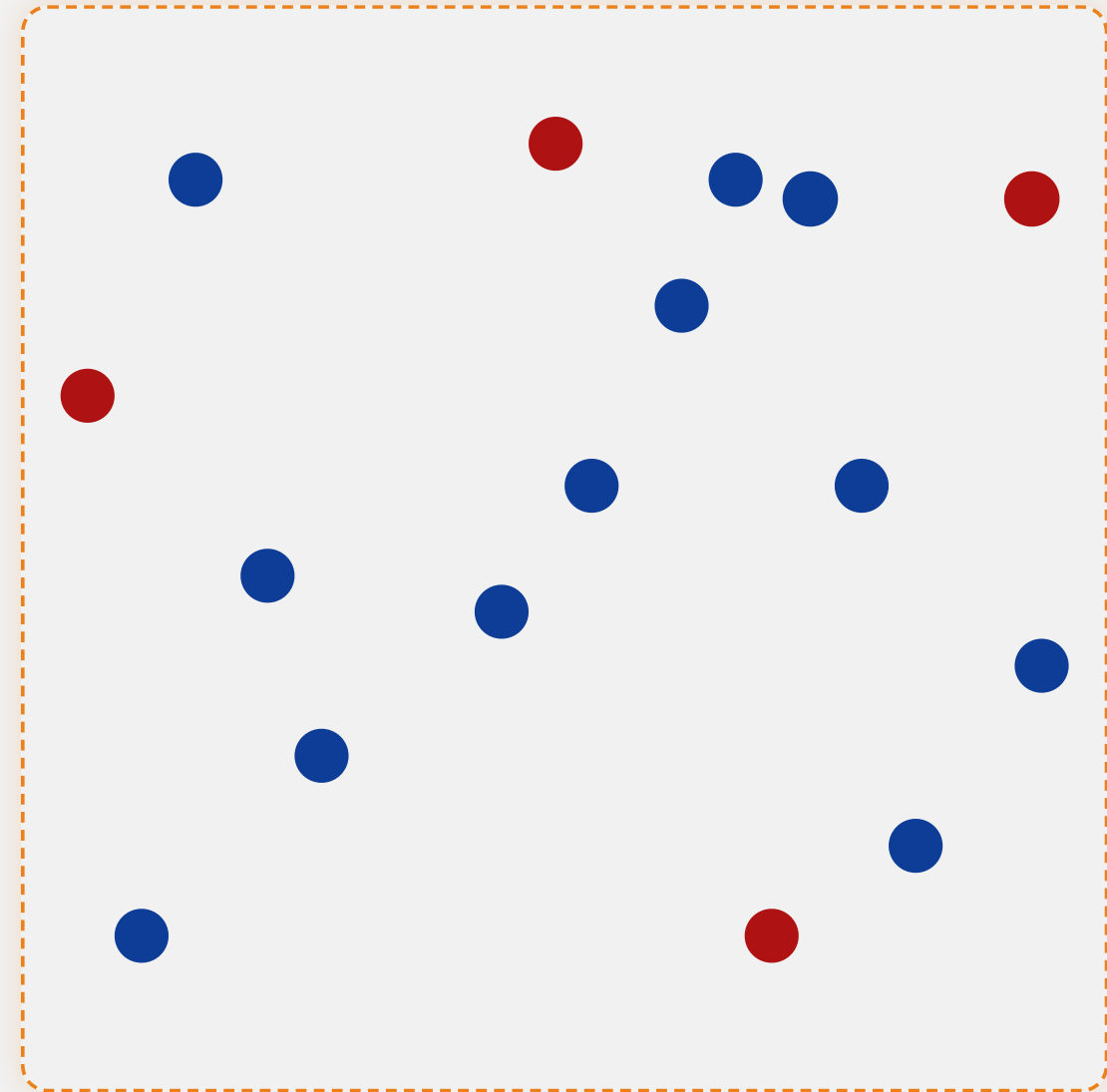


Finite Sphaleron Rate ( $\Gamma_{\text{sphal}} \neq 0$ )



# 1) Chiral Magnetic Effect

Sphaleron Transition occurs! ( $N_R \rightarrow N_L$ )



**Finite Sphaleron Rate ( $\Gamma_{\text{sphal}} \neq 0$ )**

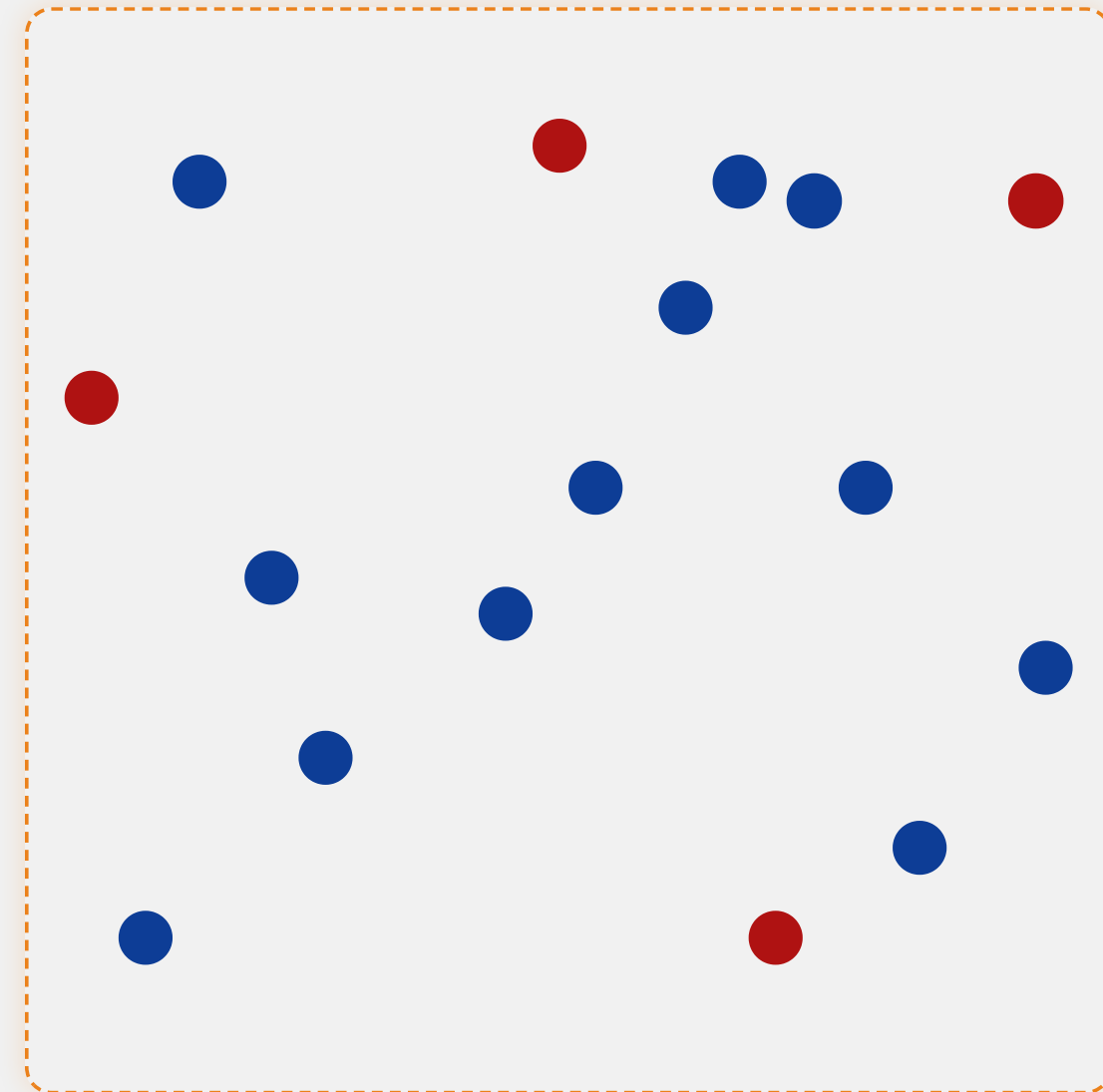


**Barrier Crossing:**

Thermal fluctuations overcome the energy barrier separating distinct topological vacua.

# 1) Chiral Magnetic Effect

Sphaleron Transition occurs! ( $N_R \rightarrow N_L$ )



**Finite Sphaleron Rate** ( $\Gamma_{\text{sphal}} \neq 0$ )



**Barrier Crossing:**

Thermal fluctuations overcome the energy barrier separating distinct topological vacua.

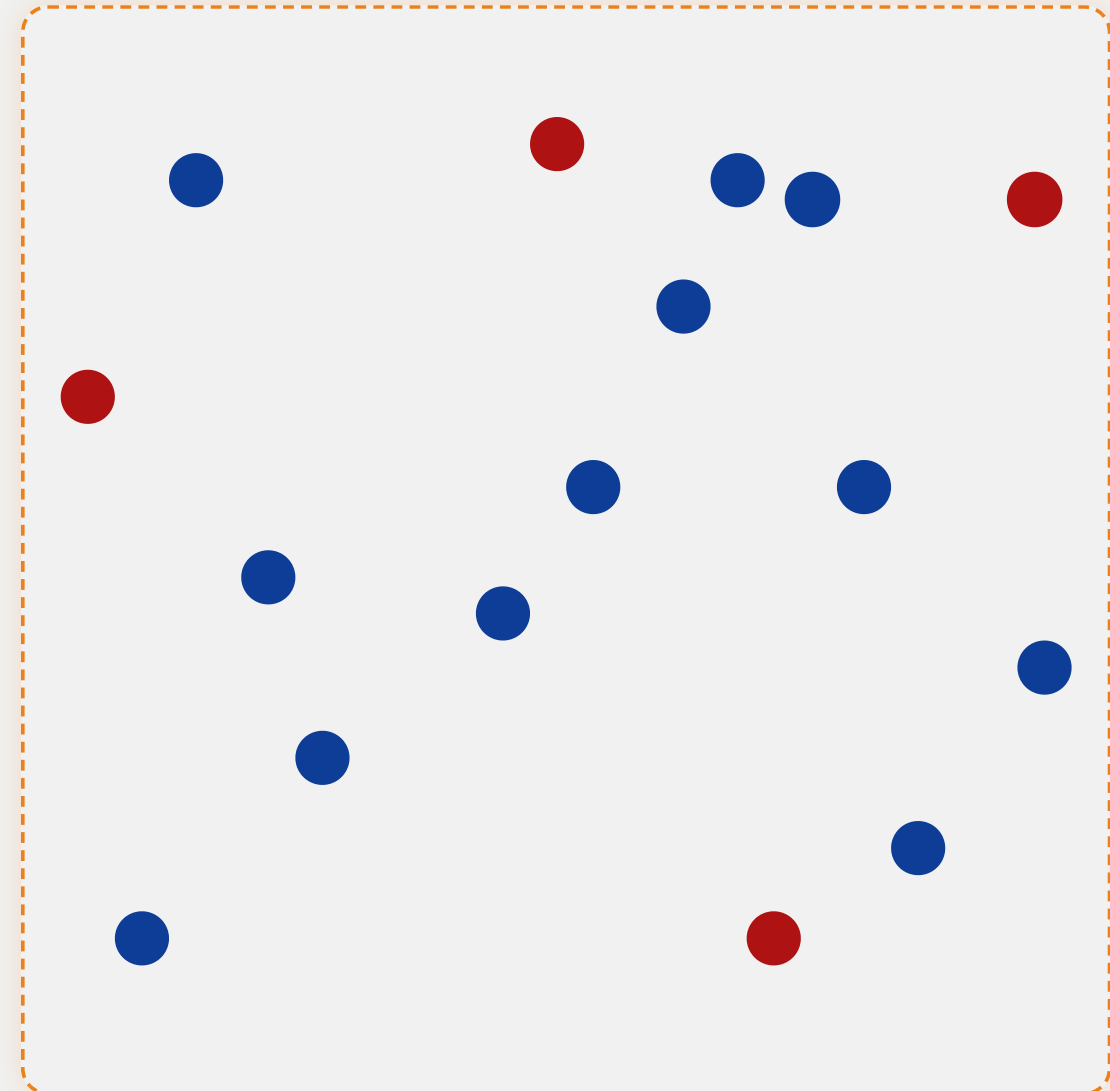
**The Anomaly:**

Transitions change  $Q$ , driving axial charge via:

$$\partial_\mu j_5^\mu = 2N_f \underbrace{\frac{g^2}{32\pi^2} G_{\mu\nu} \tilde{G}^{\mu\nu}}_{q(x)}$$

# 1) Chiral Magnetic Effect

Sphaleron Transition occurs! ( $N_R \rightarrow N_L$ )



**Finite Sphaleron Rate** ( $\Gamma_{\text{sphal}} \neq 0$ )



**Barrier Crossing:**

Thermal fluctuations overcome the energy barrier separating distinct topological vacua.

**The Anomaly:**

Transitions change  $Q$ , driving axial charge via:

$$\partial_\mu j_5^\mu = 2N_f \underbrace{\frac{g^2}{32\pi^2} G_{\mu\nu} \tilde{G}^{\mu\nu}}_{q(x)}$$

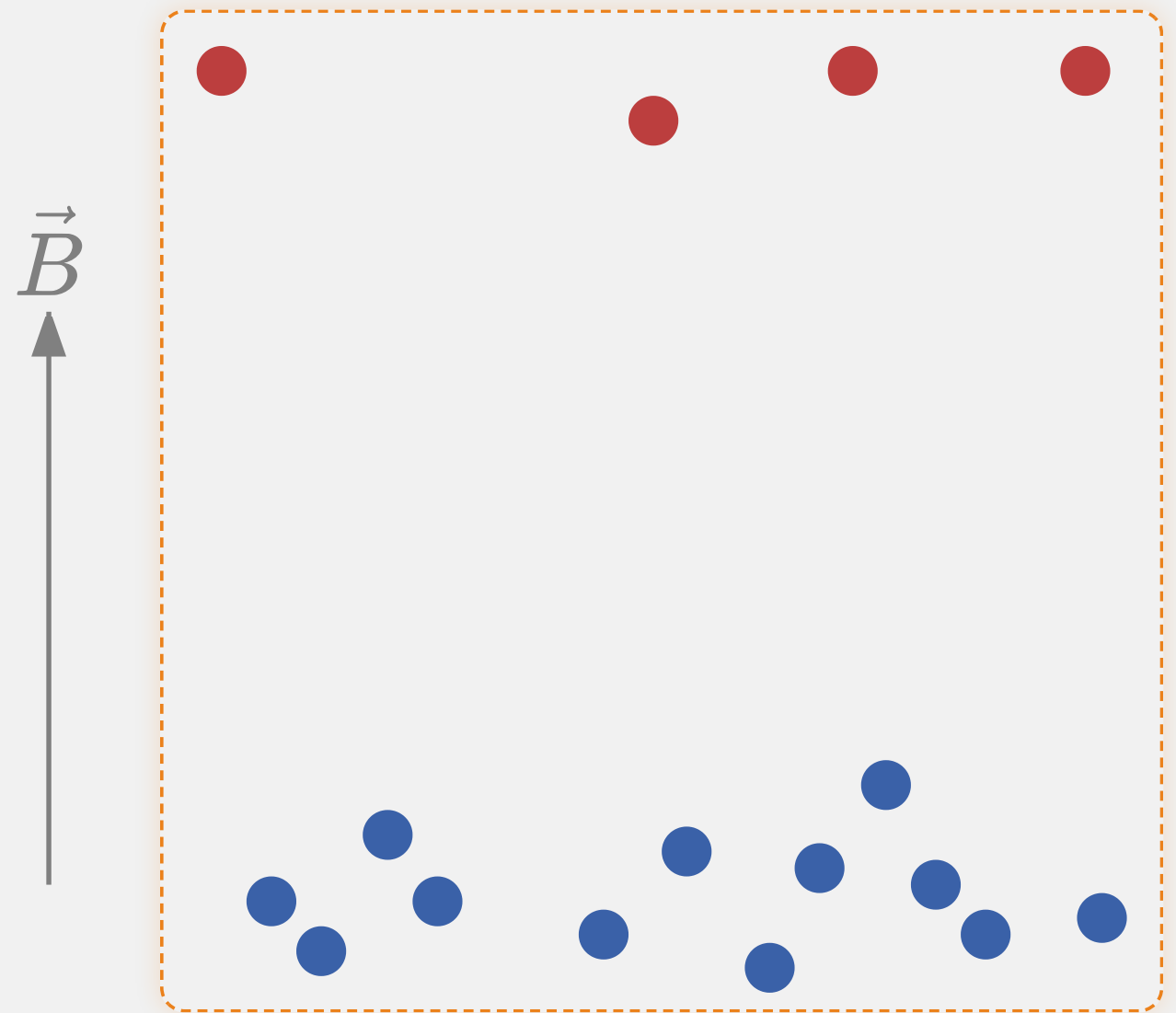
**Result:**

Creation of local **Chiral Imbalance**:

$$\Delta Q \neq 0 \Rightarrow \Delta N_5 \neq 0 \Rightarrow \text{e. g. } N_L > N_R$$

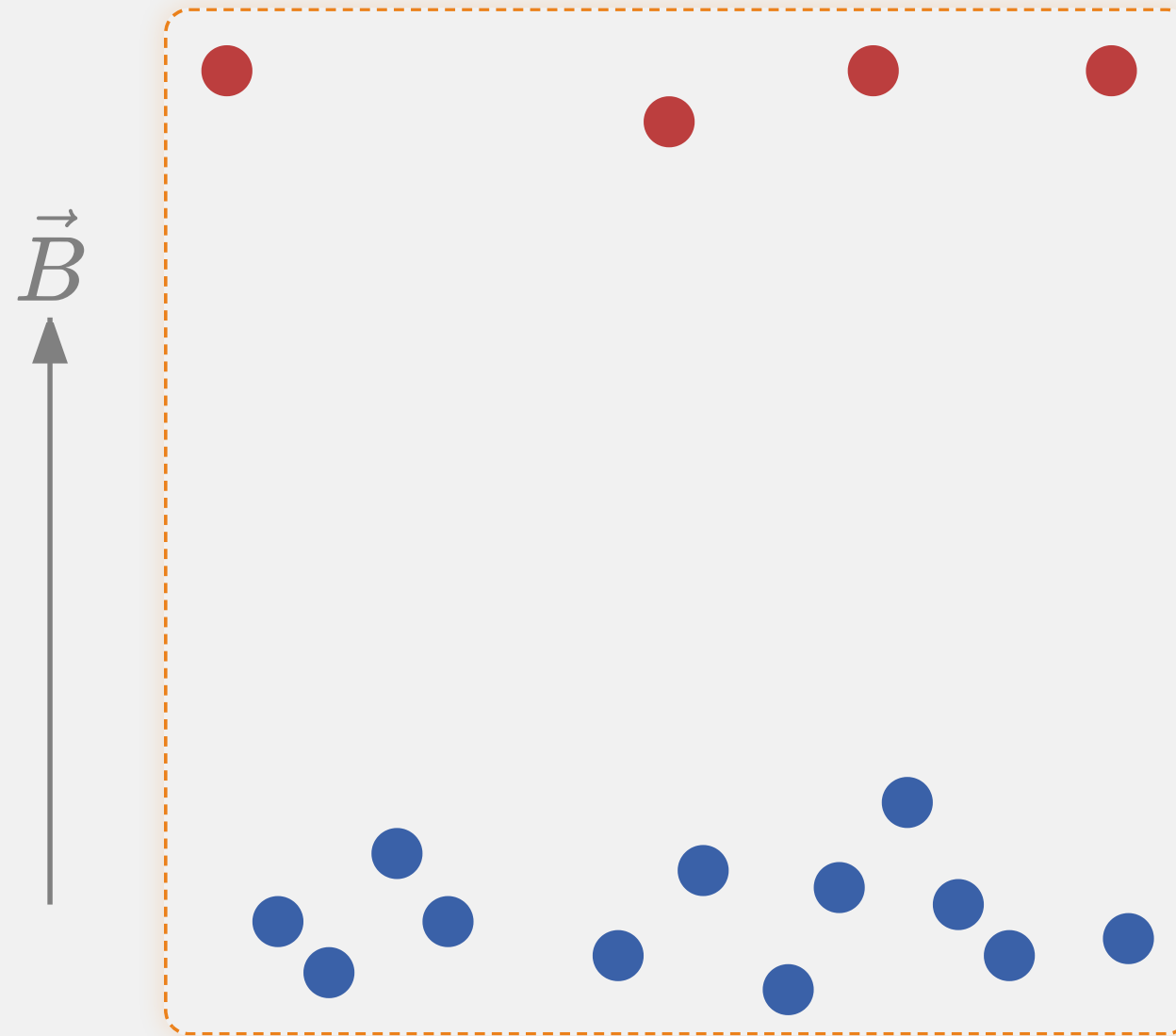
# 1) Chiral Magnetic Effect

Magnetic Field  $\vec{B}$  + Imbalance  $\rightarrow$  Electric Current  $\vec{J}$



# 1) Chiral Magnetic Effect

Magnetic Field  $\vec{B}$  + Imbalance  $\rightarrow$  Electric Current  $\vec{J}$

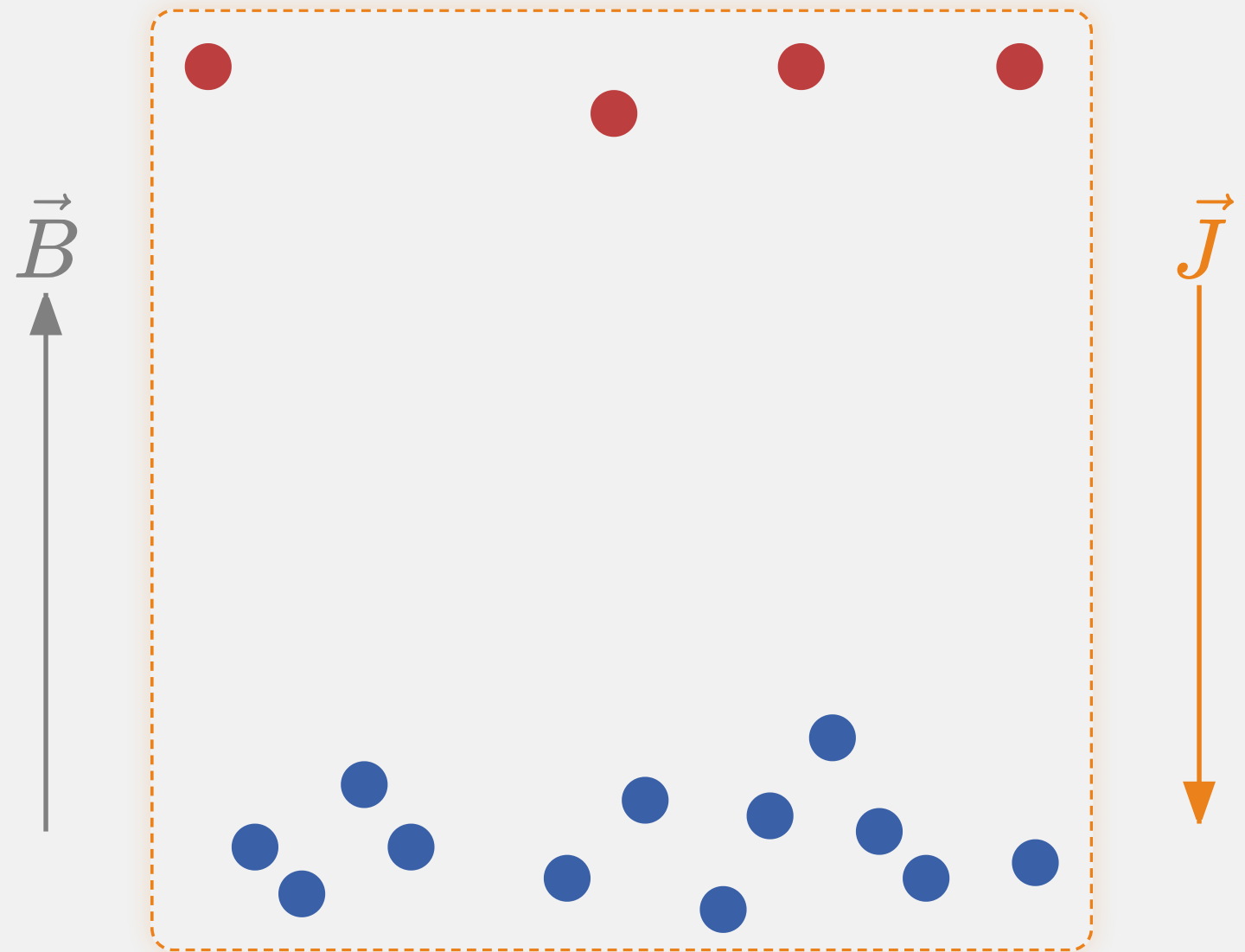


- $\vec{B}$  aligns all spins ( $\downarrow$ )
- **Left-handed:**  $\vec{p} \parallel -\vec{s} \rightarrow$  move **Down**
- **Right-handed:**  $\vec{p} \parallel \vec{s} \rightarrow$  move **Up**

Net motion is dominated (e.g.) by **Left-handed** fermions

# 1) Chiral Magnetic Effect

Magnetic Field  $\vec{B}$  + Imbalance  $\rightarrow$  Electric Current  $\vec{J}$



- $\vec{B}$  aligns all spins ( $\downarrow$ )
- **Left-handed:**  $\vec{p} \parallel -\vec{s} \rightarrow$  move **Down**
- **Right-handed:**  $\vec{p} \parallel \vec{s} \rightarrow$  move **Up**

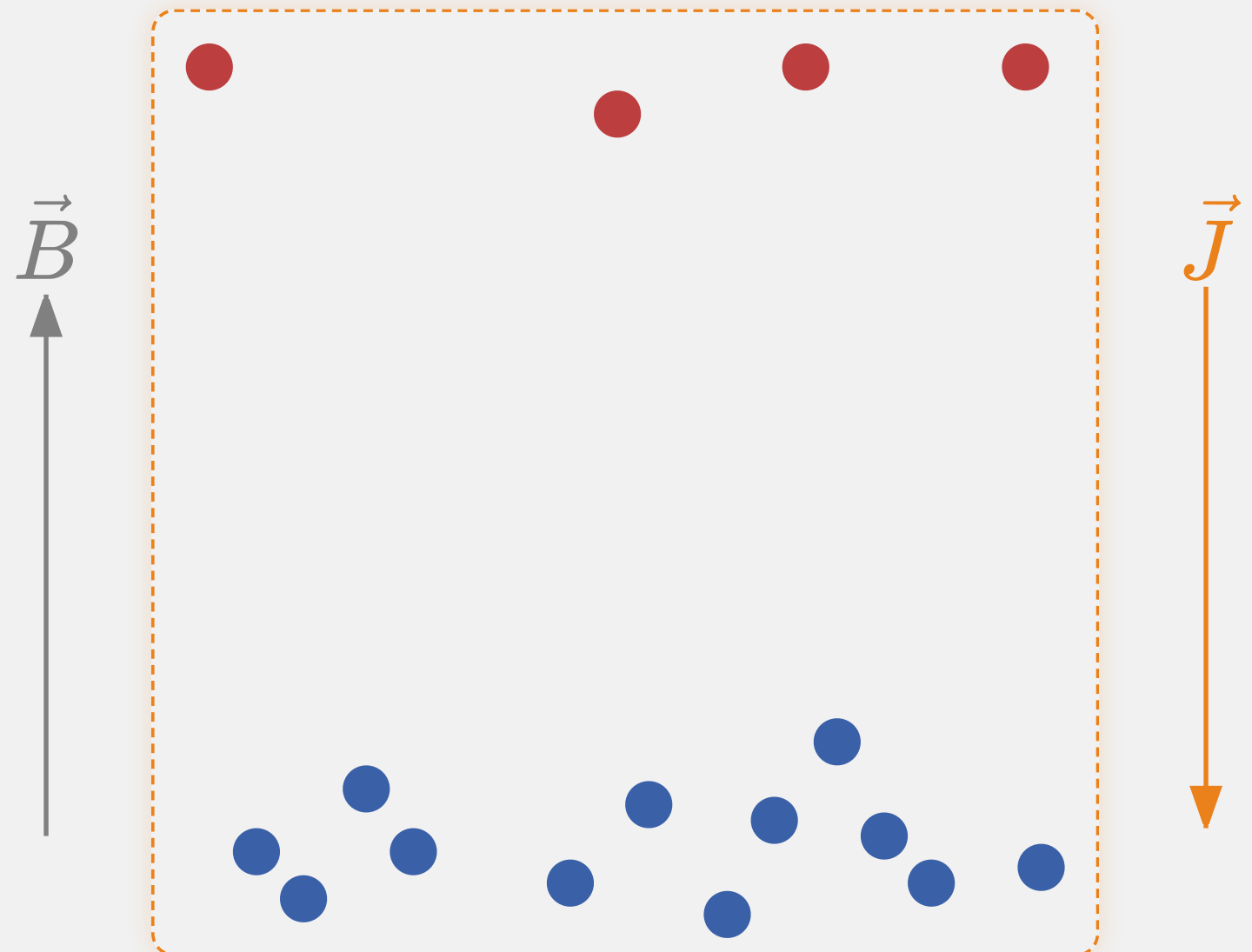
Net motion is dominated (e.g.) by **Left-handed** fermions

A chiral imbalance ( $N_5 \neq 0$ ) together with  $\vec{B}$  produces a CME current **opposite** to  $\vec{B}$ :

$$\vec{J}_{\text{CME}} \propto N_5 \vec{B}$$

# 1) Chiral Magnetic Effect

Magnetic Field  $\vec{B}$  + Imbalance  $\rightarrow$  Electric Current  $\vec{J}$



- $\vec{B}$  aligns all spins ( $\downarrow$ )
- **Left-handed:**  $\vec{p} \parallel -\vec{s} \rightarrow$  move **Down**
- **Right-handed:**  $\vec{p} \parallel \vec{s} \rightarrow$  move **Up**

Net motion is dominated (e.g.) by **Left-handed** fermions

A chiral imbalance ( $N_5 \neq 0$ ) together with  $\vec{B}$  produces a CME current **opposite** to  $\vec{B}$ :

$$\vec{J}_{\text{CME}} \propto N_5 \vec{B}$$

*Intense ongoing experimental efforts  
CME currents at heavy-ion colliders RHIC and LHC*

## 2) Axion Cosmology & Sphalerons



## 2) Axion Cosmology & Sphalerons

### The Axion:

A pseudo-Goldstone boson proposed to solve the **Strong CP Problem** and also a leading **Dark Matter** candidate.

## 2) Axion Cosmology & Sphalerons

### The Axion:

A pseudo-Goldstone boson proposed to solve the **Strong CP Problem** and also a leading **Dark Matter** candidate.

### Thermal Production:

Early Universe ( $T \sim T_c \div 10T_c$ ) → axions produced via hadronic scatterings:

$$\pi + \pi \rightarrow a + a$$

## 2) Axion Cosmology & Sphalerons

### The Axion:

A pseudo-Goldstone boson proposed to solve the **Strong CP Problem** and also a leading **Dark Matter** candidate.

### Thermal Production:

Early Universe ( $T \sim T_c \div 10T_c$ ) → axions produced via hadronic scatterings:

$$\pi + \pi \rightarrow a + a$$

The axion relic abundance is governed by the **Boltzmann Equation** [cite: 81-82]:

$$\frac{df_{\vec{p}}}{dt} = (1 + f_{\vec{p}})\Gamma_a^{(+)} - f_{\vec{p}}\Gamma_a^{(-)}$$

## 2) Axion Cosmology & Sphalerons

### The Axion:

A pseudo-Goldstone boson proposed to solve the **Strong CP Problem** and also a leading **Dark Matter** candidate.

### Thermal Production:

Early Universe ( $T \sim T_c \div 10T_c$ ) → axions produced via hadronic scatterings:

$$\pi + \pi \rightarrow a + a$$

The axion relic abundance is governed by the **Boltzmann Equation** [cite: 81-82]:

$$\frac{df_{\vec{p}}}{dt} = (1 + f_{\vec{p}})\Gamma_a^{(+)} - f_{\vec{p}}\Gamma_a^{(-)}$$

**The Key Input:** The interaction rates  $\Gamma_a$  are related to the **Sphaleron Rate** [cite: 84]:

$$\Gamma_a^{(-)} = e^{E/T} \quad \Gamma_a^{(+)} = \frac{\Gamma_{\text{sphal}}}{2Ef_a^2}$$

# From Real Time to Euclidean Time



The Sphaleron Rate is a **Real-Time** Transport Coefficient:

$$\Gamma_{\text{sphal}} = \int dt d^3x \langle q(\vec{x}, t) q(\vec{0}, 0) \rangle_T$$

# From Real Time to Euclidean Time



The Sphaleron Rate is a **Real-Time** Transport Coefficient:

$$\Gamma_{\text{sphal}} = \int dt d^3x \langle q(\vec{x}, t) q(\vec{0}, 0) \rangle_T$$

But lattice simulations live in **Euclidean time** ( $t \rightarrow -i\tau$ ):

$$0 \leq \tau \leq 1/T$$

# From Real Time to Euclidean Time



The Sphaleron Rate is a **Real-Time** Transport Coefficient:

$$\Gamma_{\text{sphal}} = \int dt d^3x \langle q(\vec{x}, t) q(\vec{0}, 0) \rangle_T$$

But lattice simulations live in **Euclidean time** ( $t \rightarrow -i\tau$ ):

$$0 \leq \tau \leq 1/T$$

We measure the **Euclidean Correlator** (spatially integrated):

$$G_E(\tau) = \int d^3x \langle q(\vec{x}, \tau) q(\vec{0}, 0) \rangle$$

# From Real Time to Euclidean Time



The Sphaleron Rate is a **Real-Time** Transport Coefficient:

$$\Gamma_{\text{sphal}} = \int dt d^3x \langle q(\vec{x}, t) q(\vec{0}, 0) \rangle_T$$

But lattice simulations live in **Euclidean time** ( $t \rightarrow -i\tau$ ):

$$0 \leq \tau \leq 1/T$$

We measure the **Euclidean Correlator** (spatially integrated):

$$G_E(\tau) = \int d^3x \langle q(\vec{x}, \tau) q(\vec{0}, 0) \rangle$$

## ***The Challenge:***

*How to recover dynamic transport  $\Gamma_{\text{sphal}}$  from lattice data  $G_E(\tau)$ ?*

# Spectral Representation



Spectral Decomposition of Euclidean Correlators

$$G(\tau) = - \int_0^\infty \frac{d\omega}{\pi} K(\tau, \omega) \rho(\omega)$$

# Spectral Representation



Spectral Decomposition of Euclidean Correlators

$$G(\tau) = - \int_0^\infty \frac{d\omega}{\pi} K(\tau, \omega) \rho(\omega)$$

# Spectral Representation

Spectral Decomposition of Euclidean Correlators

$$G(\tau) = - \int_0^\infty \frac{d\omega}{\pi} K(\tau, \omega) \rho(\omega)$$

with the thermal Laplace basis

$$K(\tau, \omega) = \frac{\cosh\left(\omega(\tau - \frac{1}{2T})\right)}{\sinh\left(\frac{\omega}{2T}\right)}$$

# Spectral Representation

Spectral Decomposition of Euclidean Correlators

$$G(\tau) = - \int_0^\infty \frac{d\omega}{\pi} K(\tau, \omega) \rho(\omega)$$

with the thermal Laplace basis

$$K(\tau, \omega) = \frac{\cosh\left(\omega(\tau - \frac{1}{2T})\right)}{\sinh\left(\frac{\omega}{2T}\right)}$$

The **spectral function** encodes:

- excitations at finite  $\omega$
- **transport** from its behaviour at  $\omega \rightarrow 0$

# Spectral Representation



Spectral Decomposition of Euclidean Correlators

$$G(\tau) = - \int_0^\infty \frac{d\omega}{\pi} K(\tau, \omega) \rho(\omega)$$

with the thermal Laplace basis

$$K(\tau, \omega) = \frac{\cosh\left(\omega\left(\tau - \frac{1}{2T}\right)\right)}{\sinh\left(\frac{\omega}{2T}\right)}$$

The **spectral function** encodes:

- excitations at finite  $\omega$
- **transport** from its behaviour at  $\omega \rightarrow 0$

- **For the Sphaleron Rate:** []

$$\Gamma_{\text{sphal}} = \lim_{\omega \rightarrow 0} \frac{2T}{\omega} \rho(\omega)$$

# The Inverse Problem: A Mathematical Wall



# The Inverse Problem: A Mathematical Wall



$$G_E(\tau_i) = - \int_0^\infty \frac{d\omega}{\pi} K(\tau_i, \omega) \rho(\omega)$$

**Input from the Lattice:**

- Finite set of points:  $N_\tau \sim \mathcal{O}(10 - 20)$
- Noisy data:  $G_E(\tau_i) \pm \sigma_i$

# The Inverse Problem: A Mathematical Wall



$$G_E(\tau_i) = - \int_0^\infty \frac{d\omega}{\pi} K(\tau_i, \omega) \rho(\omega)$$

## Input from the Lattice:

- Finite set of points:  $N_\tau \sim \mathcal{O}(10 - 20)$
- Noisy data:  $G_E(\tau_i) \pm \sigma_i$

## The Unknown (Physics):

- Continuous function  $\rho(\omega) = \mathcal{L}^{-1}\{G_E\}(\omega)$
- Infinite degrees of freedom

# The Inverse Problem: A Mathematical Wall



$$G_E(\tau_i) = - \int_0^\infty \frac{d\omega}{\pi} K(\tau_i, \omega) \rho(\omega)$$

## Input from the Lattice:

- Finite set of points:  $N_\tau \sim \mathcal{O}(10 - 20)$
- Noisy data:  $G_E(\tau_i) \pm \sigma_i$

## The Output (Physics):

- Continuous function  $\rho(\omega) = \mathcal{L}^{-1}\{G_E\}(\omega)$
- Infinite degrees of freedom

### The Problem:

This is a **Fredholm Integral Equation of the 1st Kind**  $\Rightarrow$  **Ill-Posed**.

An infinite number of solutions  $\rho(\omega)$  can fit the discrete data within error bars.

# Discretization & Mock Tests

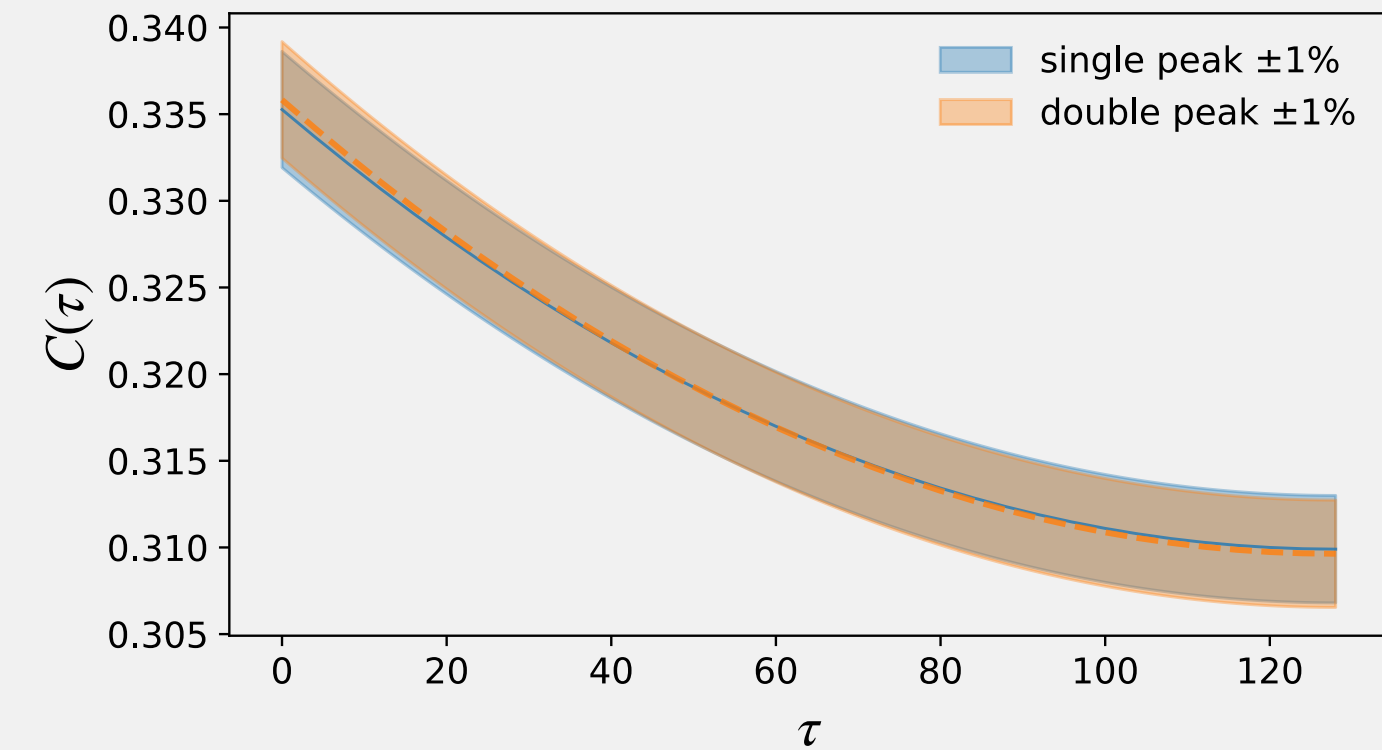
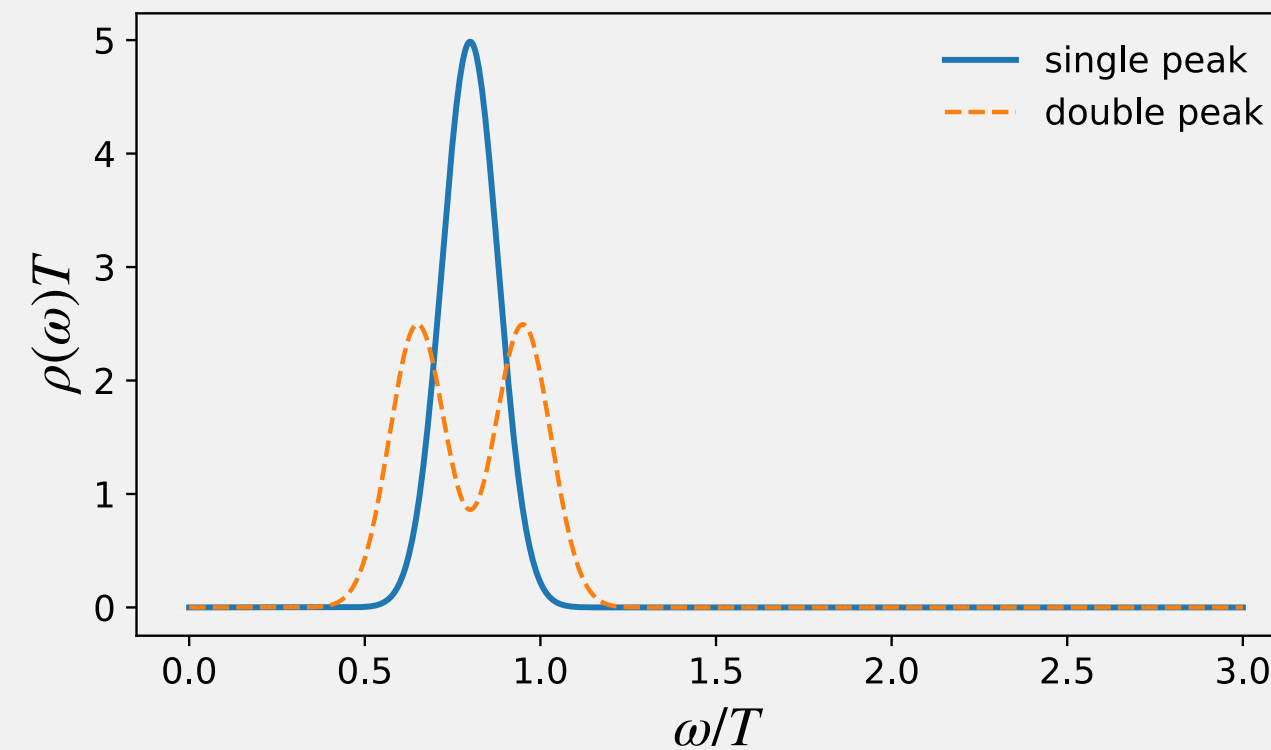


Synthetic Data  $\Rightarrow G(\tau_i) = \sum_j K(\tau_i, \omega_j) \rho(\omega_j)$

# Discretization & Mock Tests



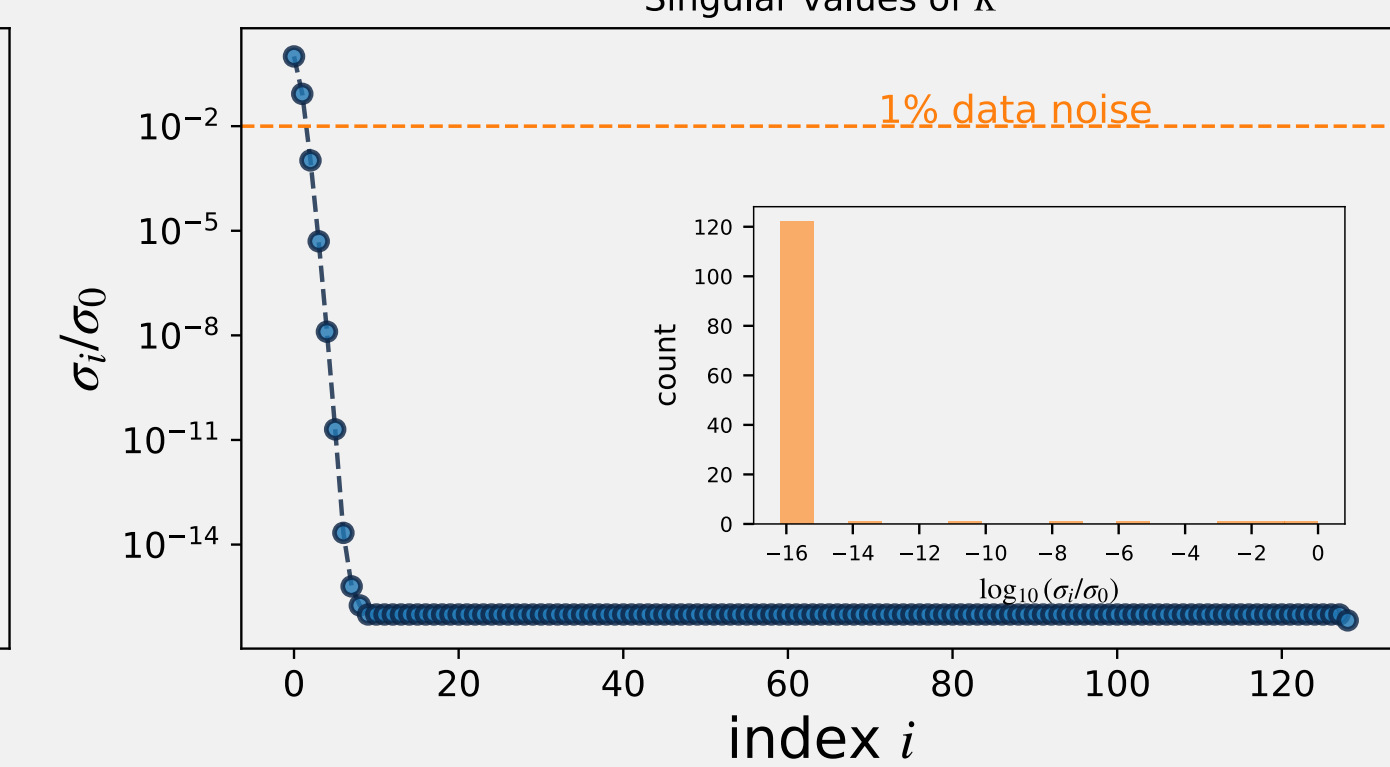
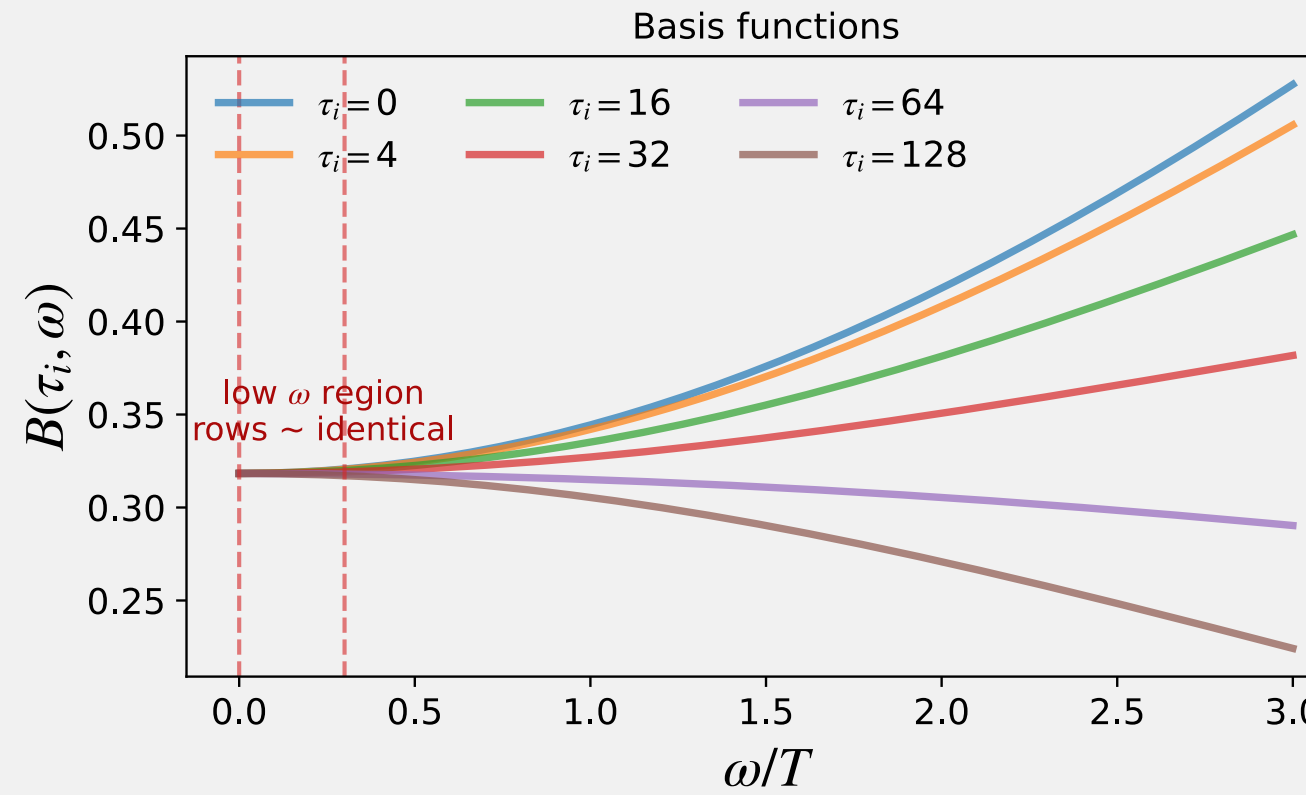
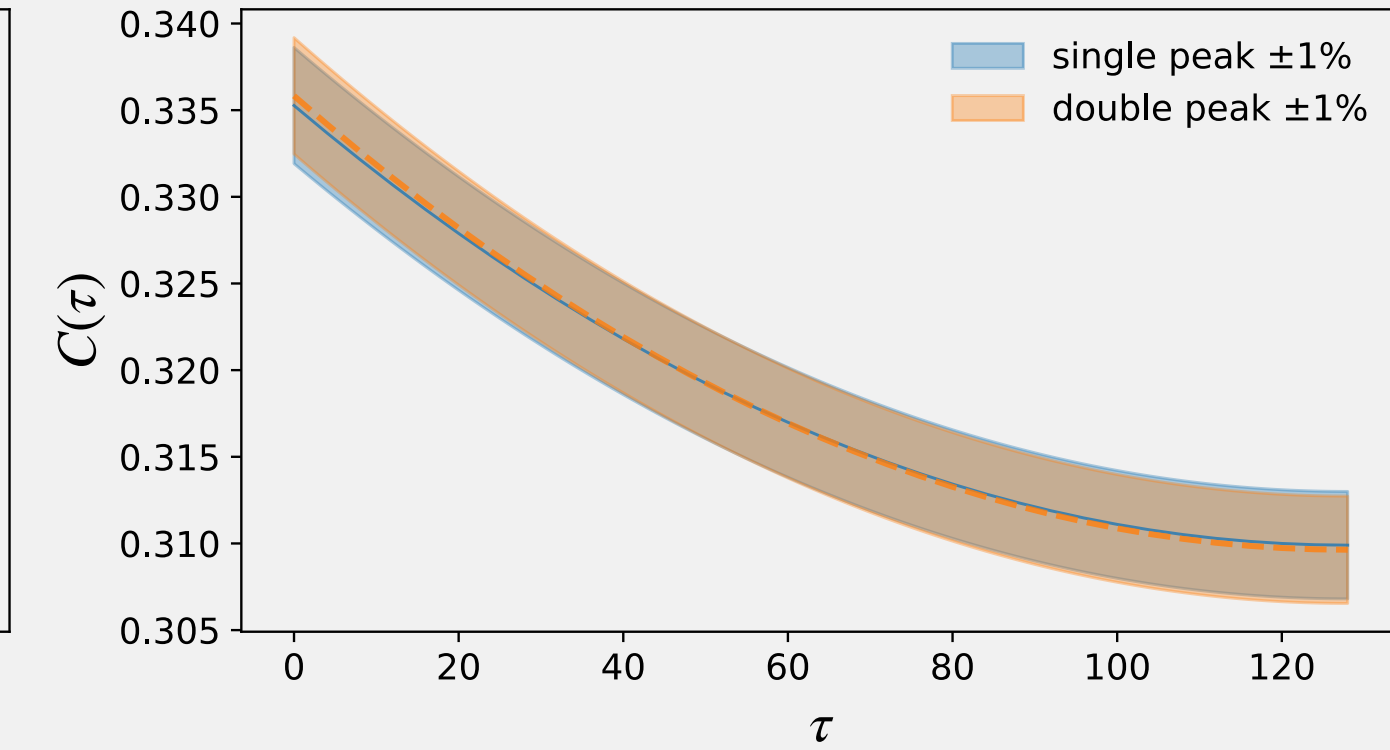
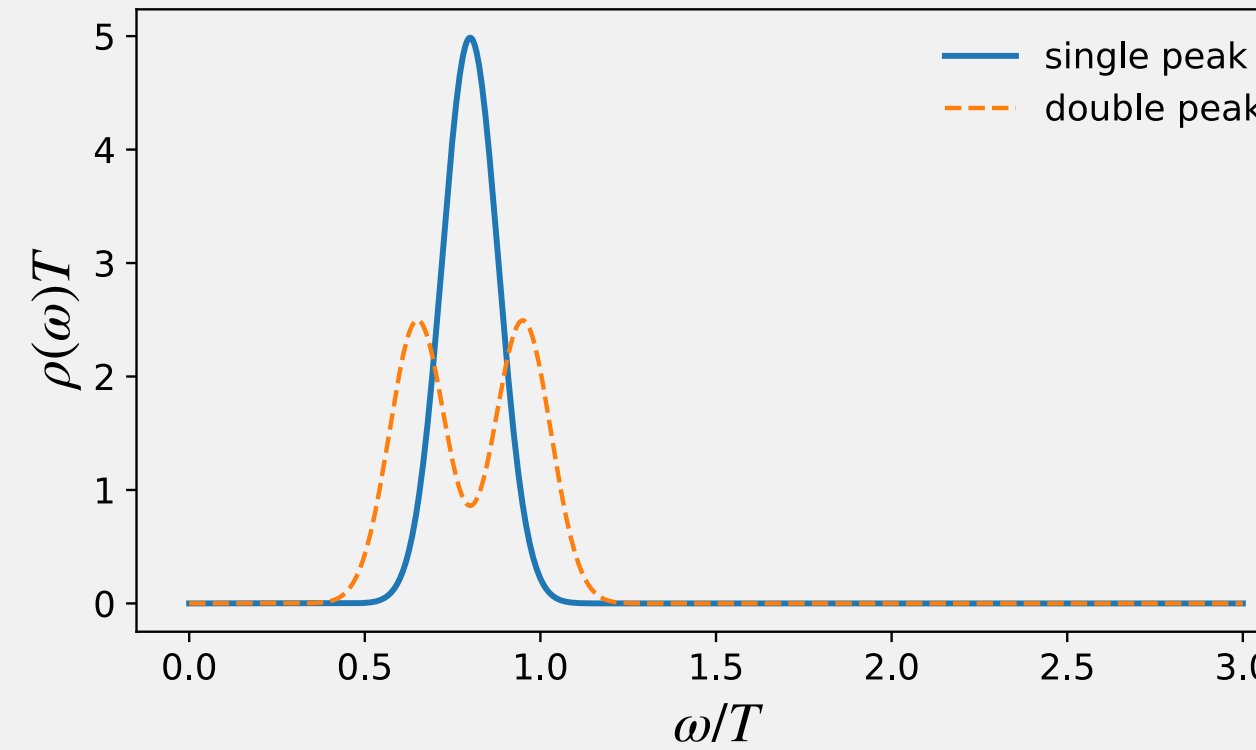
$$\text{Synthetic Data} \Rightarrow G(\tau_i) = \sum_j K(\tau_i, \omega_j) \rho(\omega_j)$$



# Discretization & Mock Tests



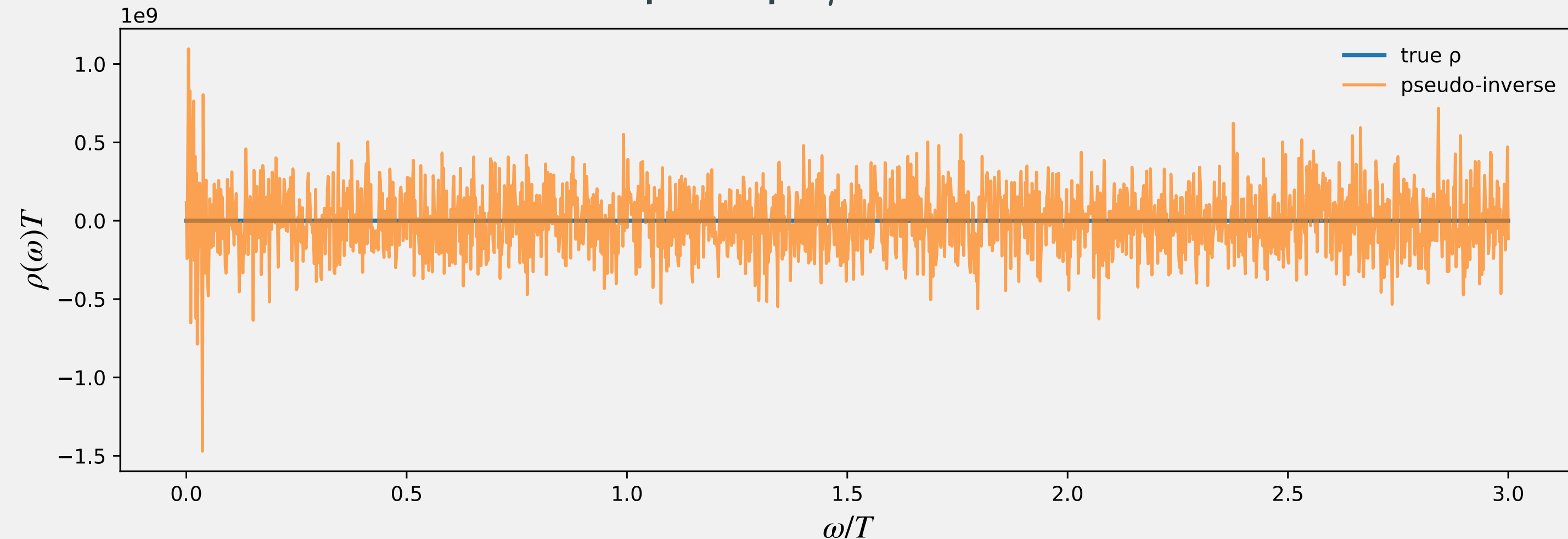
$$\text{Synthetic Data} \Rightarrow G(\tau_i) = \sum_j K(\tau_i, \omega_j) \rho(\omega_j)$$



# Direct Inversion: a Catastrophe!



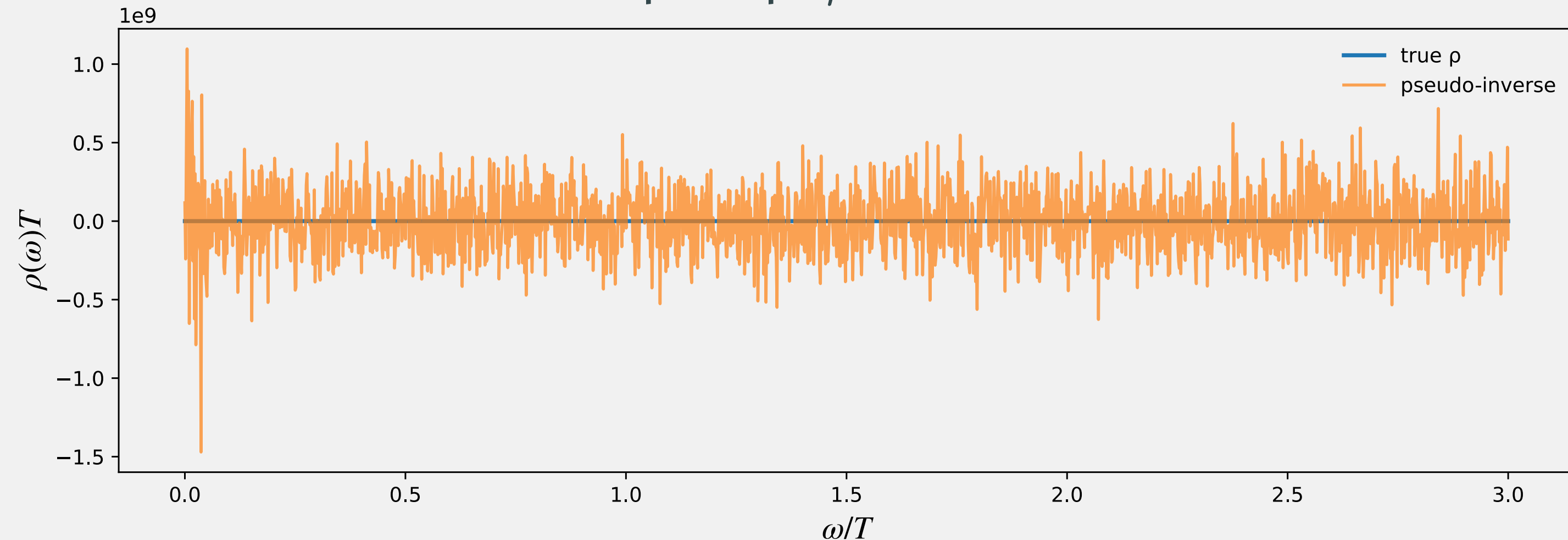
Naïve oversæd:  $\rho \sim K^{-1} G$



# Direct Inversion: a Catastrophe!



Naïve oversæp:  $\rho \sim K^{-1} G$



---

To overcome ill-posedness, we must abandon pointwise reconstruction.  
We instead target a **smeared spectral density** using a **regularized estimator** that suppresses noise amplification.

# Breaking the Wall: 1. Smearing

Sharp features  $\rho(\omega)$  cannot be reconstructed → **Smeared Spectral Density:**

$$\bar{\rho}_\sigma(\bar{\omega}) = \int_0^\infty d\omega \Delta_\sigma(\bar{\omega}, \omega) \frac{\rho(\omega)}{\omega}$$

# Breaking the Wall: 1.Smeearing

Sharp features  $\rho(\omega)$  cannot be reconstructed → **Smeared Spectral Density:**

$$\bar{\rho}_\sigma(\bar{\omega}) = \int_0^\infty d\omega \Delta_\sigma(\bar{\omega}, \omega) \frac{\rho(\omega)}{\omega}$$

Here  $\Delta_\sigma$  is a **target smearing kernel** which replaces the ideal  $\delta(\omega - \bar{\omega})$  that we cannot resolve.

# Breaking the Wall: 1. Smearing

Sharp features  $\rho(\omega)$  cannot be reconstructed → **Smeared Spectral Density:**

$$\bar{\rho}_\sigma(\bar{\omega}) = \int_0^\infty d\omega \Delta_\sigma(\bar{\omega}, \omega) \frac{\rho(\omega)}{\omega}$$

Here  $\Delta_\sigma$  is a **target smearing kernel** which replaces the ideal  $\delta(\omega - \bar{\omega})$  that we cannot resolve.

## The HLT Strategy:

Rather than solving directly for  $\rho(\omega)$ , we determine coefficients  $g_\tau(\bar{\omega})$  such that

$$\Delta_\sigma(\bar{\omega}, \omega) \approx \sum_{\tau=t_{\min}}^{N_\tau/2} g_\tau(\bar{\omega}) K(\tau, \omega).$$

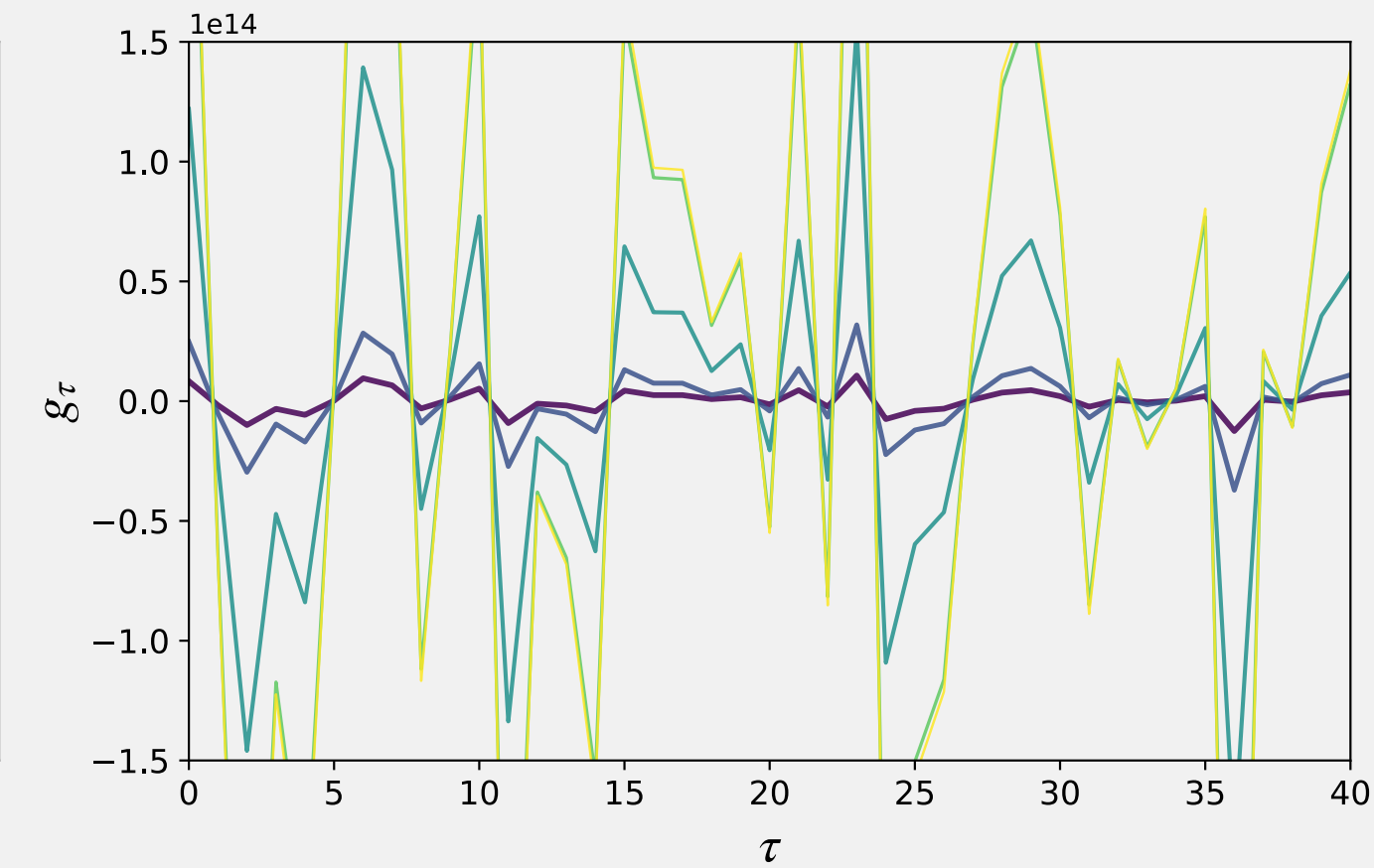
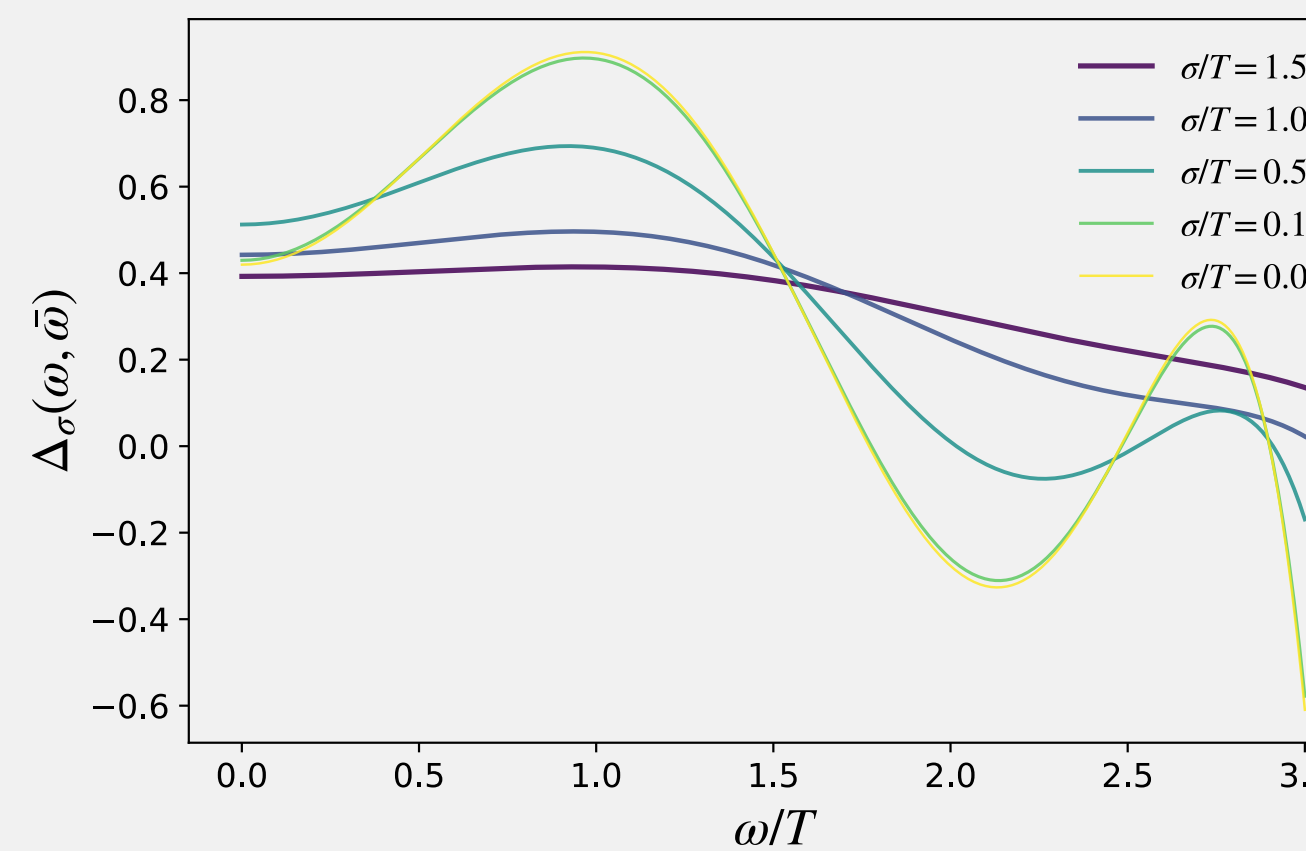
Then the smeared estimator becomes:

$$\bar{\rho}_\sigma(\bar{\omega}) \approx \sum_{\tau=t_{\min}}^{N_\tau/2} g_\tau(\bar{\omega}) G_E(\tau)$$

# Smearing Mock Test



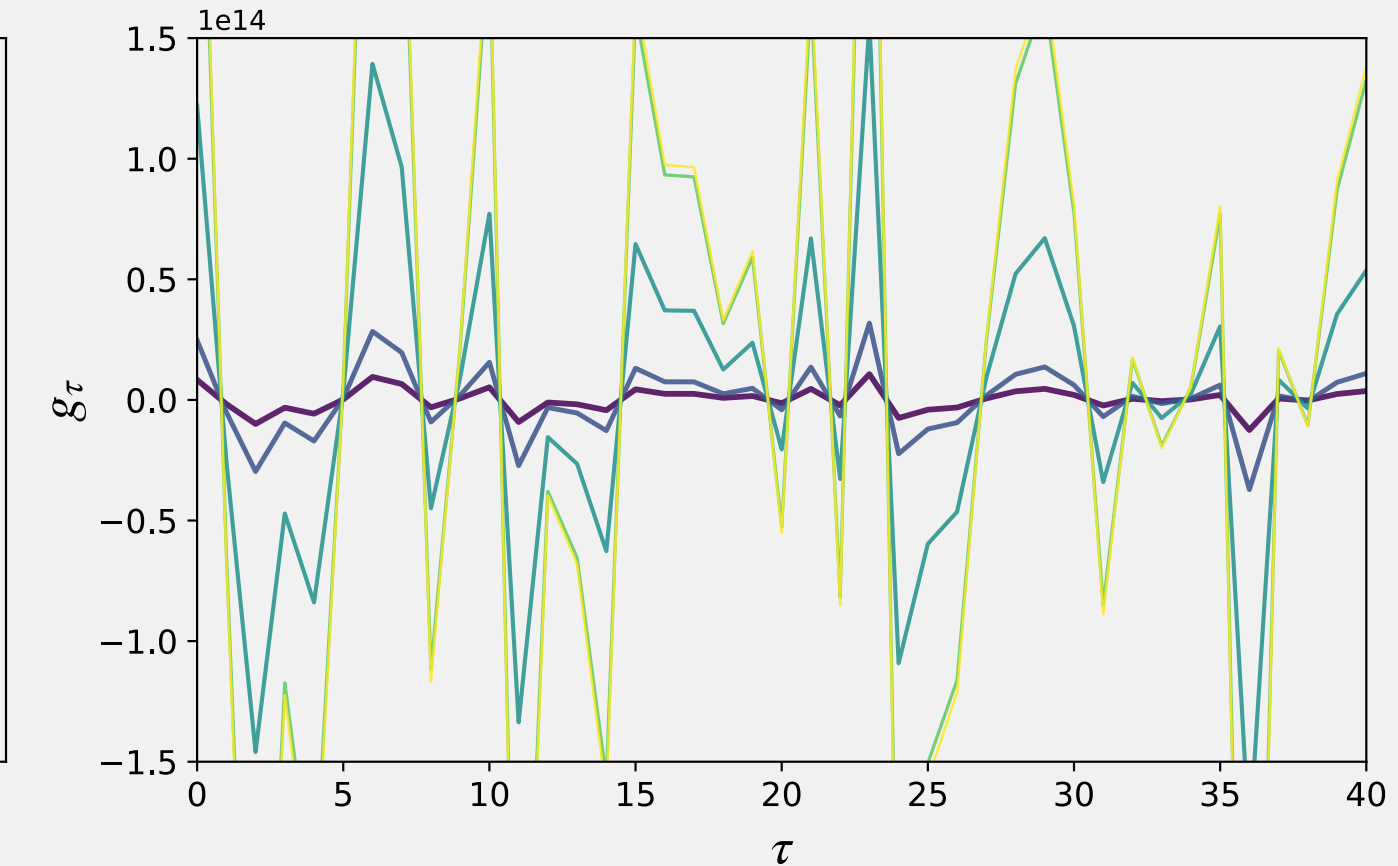
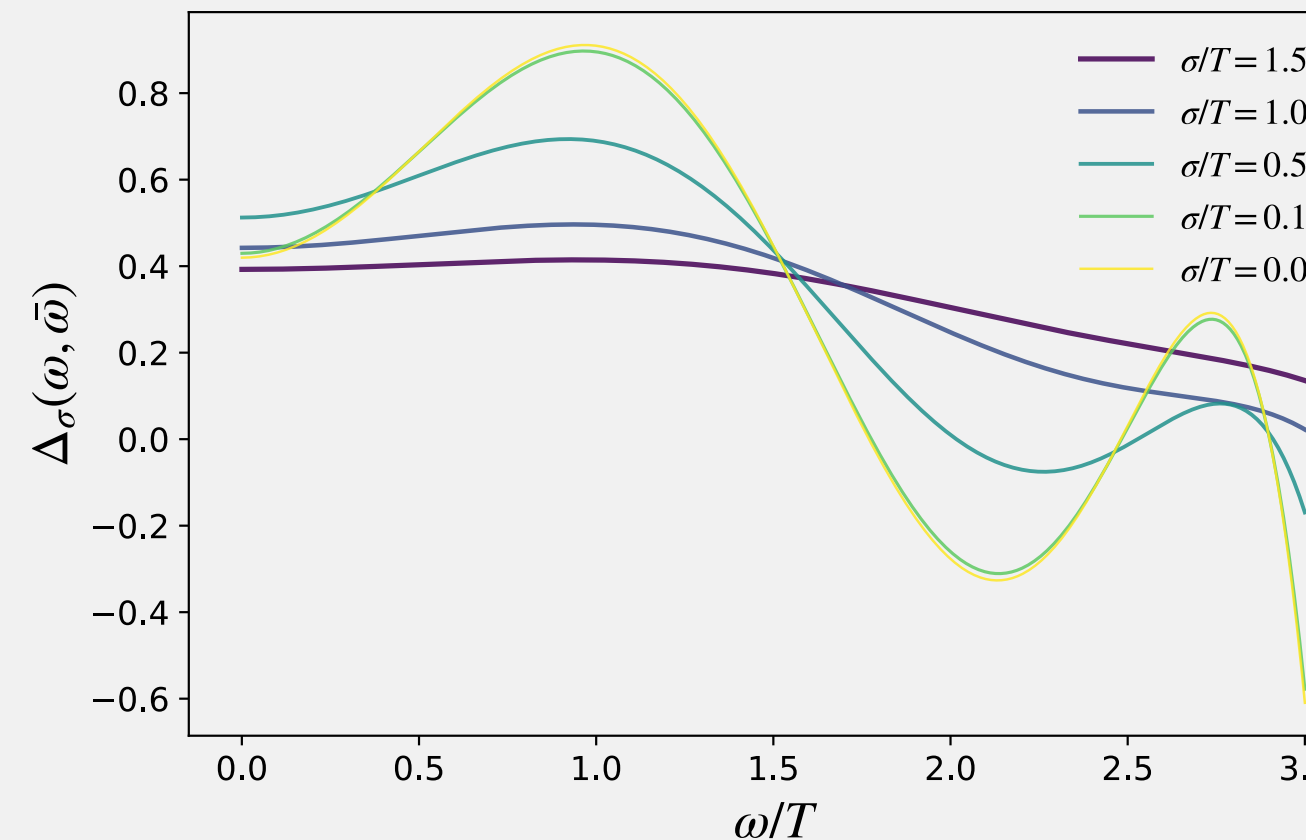
# Smearing Mock Test



# Smearing Mock Test

## The Trade-off

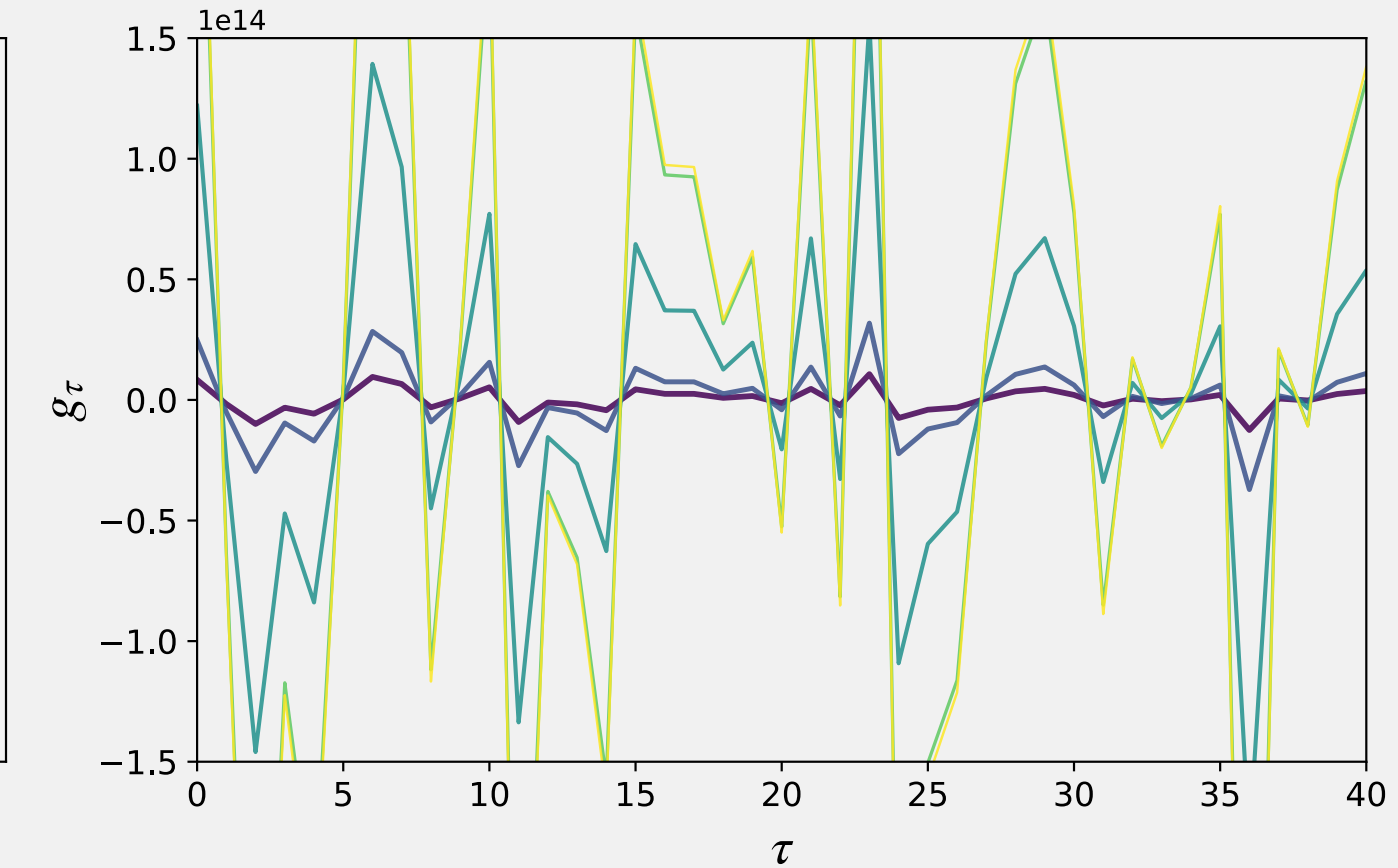
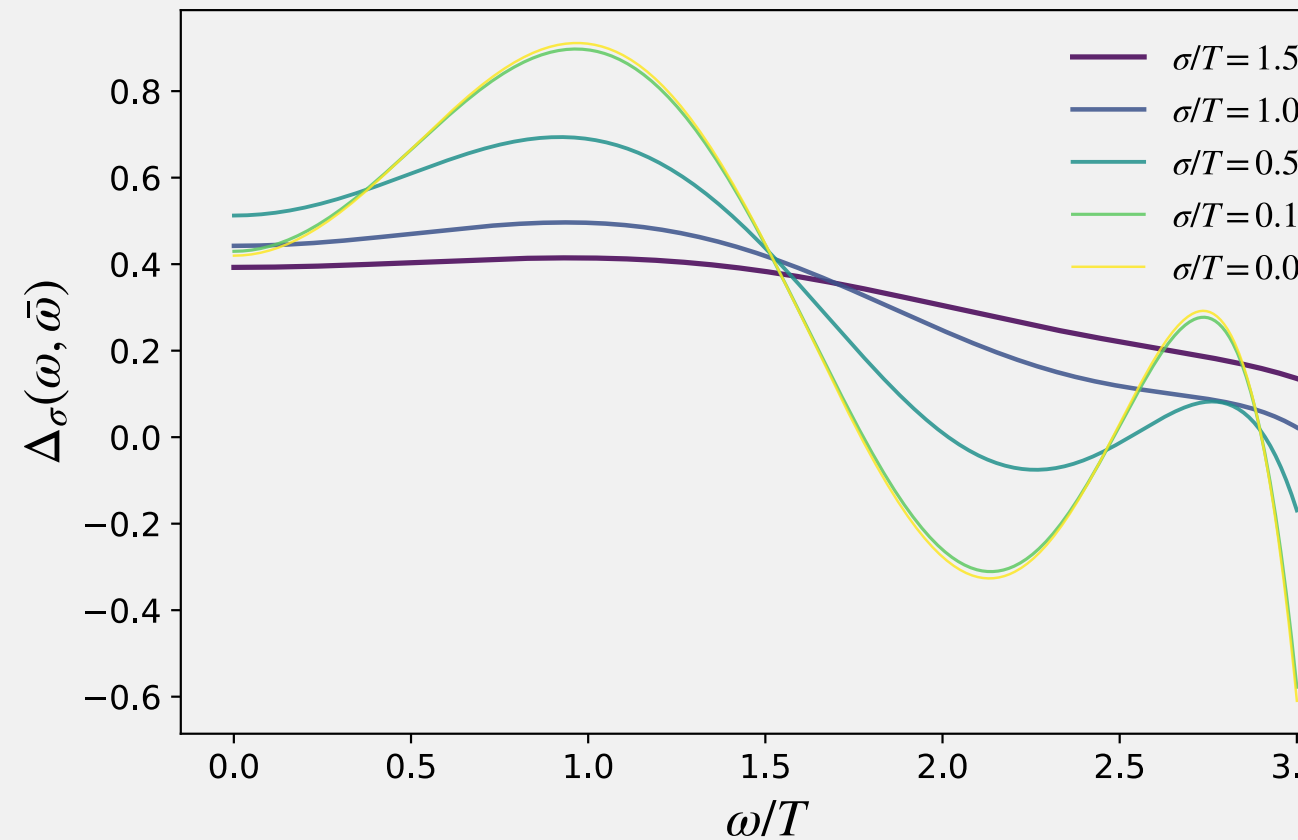
- **Narrower target  $\sigma$**   $\Rightarrow$  sharper  $\Delta$  but  $\|g\| \uparrow$  (variance explodes).
- **Broader  $\sigma$**   $\Rightarrow$  stable  $\Delta$ , reduced variance, but poorer resolution.
- **Goal:** Need optimal  $\sigma +$  damping ( $\lambda$ ) to balance width vs. noise.



# Smearing Mock Test

## The Trade-off

- **Narrower target  $\sigma$**   $\Rightarrow$  sharper  $\Delta$  but  $\|g\| \uparrow$  (variance explodes).
- **Broader  $\sigma$**   $\Rightarrow$  stable  $\Delta$ , reduced variance, but poorer resolution.
- **Goal:** Need optimal  $\sigma +$  damping ( $\lambda$ ) to balance width vs. noise.



We now introduce regularization (Modified Backus–Gilbert / HLT) to set  $\sigma$  and suppress unstable modes.

# the HLT functional

We determine the coefficients  $g_\tau(\bar{\omega})$  by minimizing the functional:

$$W_\lambda[g] = (1 - \lambda) \frac{A[g]}{A_{\text{norm}}} + \lambda B[g]$$

# the HLT functional

We determine the coefficients  $g_\tau(\bar{\omega})$  by minimizing the functional:

$$W_\lambda[g] = (1 - \lambda) \frac{A[g]}{A_{\text{norm}}} + \lambda B[g]$$

## 1. Resolution Error (Bias)

$$A[g] = \int_0^\infty d\omega |\Delta(\omega) - \delta_\sigma(\omega)|^2$$

- Penalizes deviations from the **target**  $\delta_\sigma$ .
- Enforces the correct “smearing shape.”

# the HLT functional

We determine the coefficients  $g_\tau(\bar{\omega})$  by minimizing the functional:

$$W_\lambda[g] = (1 - \lambda) \frac{A[g]}{A_{\text{norm}}} + \lambda B[g]$$

## 1. Resolution Error (Bias)

$$A[g] = \int_0^\infty d\omega |\Delta(\omega) - \delta_\sigma(\omega)|^2$$

- Penalizes deviations from the **target**  $\delta_\sigma$ .
- Enforces the correct “smearing shape.”

## 2. Statistical Error (Variance)

$$B[g] = \mathbf{g}^T \cdot \mathbf{Cov} \cdot \mathbf{g}$$

- Penalizes the **variance** of the estimator due to data noise.
- Reduces explosion of coefficients  $g_\tau$ .

# the HLT functional

We determine the coefficients  $g_\tau(\bar{\omega})$  by minimizing the functional:

$$W_\lambda[g] = (1 - \lambda) \frac{A[g]}{A_{\text{norm}}} + \lambda B[g]$$

## 1. Resolution Error (Bias)

$$A[g] = \int_0^\infty d\omega |\Delta(\omega) - \delta_\sigma(\omega)|^2$$

- Penalizes deviations from the **target**  $\delta_\sigma$ .
- Enforces the correct “smearing shape.”

## 2. Statistical Error (Variance)

$$B[g] = \mathbf{g}^T \cdot \mathbf{Cov} \cdot \mathbf{g}$$

- Penalizes the **variance** of the estimator due to data noise.
- Reduces explosion of coefficients  $g_\tau$ .

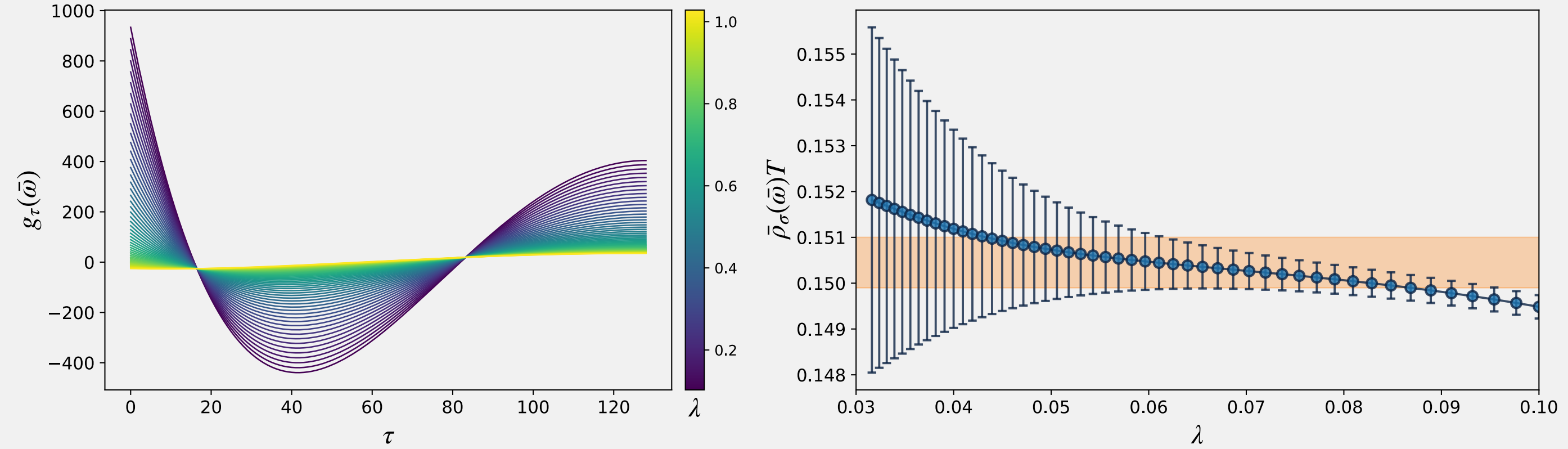
The parameter  $\lambda \in [0, 1)$  controls the trade-off.

(Unlike standard Backus-Gilbert, we fix  $\sigma$  as an input and scan  $\lambda$  for stability.)

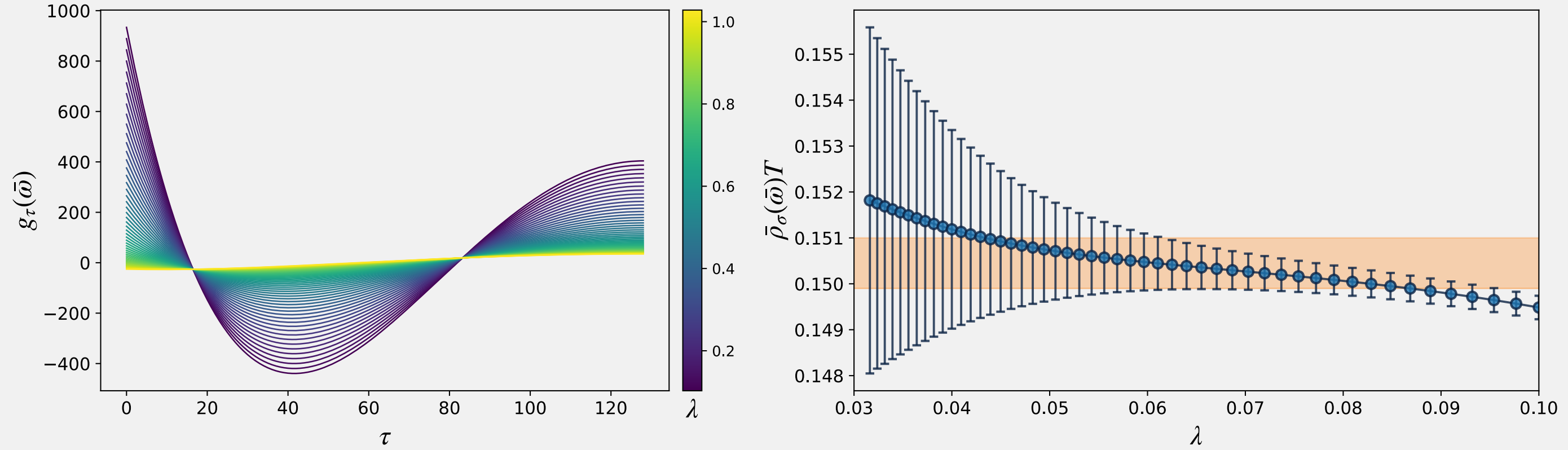
# The last Mock test



# The last Mock test



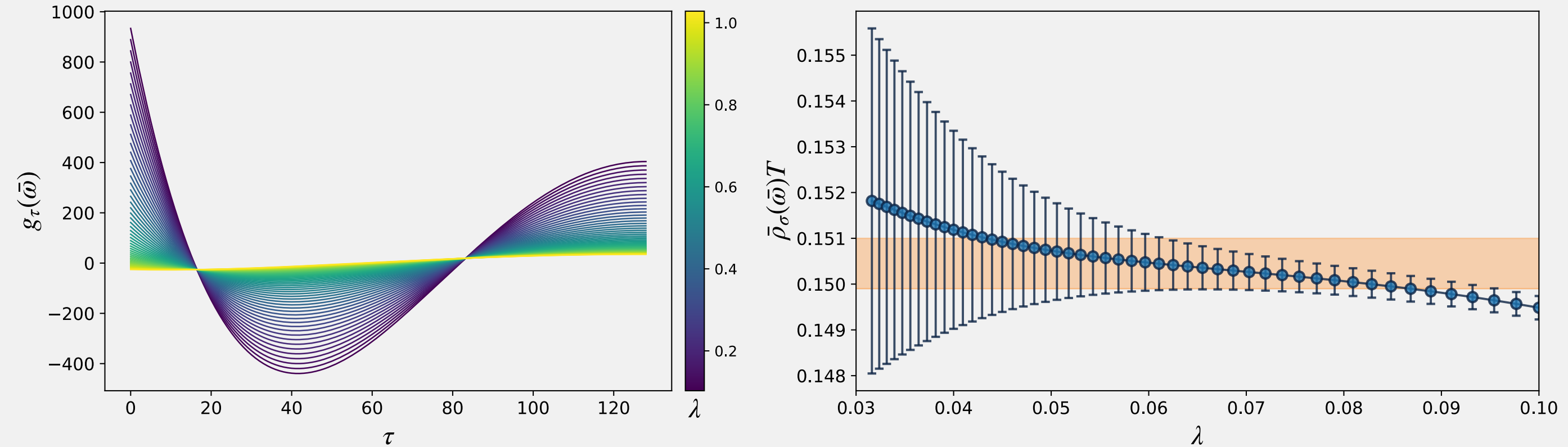
# The last Mock test



Coefficients  $g_\tau(\lambda)$ :

- Small  $\lambda \rightarrow$  unstable:  
*Coefficients explode to minimize bias  $\leftrightarrow A$ .*
- Large  $\lambda \rightarrow$  stable:  
*Coefficients are damped to minimize variance  $\leftrightarrow B$ .*

# The last Mock test



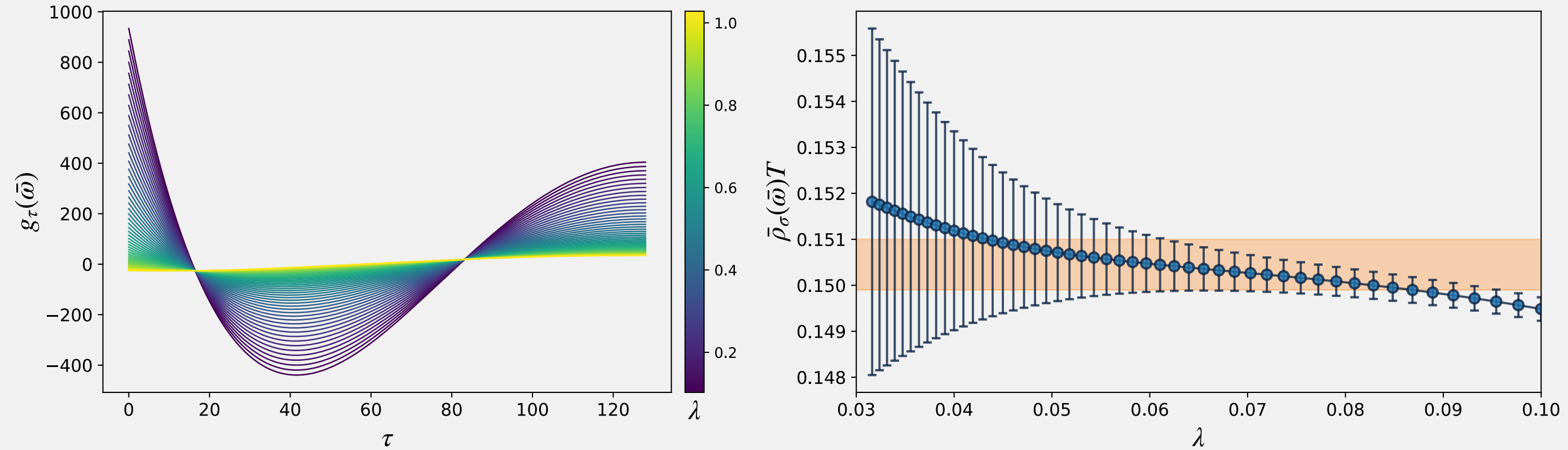
## Coefficients $g_\tau(\lambda)$ :

- Small  $\lambda \rightarrow$  unstable:  
*Coefficients explode to minimize bias  $\leftrightarrow A$ .*
- Large  $\lambda \rightarrow$  stable:  
*Coefficients are damped to minimize variance  $\leftrightarrow B$ .*

## Stability analysis:

- Small  $\lambda$ :  
*Statistical error explodes (noise amplification).*
- Large  $\lambda$ :  
*Systematic error dominates (poor resolution).*

# The last Mock test



## Coefficients $g_\tau(\lambda)$ :

- Small  $\lambda \rightarrow$  unstable:  
*Coefficients explode to minimize bias  $\leftrightarrow A$ .*
- Large  $\lambda \rightarrow$  stable:  
*Coefficients are damped to minimize variance  $\leftrightarrow B$ .*

## Stability analysis:

- Small  $\lambda$ :  
*Statistical error explodes (noise amplification).*
- Large  $\lambda$ :  
*Systematic error dominates (poor resolution).*

## The Sweet Spot:

We pick the result on the **plateau** where the value stabilizes before the noise takes over.

# The HLT Algorithm: A Recipe

**Input:** Euclidean Correlator  $G_E(\tau)$  with covariance matrix.

$$\left( \frac{2}{\sigma\pi} \right) \frac{\omega}{\sinh(\omega/\sigma)} \xrightarrow{\sigma \rightarrow 0} \delta(\omega)$$

$$W_\lambda[g] = (1 - \lambda)A[g] + \lambda B[g]$$

# The HLT Algorithm: A Recipe

**Input:** Euclidean Correlator  $G_E(\tau)$  with covariance matrix.

## 1. Choose a Target Resolution $\sigma$ :

Fix the physical width of the desired smearing  $\delta_\sigma(\omega)$ :

$$\left( \frac{2}{\sigma\pi} \right) \frac{\omega}{\sinh(\omega/\sigma)} \xrightarrow{\sigma \rightarrow 0} \delta(\omega)$$

$$W_\lambda[g] = (1 - \lambda)A[g] + \lambda B[g]$$

# The HLT Algorithm: A Recipe

**Input:** Euclidean Correlator  $G_E(\tau)$  with covariance matrix.

## 1. Choose a Target Resolution $\sigma$ :

Fix the physical width of the desired smearing  $\delta_\sigma(\omega)$ :

$$\left( \frac{2}{\sigma\pi} \right) \frac{\omega}{\sinh(\omega/\sigma)} \xrightarrow{\sigma \rightarrow 0} \delta(\omega)$$

## 2. Setup the Regularization $\lambda$ :

Minimize  $W_\lambda[g]$  for  $\lambda \in [0, 1)$ .

$$W_\lambda[g] = (1 - \lambda)A[g] + \lambda B[g]$$

# The HLT Algorithm: A Recipe



**Input:** Euclidean Correlator  $G_E(\tau)$  with covariance matrix.

## 1. Choose a Target Resolution $\sigma$ :

Fix the physical width of the desired smearing  $\delta_\sigma(\omega)$ :

$$\left( \frac{2}{\sigma\pi} \right) \frac{\omega}{\sinh(\omega/\sigma)} \xrightarrow{\sigma \rightarrow 0} \delta(\omega)$$

## 2. Setup the Regularization $\lambda$ :

Minimize  $W_\lambda[g]$  for  $\lambda \in [0, 1)$ .

$$W_\lambda[g] = (1 - \lambda)A[g] + \lambda B[g]$$

## 3. Identify the Stability Plateau:

Plot  $\Gamma_\lambda$  vs.  $d = \sqrt{A[g(\lambda)]/A[0]}$ . Find the region where systematics and statistics equilibrate.

# The HLT Algorithm: A Recipe

**Input:** Euclidean Correlator  $G_E(\tau)$  with covariance matrix.

## 1. Choose a Target Resolution $\sigma$ :

Fix the physical width of the desired smearing  $\delta_\sigma(\omega)$ :

$$\left( \frac{2}{\sigma\pi} \right) \frac{\omega}{\sinh(\omega/\sigma)} \xrightarrow{\sigma \rightarrow 0} \delta(\omega)$$

## 2. Setup the Regularization $\lambda$ :

Minimize  $W_\lambda[g]$  for  $\lambda \in [0, 1)$ .

$$W_\lambda[g] = (1 - \lambda)A[g] + \lambda B[g]$$

## 3. Identify the Stability Plateau:

Plot  $\Gamma_\lambda$  vs.  $d = \sqrt{A[g(\lambda)]/A[0]}$ . Find the region where systematics and statistics equilibrate.

## 4. Repeat over multiple $\sigma$ :

Eventually extrapolate  $\sigma \rightarrow 0$

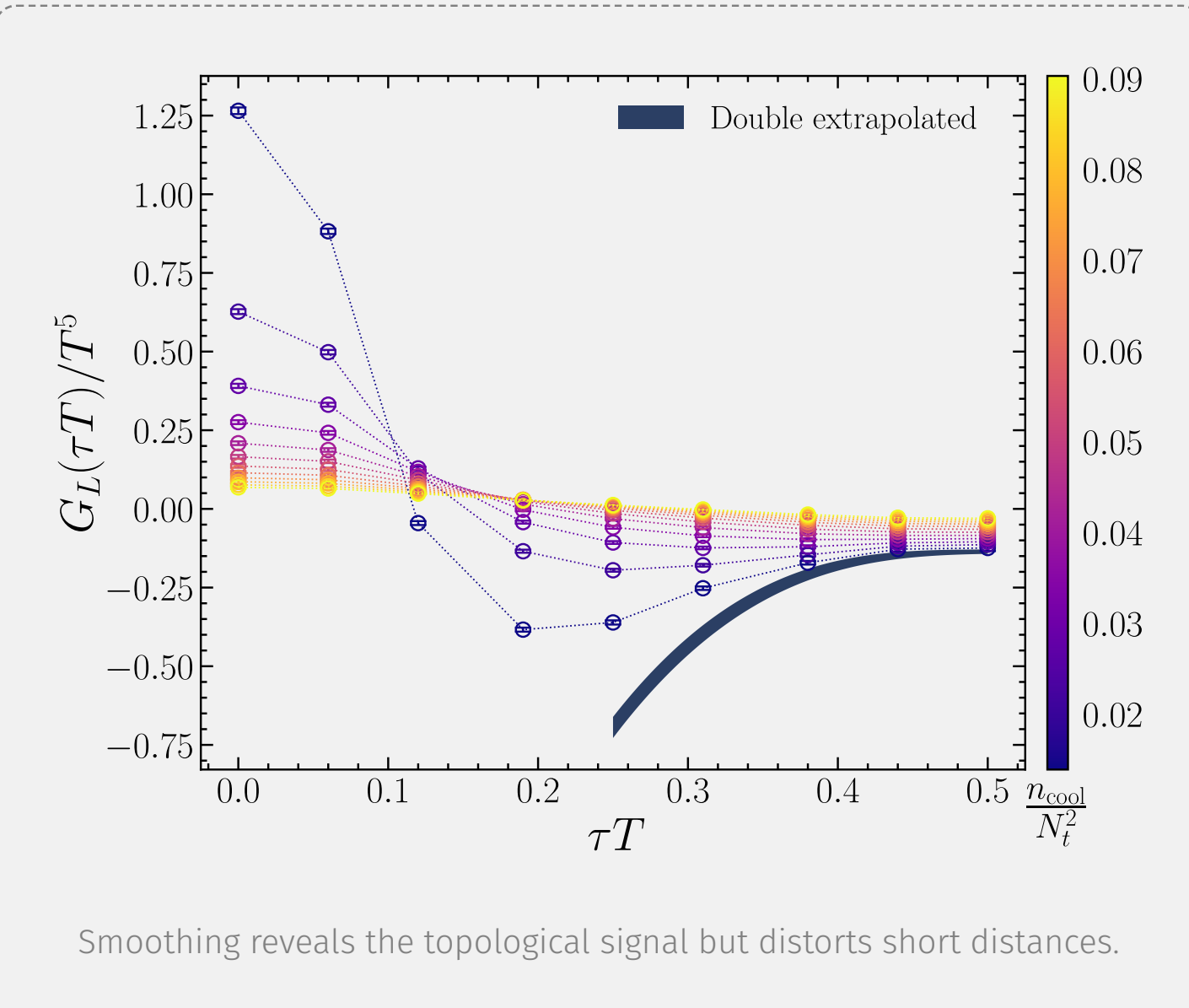
# Lattice Calculation: Extracting the Signal

To measure topological fluctuations, we must suppress UV noise.

## The Observable:

$$G_L(\tau) = \sum_{\vec{x}} \langle q_L(\vec{x}, \tau) q_L(\vec{0}, 0) \rangle$$

- **The Problem:** Standard lattice topological charge is dominated by UV fluctuations ( $1/a$  divergent).
- **The Solution: Smoothing** (Gradient Flow / Cooling).



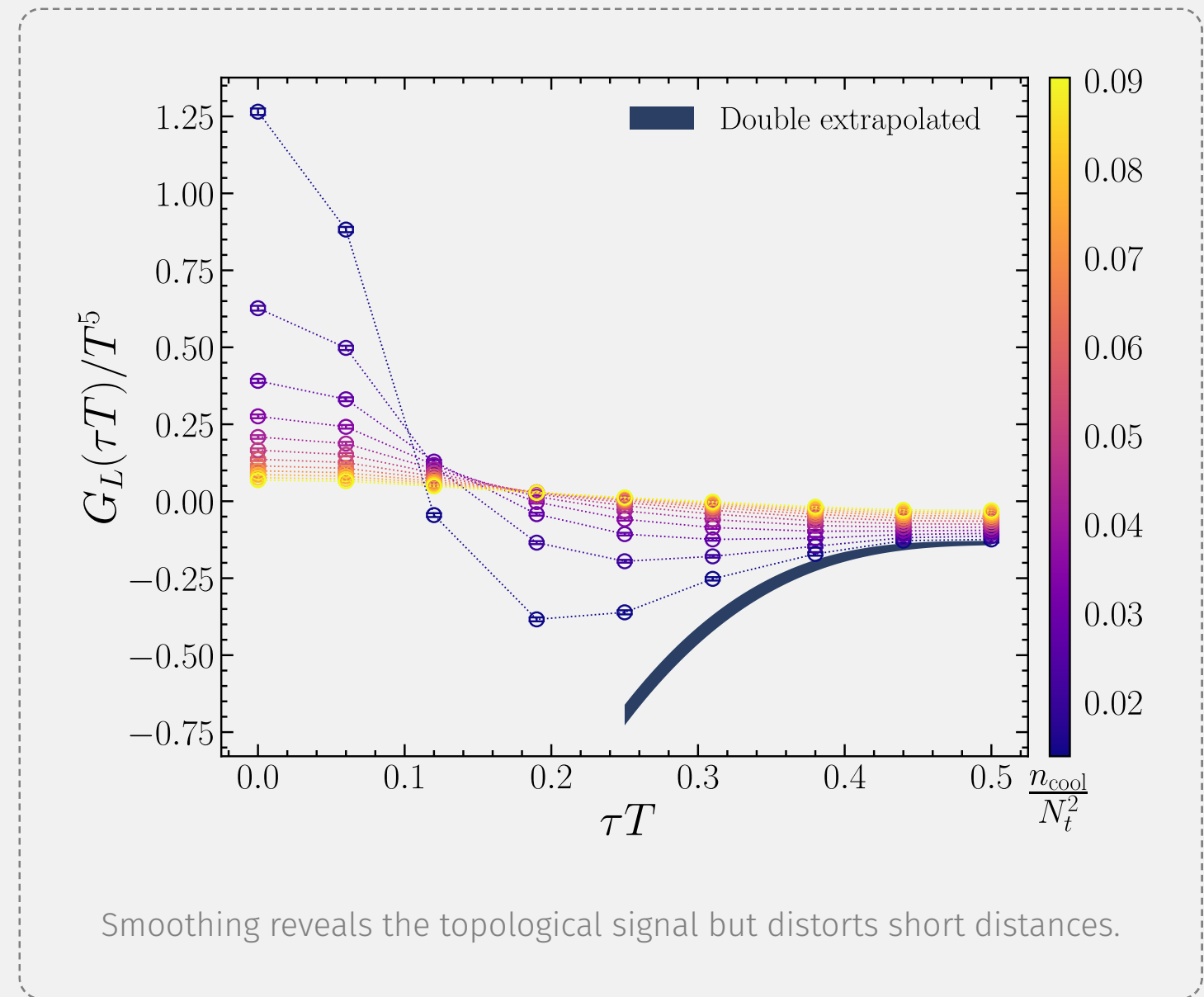
# Lattice Calculation: Extracting the Signal

To measure topological fluctuations, we must suppress UV noise.

## The Observable:

$$G_L(\tau) = \sum_{\vec{x}} \langle q_L(\vec{x}, \tau) q_L(\vec{0}, 0) \rangle$$

- **The Problem:** Standard lattice topological charge is dominated by UV fluctuations ( $1/a$  divergent).
- **The Solution: Smoothing** (Gradient Flow / Cooling).



**Artifacts:** Smoothing introduces a new scale  $R_s \propto \sqrt{n_{\text{cool}}}$ .  
*We must remove this dependence to recover physical results.*

# Baseline: Zero-Momentum Results



Recent determination in full  $N_f = 2 + 1$  QCD.



## Key Findings:

- Rate determined for  $T \in [200, 600]$  MeV.
- **Unquenching effect:** Full QCD rate is  $\sim 2\times$  larger than pure gauge.
- **Scaling:**  $\Gamma \sim T^2$  (deviates from perturbative  $\sim T^4$ ).

---

**But Axion physics requires  $\Gamma(\vec{p})$ !**

# New Frontier: Finite Momentum $\Gamma(p)$



We extend the calculation to non-zero spatial momentum  $\vec{p}$ .

## The Observable

Spatial Fourier Transform:

$$Q_L^{\vec{p}}(n_t) = \sum_{\vec{n}} e^{i\vec{p}\cdot\vec{n}} q_L(n_t, \vec{n})$$

We compute the correlator:

$$G^{\vec{p}}(\tau) = \langle Q_L^{\vec{p}}(\tau) Q_L^{-\vec{p}}(0) \rangle$$

**Why?** \* Essential for Axion thermal production rates. \*  
Probes the spatial structure of topological fluctuations.

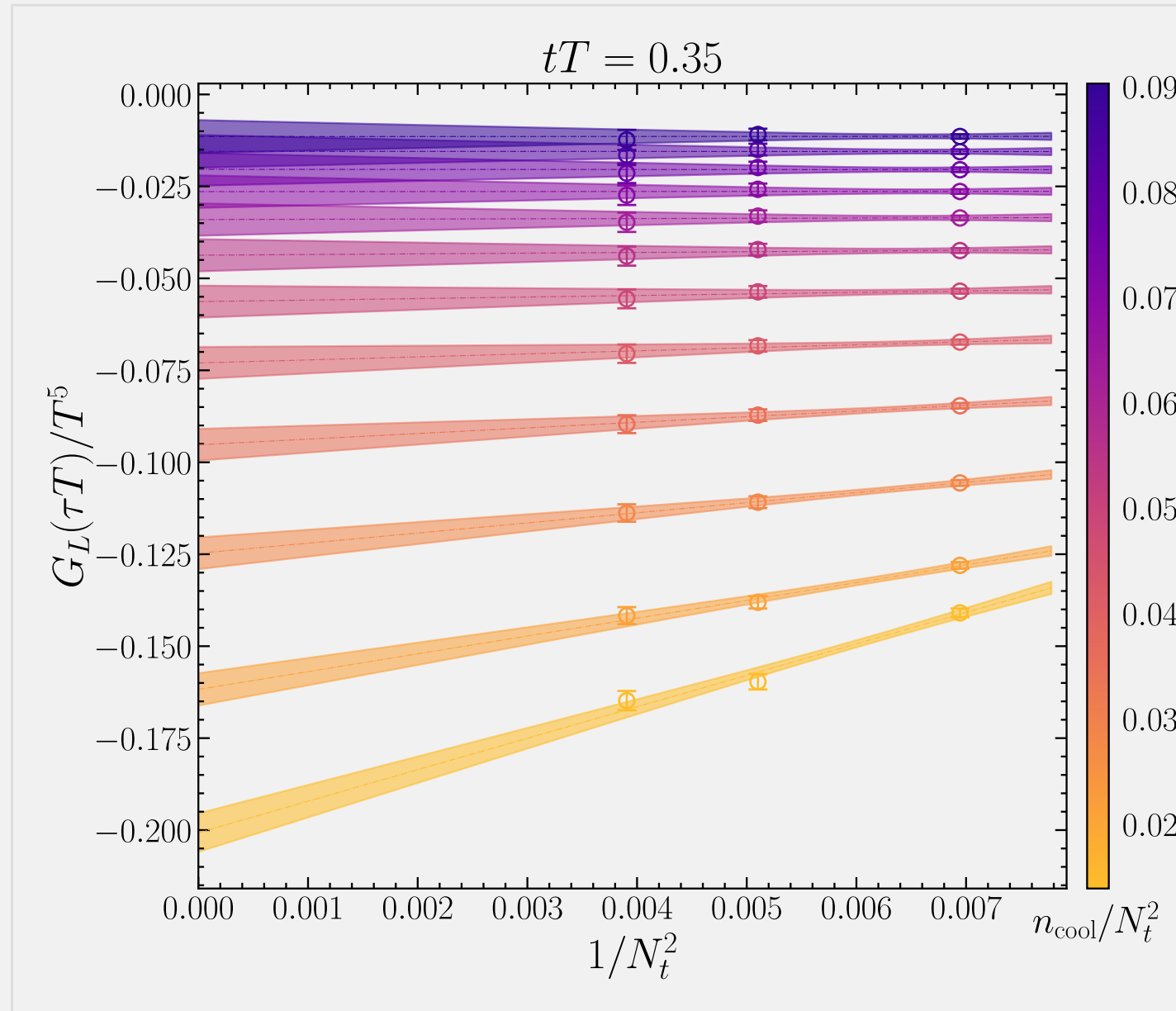
**Methodology:** \* Pure SU(3) Gauge Theory. \*  
 $T \simeq 1.24 T_c$ . \* **Rigorous Double Extrapolation.**

# Removing Artifacts: Double Extrapolation

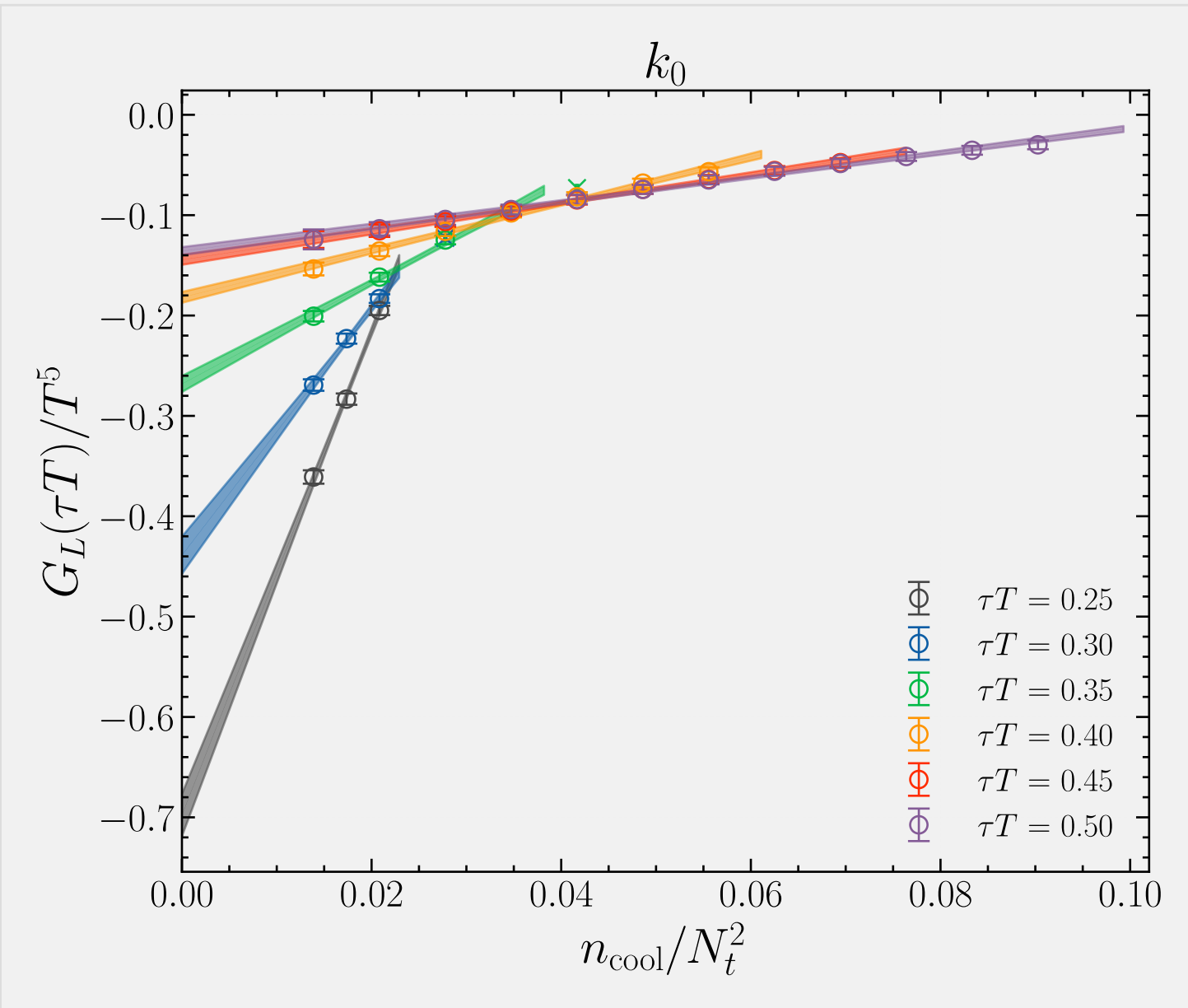


We perform a precise chain of limits to isolate the physical signal.

**Step 1: Continuum Limit ( $a \rightarrow 0$ )**



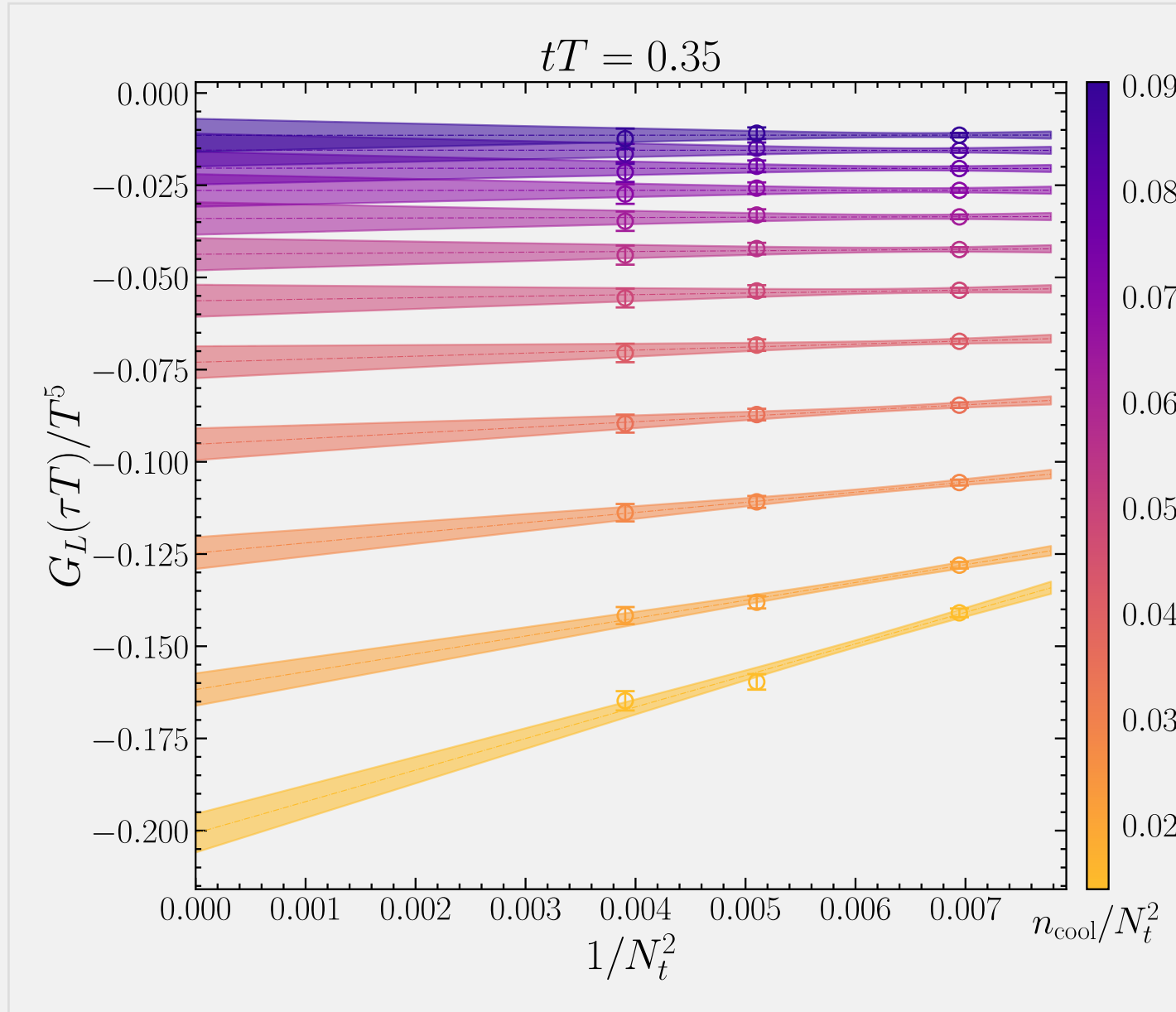
**Step 2: Zero-Smoothing ( $n_{\text{cool}} \rightarrow 0$ )**



# Removing Artifacts: Double Extrapolation

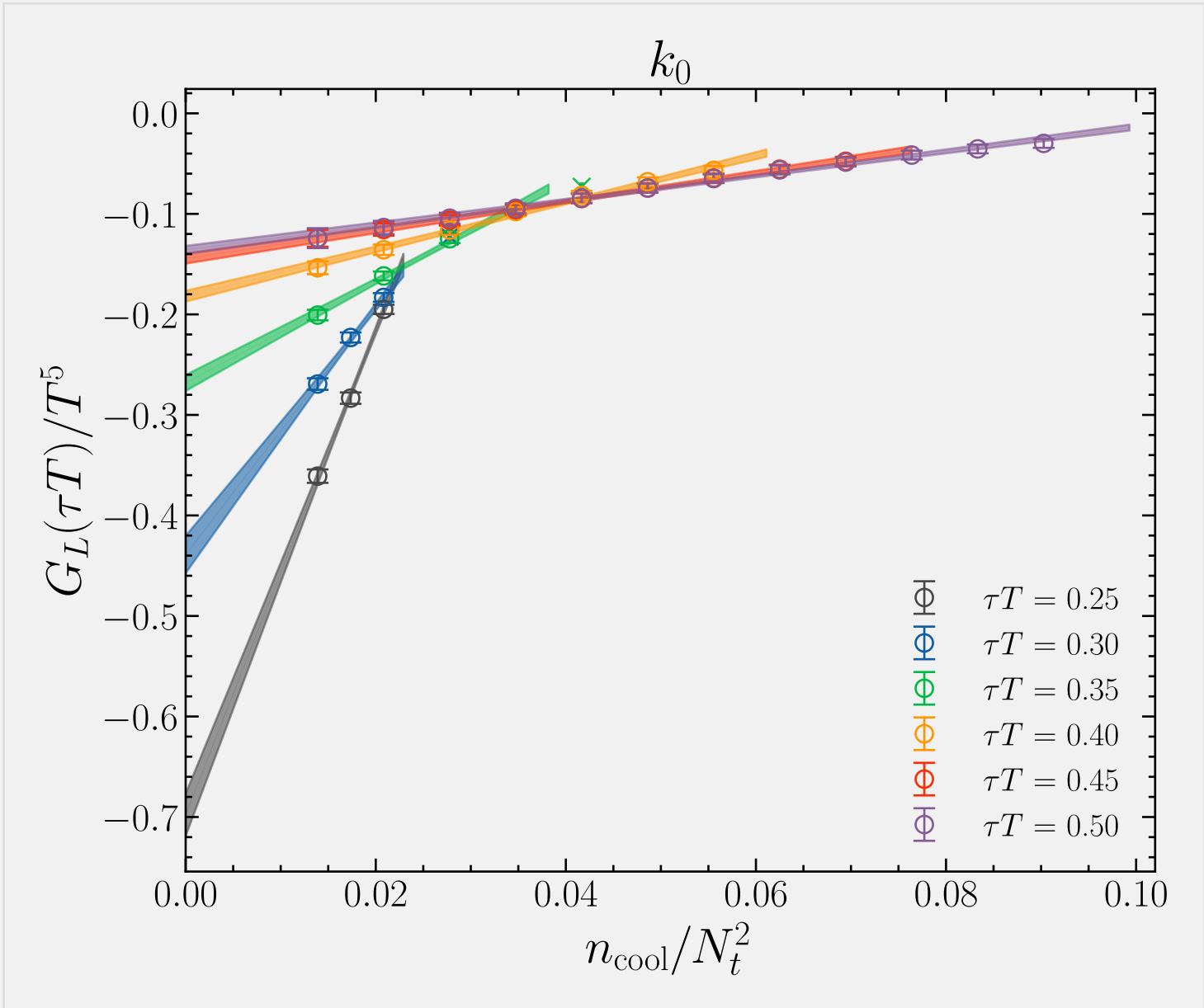
We perform a precise chain of limits to isolate the physical signal.

**Step 1: Continuum Limit ( $a \rightarrow 0$ )**



Scaling at fixed physical smoothing  $r_s$ .

**Step 2: Zero-Smoothing ( $n_{\text{cool}} \rightarrow 0$ )**

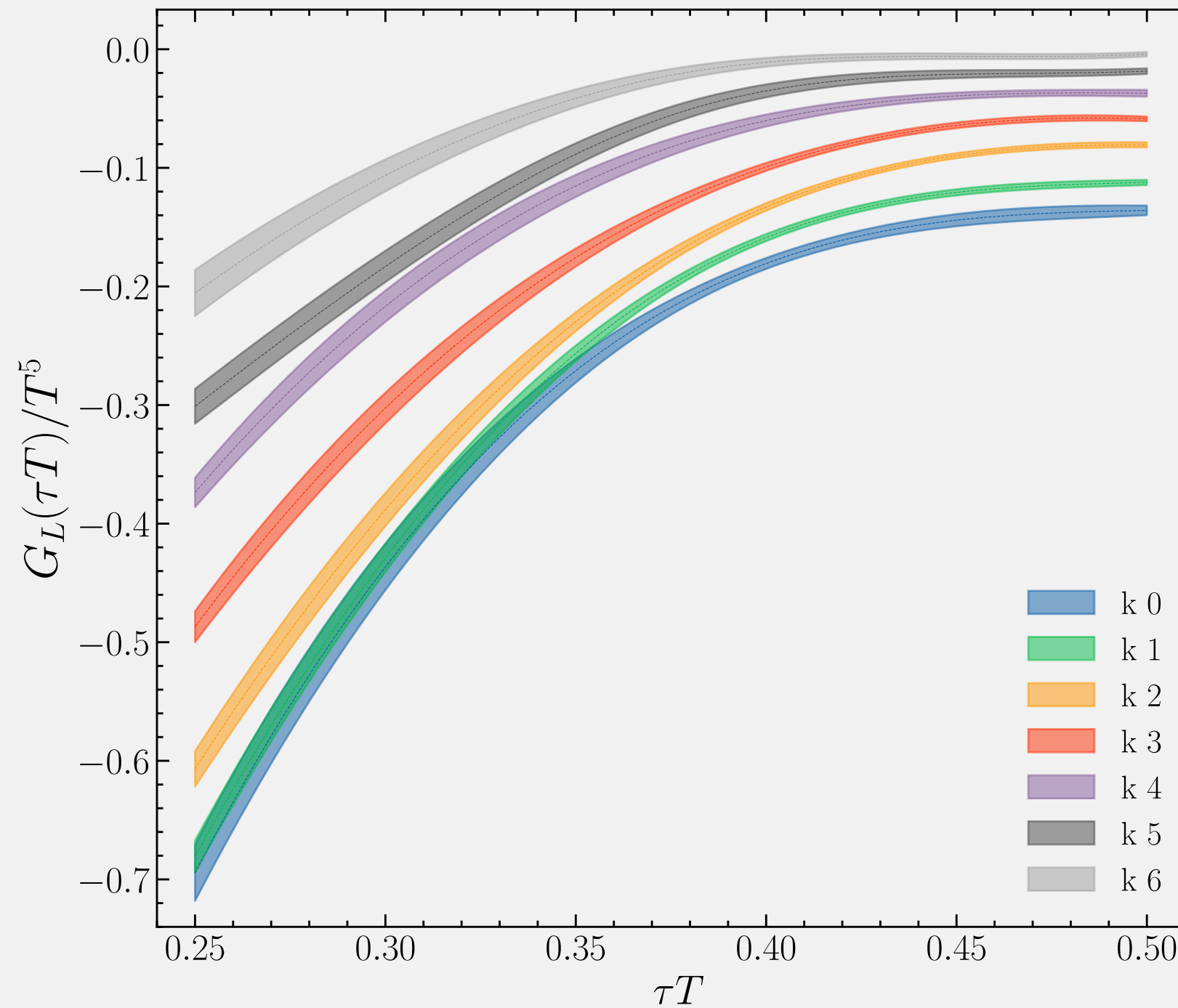


Extrapolating residual smoothing effects to zero.

*This procedure is repeated for every momentum mode  $\vec{p}$ .*

# Results: Momentum Suppression

The physical, double-extrapolated correlators  $G^{\vec{p}}(\tau)$ .



## Observation:

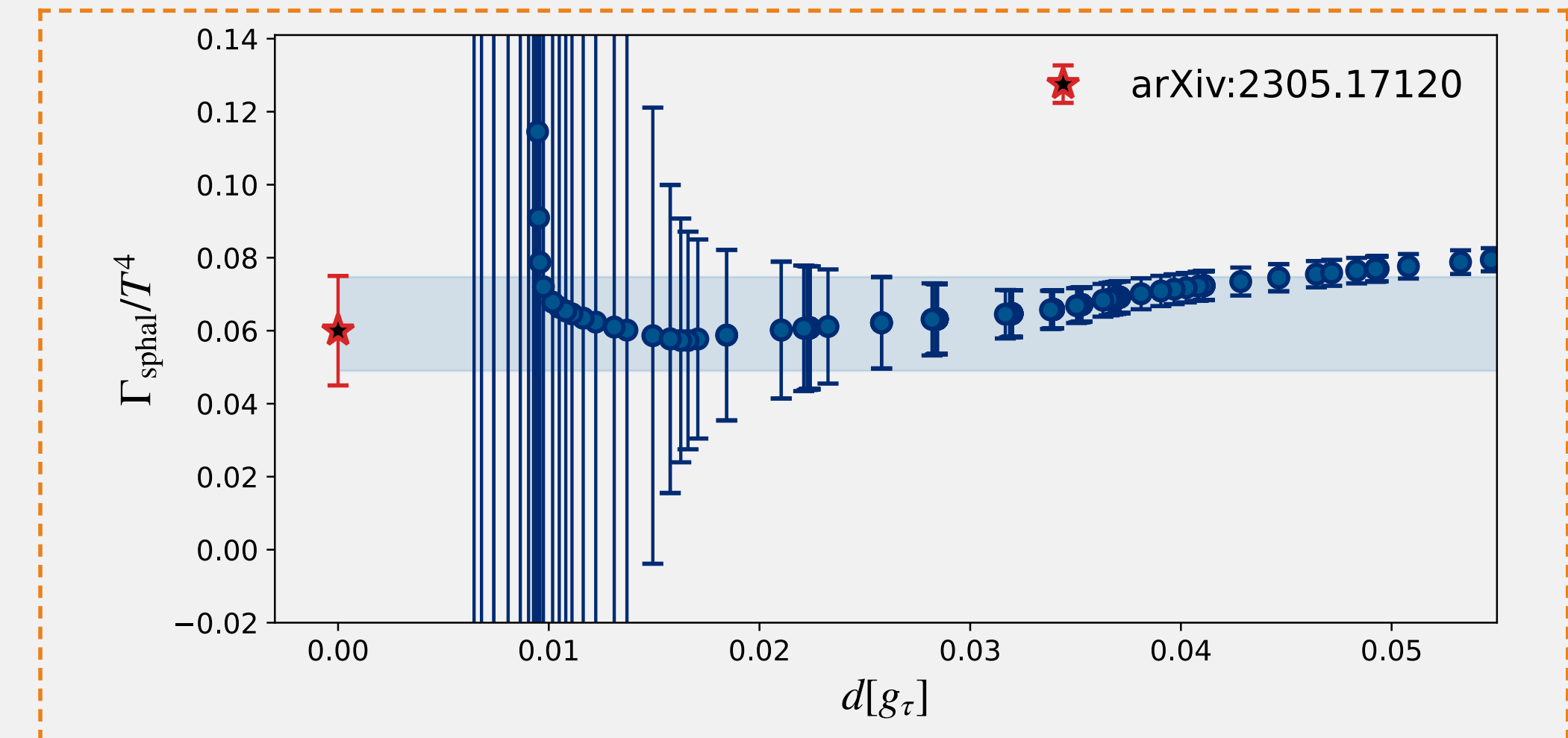
- Strong suppression of the topological fluctuations as  $p/T$  increases.
- For  $p/T \sim 9$ , the signal is suppressed by  $\sim 80\%$ .

\*\*Physical Implication:\*\*  
 This implies the \*\*Topological Rate\*\*  $\Gamma(p)$  decreases at large momenta.

# Inversion Results: Rate vs Momentum



Applying HLT inversion to the extrapolated correlators.



Preliminary determination suggests  $\Gamma(p)$  [stays constant / decays] up to sphaleron scale  $p_s \sim \alpha_s T$ .

# Conclusions

- **The Method:** The HTL (Backus-Gilbert) strategy successfully extracts spectral information from noisy lattice correlators, provided a careful stability analysis is performed.
- **Static Results:** Non-perturbative determination of  $\Gamma_{\text{sphal}}$  in full QCD shows significant enhancement over quenched approximations.
- **Finite Momeptum (Novel):**
  - We implemented a rigorous **double extrapolation** ( $a \rightarrow 0, r_s \rightarrow 0$ ) for finite- $p$  correlators.
  - Clear signal of **momeptum suppression** observed in the pure gauge theory.
  - First steps toward a full momentum-dependent axion production rate.

# Conclusions

- **The Method:** The HLT (Backus-Gilbert) strategy successfully extracts spectral information from noisy lattice correlators, provided a careful stability analysis is performed.
- **Static Results:** Non-perturbative determination of  $\Gamma_{\text{sphal}}$  in full QCD shows significant enhancement over quenched approximations.
- **Finite Momeptum (Novel):**
  - We implemented a rigorous **double extrapolation** ( $a \rightarrow 0, r_s \rightarrow 0$ ) for finite- $p$  correlators.
  - Clear signal of **momeptum suppression** observed in the pure gauge theory.
  - First steps toward a full momentum-dependent axion production rate.

**Future Work: Extend finite- $p$  analysis to Full QCD ( $T \sim 1$  GeV).**

prova

